



DSM-based design approach against flexural-torsional and global-global interactive failures in CFS fixed-ended columns

Elisa Cerqueira¹, Alexandre Landesmann¹, Dinar Camotim², André D. Martins², Pedro B. Dinis²

Abstract

The work reported in this paper is a sequel of previous numerical investigations carried out by the authors on the post-buckling behavior, strength and Direct Strength Method (DSM) design of cold-formed steel fixed-ended plain (Dinis *et al.* 2020a) and lipped (Cerqueira *et al.* 2021) channel columns buckling in flexural-torsional modes and experiencing global-global interaction – a coupling phenomenon involving major-axis flexural-torsional (F_{MT}) and minor-axis flexural (F_m) buckling that was first unveiled in the above studies. On the basis of the plain and lipped channel failure load data gathered, a DSM-based design approach for columns buckling in F_{MT} modes and failing in either pure F_{MT} or F_{MT} - F_m interactive modes was developed and recently shown to provide accurate, mostly safe and reliable predictions of the experimental (only a few) and numerical failure loads available (Dinis *et al.* 2022). The success of this research effort encouraged the authors to investigate whether the findings obtained remain qualitatively valid for fixed-ended columns with other cross-section shapes, such as return-lip, web-stiffened and web/flange-stiffened lipped channels, hat-sections and rack-sections. Therefore, the aim of this work is to report the available results of this ongoing investigation, intended to find an efficient and reliable DSM-based design approach for arbitrary CFS columns failing in pure F_{MT} or F_{MT} - F_m interactive modes. Such results concern the post-buckling behavior, strength and DSM design of the columns analyzed in this work, and include fairly extensive failure load sets – ANSYS non-linear shell finite element models are used. It is shown that the numerical failure loads assembled are quite efficiently predicted by the existing DSM-based design approach, developed exclusively in the context of plain and lipped channel columns.

1. Introduction and Background

Cold-formed steel (CFS) members used in the construction industry often are made of high-strength steels and exhibit slender cross-sections, a combination making them highly prone to the occurrence of several buckling phenomena – Figs. 1(a)-(d) show rack-section (R) column cross-sections buckled in some of them, namely local, distortional, major-axis flexural-torsional and minor-axis flexural modes. Naturally, the overall structural response and ultimate strength of such columns are invariably affected, to a greater or lesser extent, by the occurrence of the above buckling phenomena, as well as by the interaction between them – this is why provisions dealing with them must be included in CFS specifications.

¹ Programa de Engenharia Civil, COPPE, Universidade Federal do Rio de Janeiro, Brazil. <elisa.cerqueira@coc.ufrj.br; alandes@coc.ufrj.br>

² CERIS, DECivil, Instituto Superior Técnico (IST), Universidade de Lisboa, Portugal. <dcamotim@civil.ist.utl.pt; andrerdmartins@tecnico.ulisboa.pt; dinis@civil.ist.utl.pt>

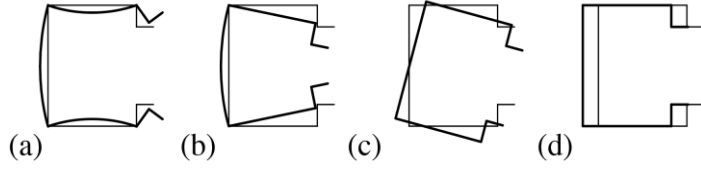


Figure 1: Rack-section column cross-sections buckled in (a) local, (b) distortional, (c) major-axis flexural-torsional and (d) minor-axis flexural modes

Nowadays, it is fair to claim that the Direct Strength Method (DSM – *e.g.*, Schafer 2008, 2019 or Camotim *et al.* 2016), first proposed by Schafer & Peköz (1998) and based on an original idea of Hancock *et al.* (1994), is the most rational and efficient approach for the design of cold-formed steel members (columns and beams, to be more precise) – this explains its fast growing and widespread popularity around the world. Moreover, it should be noted that the domain of application of the DSM has been recently extended to cover also beam-columns (Torabian & Schafer 2018), even if this research effort did not yet reach the codification stage. The currently codified design/strength curves are able to handle local, distortional, global and local-global interactive failures. In the context of this investigation, the relevant column nominal strength is the global one (P_{nG}), given by (AISI 2020)

$$P_{nG} = \begin{cases} P_y \left(0.658 \lambda_G^2 \right) & \text{if } \lambda_G \leq 1.5 \\ P_y \left(\frac{0.877}{\lambda_G^2} \right) & \text{if } \lambda_G > 1.5 \end{cases} \quad \text{with} \quad \lambda_G = \sqrt{\frac{P_y}{P_{cr.G}}} \quad , \quad (1)$$

where $P_{cr.G}$ and λ_G are the column global critical buckling load and slenderness, and $P_y = A \cdot f_y$ is the column squash load (A and f_y are the cross-sectional area and steel yield stress, respectively). Recently, Dinis *et al.* (2019, 2020b) reported numerical investigations on the accuracy of the Eq. (1) in predicting the failure loads of fixed-ended CFS columns collapsing in pure F_MT or F_m modes – a wide parametric study was carried out to gather failure loads of columns with (i) several cross-sections (plain channels, unstiffened, return lip, web-stiffened and web/flange-stiffened lipped channels, lipped zed-sections, hat-sections, rack-sections and I-sections formed by back-to-back plain channels), (ii) various geometries (cross-section dimensions and lengths) and (iii) many slenderness values. While the column failure loads associated with F_m collapses were found to be generally well predicted (even if there is room for slight improvements in the low and intermediate slenderness ranges), it was clearly shown that those associated with F_MT collapses are often considerably underestimated by the current design curve in the moderate and high slenderness ranges. This fact led the authors to propose a novel DSM-based strength curve set dependent on the non-dimensional cross-section geometric parameter

$$\beta_{FT} = \frac{I_I + I_w/A}{I_{II}} \quad , \quad (2)$$

where A , I_I , I_{II} and I_w are the cross-sectional area, major and minor moments of inertia, and warping constant (Dinis *et al.* 2020b). This strength curve set, termed P_{nFT} and defined by

$$P_{nFT} = \begin{cases} P_y \left(0.658 \lambda_{FT}^2 \right) & \text{if } \lambda_{FT} \leq 1.5 \\ P_y \left(\frac{a}{\lambda_{FT}^b} \right) & \text{if } \lambda_{FT} > 1.5 \end{cases} \quad \text{with} \quad \lambda_{FT} = \sqrt{\frac{P_y}{P_{cr.FT}}} \quad , \quad (3)$$

where subscript “G” was replaced by “FT”, in order to avoid confusion with the current DSM global design curve, and the β_{FT} dependence is felt through parameters a and b , obtained by means of a “trial-and-error curve fitting procedure”, which read

$$a = 0.39 \times 1.5^b \quad b = 0.06\beta_{FT} + 0.71 \leq 2.0 \quad (4)$$

It should be noted that Eqs. (3) and (1) only differ for $\lambda_{FT} > 1.5$ (moderate and high slenderness ranges) – the exponential expression is kept in the low-to-moderate slenderness range ($\lambda_{FT} \leq 1.5$). Each β_{FT} value leads to a and b values defining a different strength curve. For $\beta_{FT} \geq 21.5$, one has $b=2.0$ and $a=0.877$, which means that Eq. (3) and (1) coincide. Figs. 2(a)-(b) plot, against λ_{FT} ($=\lambda_G$), the P_u/P_{nG} and P_u/P_{nFT} values concerning all numerical failure loads considered by Dinis *et al.* (2020b) – recall that the two plots only differ for $\lambda_{FT} > 1.5$. Both figures include the P_u/P_{nG} and P_u/P_{nFT} means, standard deviations and maximum/minimum values, as well as the LRFD resistance factor ϕ values (AISI 2020) they lead to. It is clear that Eq. (3) yields accurate and mostly safe FMT failure load predictions: the P_u/P_{nFT} mean and standard deviation are equal to 1.061-0.054 and lead to an LRFD resistance factor much higher than that prescribed by AISI (2020) for compression members ($\phi_c=0.85$). Moreover, the large underestimations and scatter exhibited by the P_{nG} failure load estimates, for $\lambda_{FT} > 1.5$, are eliminated.

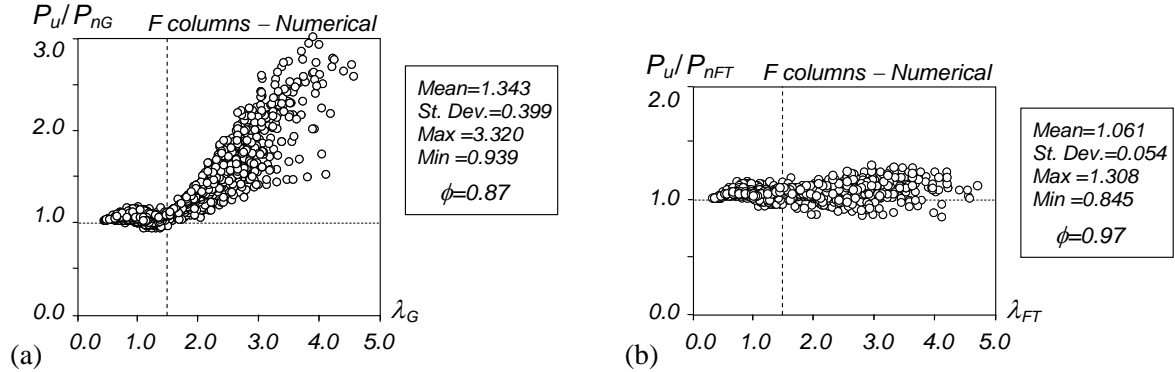


Figure 2: Plots (a) P_u/P_{nG} vs. λ_G and (b) P_u/P_{nFT} vs. λ_{FT} for the numerical FMT failure loads considered by Dinis *et al.* (2020b)

Subsequent investigations on the post-buckling behavior and failure of CFS columns buckling in FMT modes and exhibiting other than fixed-ended support conditions (three types of pinned supports, all fixed with respect to torsion and having warping fully prevented: supports consisting of either cylindrical or spherical hinges) revealed some unexpected behavioral features (Dinis *et al.* 2020b). In particular, such features raised the suspicion, and eventually convinced the authors, that the column FMT post-buckling behavior and failure are affected by coupling between FMT and Fm buckling – the closeness between the corresponding bifurcation loads ($P_{b,Fm}$ and $P_{cr,FT}$) quantifies the relevance of this interaction phenomenon. Note that, to the authors’ best knowledge, a global-global interaction had only been reported in short-to-intermediate equal-leg angle columns (e.g., Camotim *et al.* 2020), due to their very specific geometry (formed by just two outstand walls). On the other hand, the type of global-global interaction unveiled occurs in moderately long columns singly symmetric with respect to the major-axis that exhibit FMT critical and Fm non-critical buckling modes.

In order to confirm the above suspicion, Dinis *et al.* (2022) compared the failure loads of sets of CFS fixed-ended plain (U) and lipped (C) channel columns sharing the same cross-section dimensions ($b_w=100\text{mm}$, $b_f=40\text{mm}$, $t=1.2\text{mm}$ and $b_w=95\text{mm}$, $b_f=50\text{mm}$, $b_f=10\text{mm}$, $t=1.8\text{mm}$, respectively), yield stresses and initial geometrical imperfections (critical-mode FMT imperfections with amplitude $L/1000$).

Within each pair of (U or C) column sets, the only difference between the columns are the lengths, selected to have $R_G = P_{b,Fm}/P_{cr,FT}$ values either well above 1.0 (first set) or quite close to 1.0 (second set) – all the columns considered buckle in critical F_{MT} modes and have slenderness values above 1.5, as the coupling effects are more pronounced in slender columns. Figs. 3(a)-(b) show the plots P_u/P_{nFT} vs λ_{FT} for the U and C fixed-ended columns sets, where the white and grey circles stand for columns with R_G well above 1.0 (≥ 1.45) and closer to 1.0 (< 1.45), respectively – this quite arbitrary “border” is merely intended to separate columns likely or unlikely to experience F_{MT}-F_m interaction. As expected, the grey P_u/P_{nFT} values consistently fall below the white ones, thus evidencing the failure load erosion due to the interaction. It is also observed that the P_{nFT} estimation of the grey circles is inaccurate and unsafe – the vast majority of P_u/P_{nFT} values are below 1.0, many of them substantially, while the same estimation of the white circles is quite good. The P_u/P_{nFT} mean, standard deviation and maximum/minimum values read 0.74-0.14-1.01-0.50 + 0.86-0.13-1.06-0.64 (grey circles) and 1.08-0.08-1.21-0.85 + 1.07-0.05-1.21-0.99 (white circles), respectively for the U and C columns – it is clear that the P_{nFT} values are inadequate to estimate failure loads of columns undergoing global-global interaction.

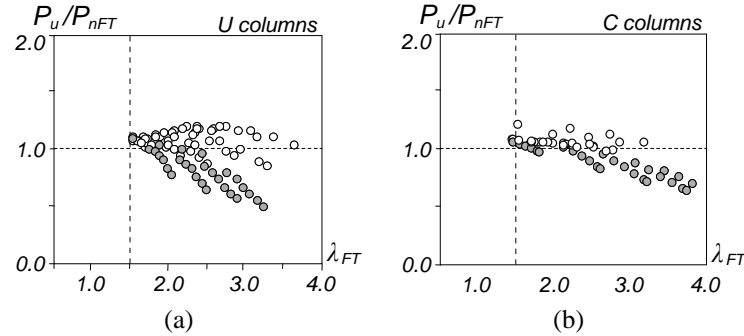


Figure 3: Plots P_u/P_{nFT} vs. λ_{FT} of (a) U and (b) C columns having $P_{b,Fm}/P_{cr,FT}$ below (grey circles) and above (white circles) 1.45.

This above finding/confirmation fact provided the motivation for the authors (Dinis *et al.* 2022) to modify the column strength curve set proposed by Dinis *et al.* (2020b), by including the buckling load ratio R_G to account for the F_{MT}-F_m interaction. Initially, they gathered a total of 835 failure loads, concerning columns having (i) 47U+48C geometries combining various cross-section dimensions and lengths, selected to ensure various levels of global-global (F_{MT}-F_m) interaction, (ii) initial geometrical imperfections with $L/1000$ amplitude (each column was analyzed with pure F_{MT} and F_m imperfections – the lowest failure load was retained for design purposes) and (iii) five yield stresses, making it possible to cover a wide critical slenderness range (λ_{FT}). Then, these failure load data were used (i) to confirm that the DSM-based design curve set proposed by Dinis *et al.* (2020b) is unable to predict them adequately and (ii) as the starting point to search for a DSM-based design approach capable of handling also F_{MT}-F_m interactive failures of columns buckling in F_{MT} modes. This search was successful and led to a modified column strength curve set defined by the expressions

$$P_{nFT-Fm} = \begin{cases} P_y \left(0.658^{\lambda_{FT}^2} \right) & \text{if } \lambda_{FT} \leq 1.5 \\ P_y \left(\frac{a}{\lambda_{FT}^b} \right) & \text{if } \lambda_{FT} > 1.5 \end{cases} \quad \text{with} \quad \lambda_{FT} = \sqrt{\frac{P_y}{P_{cr,FT}}} \quad , \quad (5)$$

$$b = 0.06\beta_{FT} + c \leq 2.0 \quad , \quad (6)$$

$$c = -19.5 R_G^3 + 73.6 R_G^2 - 94.1 R_G + 42 \geq 0.71 \quad , \quad (7)$$

where (i) subscript “FT-FM” indicates that F_{MT}-F_m interactive is handled, (ii) a and β_{FT} are still given by Eqs. (2) and (4), respectively, and, as mentioned before, (iii) $R_G = P_{b,Fm}/P_{cr,FT}$ is the ratio between the F_m (non-critical – $P_{b,Fm}$) and F_{MT} (critical – $P_{cr,FT}$) buckling loads. It should be noted that Eqs. (3)-(4) are retrieved for $R_G \geq 1.49$ (one has then $c=0.71$), which means that the CFS fixed-ended U and C column F_{MT} failure load prediction quality achieved by Dinis *et al.* (2020b), for columns not affected (or only slightly affected) by F_{MT}-F_m interaction, remains unaltered. Finally, note also that, for columns with $\lambda_{FT} \leq 1.5$, the (single) design curve is still given by Eq. (1), *i.e.*, the F_{MT} failure load estimates are provided by the current DSM global strength curve (AISC 2020).

The modified DSM-based design approach was shown to provide efficient (safe, accurate and reliable) failure loads for fixed-ended U and C columns buckling in F_{MT} modes, regardless of the R_G value (*i.e.*, whether F_{MT}-F_m interaction is present or not). Figs. 4(a)-(b) make it possible to assess the performance and merits of the proposed strength curve set. They show the P_u/P_{nFT-Fm} vs. λ_{FT} plots concerning the U and C columns considered by Dinis *et al.* (2022), affected by different F_{MT}-F_m interaction levels – note that these figures include the P_u/P_{nFT-Fm} statistical indicators. Moreover, Table 1 provides the P_u/P_{nFT-Fm} averages, standard deviations and maximum/minimum values, separating the columns with $\lambda_{FT} \leq 1.5$ and $\lambda_{FT} > 1.5$. The proposed P_{nFT-Fm} DSM-based column strength curve set, dependent on β_{FT} and R_G , provides high-quality failure load predictions for all U and C columns considered by Dinis *et al.* (2022), regardless of the interaction level. Finally, it was also shown that the P_u/P_{nFT-Fm} values concerning these columns lead to LRFD resistance factors of $\phi=0.962, 0.957, 0.958$, respectively for the U, C and U+C columns, values well above that prescribed in AISI (2020) for compression members – $\phi_c=0.85$.

Although the P_{nFT-Fm} DSM-based strength curves were shown to estimate fairly well the vast majority of the available fixed-ended U and C columns numerical failure loads, it remains an open question whether

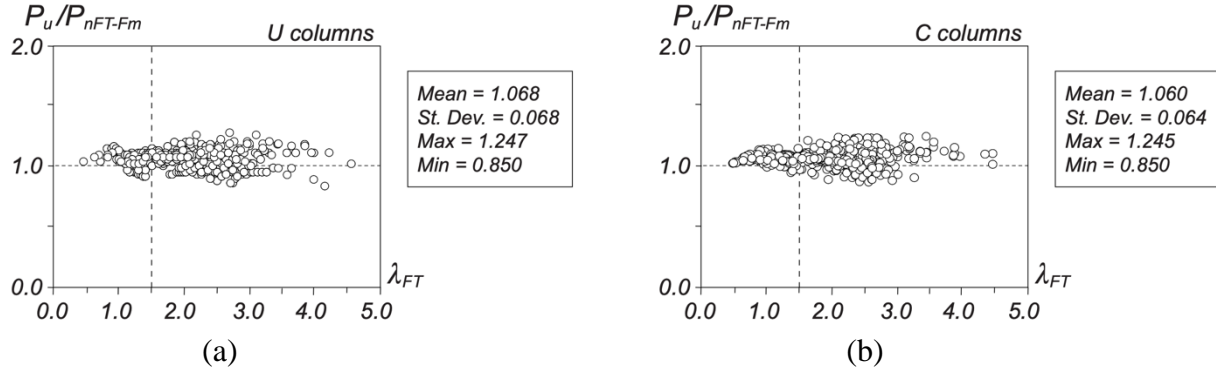


Figure 4: Plots P_u/P_{nFT-Fm} vs. λ_{FT} for the (a) U and (b) C columns considered by Dinis *et al.* (2022)

Table 1: Statistical indicators of the P_u/P_{nFT-Fm} values concerning U and C CFS columns considered by Dinis *et al.* (2022)

Parameter	U columns		C columns		U+C columns	
	$\lambda_{FT} \leq 1.5$	$\lambda_{FT} > 1.5$	$\lambda_{FT} \leq 1.5$	$\lambda_{FT} > 1.5$	$\lambda_{FT} \leq 1.5$	$\lambda_{FT} > 1.5$
n	85	240	187	323	272	563
Mean	1.052	1.074	1.056	1.062	1.055	1.067
Sd. Dev.	0.048	0.073	0.038	0.075	0.042	0.075
Max	1.139	1.247	1.146	1.245	1.146	1.247
Min	0.933	0.850	0.933	0.850	0.933	0.850

they perform equally well for columns with other cross-section shapes and/or boundary conditions – naturally, experimental validation is also required before codification can be achieved. The aim of this work is to extend the scope of the investigation reported by Dinis *et al.* (2022), by analyzing CFS fixed-ended columns with a wide variety of cross-section shapes (besides U and C), namely return-lip, web-stiffened and web/flange-stiffened lipped channels, hat-sections and rack-sections. Several cross-section dimensions lengths are considered and wide critical slenderness ranges are covered (by adopting five yield stresses). It is investigated whether and to which extent F_{MT} - F_m interaction affects the behavior, strength and DSM-based design of the columns with the new cross-section shapes.

The paper begins with the column geometry selection (Section 2), carried out by means of sequences of “trial-and-error” buckling analyses and aimed at identifying fixed-ended CFS columns with several cross-section shapes, dimensions and lengths, as well as prone to various levels of global-global (F_{MT} - F_m) interaction – all the selected columns exhibit F_{MT} critical buckling loads significantly lower than their local and distortional counterparts. Then, the elastic and elastic-plastic post-buckling behavior and strength of fixed-ended CFS columns affected by F_{MT} - F_m interaction are addressed in Section 3, adopting the approach followed by Dinis *et al.* (2022) for the U and C columns. Next, Section 4 reports the results of a fairly extensive parametric study carried out to gather the failure loads of the selected CFS columns, all associated with F_{MT} - F_m interactive collapses – in order to cover wide slenderness ranges, several yield stresses are considered. The assembled numerical failure load data, together with the fixed-ended CFS column failure loads reported by Dinis *et al.* (2020b) (concerning pure F_{MT} failures), are then used, in Section 5, to show that the DSM-based strength curve set proposed by Dinis *et al.* (2022) can also be successfully adopted to handle pure F_{MT} and F_{MT} - F_m interactive failures of CFS columns with a wide variety of cross-section shapes that buckle in F_{MT} modes – indeed, it is shown that the failure load prediction quality is similar to that reported by Dinis *et al.* (2022) for fixed-ended U and C columns. In order to achieve a general DSM-based design approach for CFS buckling in F_{MT} modes, it remains to be addressed the case of columns with other than fixed-ended support conditions, namely columns with three types of hinged supports, all fixed with respect to torsion and having warping fully prevented: supports consisting of hinges that are either cylindrical (pinned with respect to major or minor-axis bending) or spherical (pinned with respect to major and minor-axis bending) – the authors are currently working on this topic. Finally, the paper closes, in Section 6, with a few concluding remarks.

2. Column Geometry Selection – Buckling Behavior

The first task in this work consists of carefully selecting the cross-section dimensions and lengths of the fixed-ended CFS columns to be analyzed, so that they exhibit a wide variety of buckling loads ratio $R_G = P_{b,Fm}/P_{cr,FT}$. Besides the plain (U) and lipped (C) channels, already dealt with by Dinis *et al.* (2022), five additional cross-section shapes are considered, namely hat-sections (H), rack-sections (R), return lipped channels (RLC), web-stiffened lipped channels (WSC) and web-flange-stiffened lipped channels (WFSC) – the whole set of cross-section shapes and dimensions considered are displayed in Fig. 5. It is worth noting that the WSC and WFSC column “V-shaped” intermediate stiffeners are such that $d_1=d_3=10\text{ mm}$ and $d_2=d_4=20\text{ mm}$. As done previously, the selection procedure involves sequences of “trial-and-error” buckling analyses (i) performed in the code GBTUL (Bebiano *et al.* 2018), based on Generalized Beam Theory (GBT) and (ii) intended to identify columns buckling in F_{MT} modes and with R_G values comprised between 1.0 and 1.67, so that the overwhelming majority of their failures occur in F_{MT} - F_m (interactive) modes – for the sake of completion, a few of them will fail in pure F_{MT} modes.

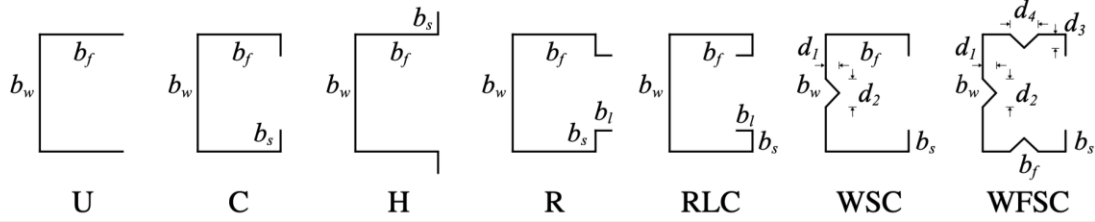


Figure 5: Column cross-section shapes and dimensions considered by Dinis *et al.* (2022) and in this work

The outputs of the above effort are 240 columns whose cross-section shapes, dimensions (b_w , b_f , b_s , b_l , t) and lengths (L_i) are given in Table 2. This table also provides the column cross-section areas (A), major (I_I) and minor (I_{II}) moments of inertia, warping constants (I_w) and β_{FT} parameter values – these geometrical properties were calculated on the basis of the cross-section mid-line dimensions. In addition, the tables included in Annex I, namely tables I.1 (H columns), I.2 (R columns), I.3 (RLC columns), I.4 (WSC columns) and I.5 (WFSC columns), provide the buckling loads ($P_{cr} \equiv P_{cr,FT}$, $P_{b,Fm}$) and ratios R_G and $R_{DL} = \text{Min}(P_{b,L}/P_{b,Fm}; P_{b,D}/P_{b,Fm})$ – $P_{b,L}$ and $P_{b,D}$ are the column local and distortional bifurcation loads.

Note that all selected columns display cross-sections dimensions such that $13.5(\text{WSC}_5) \geq b_w/b_f \geq 1.09(\text{H}_1)$ and $2.39(\text{H}_1) \geq \beta_{FT} \geq 11.62(\text{WFSC}_8)$, which are combined with six lengths comprised between 300 mm ($\text{H}_5 + \text{H}_6 + \text{RLC}_6 + \text{WSC}_2 + \text{WFSC}_8 L_i$) and 9000 mm ($\text{R}_2 + \text{WSC}_5 + \text{WSC}_6 L_6$), so that a wide R_G range can be covered: $1.68(\text{H}_5 - L_i) \geq R_G \geq \approx 1.00$ ($\text{R}_3 - L_6 + \text{R}_8 - L_6 + \text{WSC}_8 - L_6$). It was ensured that the R_{DL} ratio is never small, so that local or distortional buckling do not play any relevant role in the coupling phenomenon under consideration – the lowest R_{DL} ratios equal 1.61–1.82–2.33–1.51–1.67 and correspond to H_4 , R_7 , RLC_4 , WSC_2 and WFSC_8 columns with L_i , whose R_G values are 1.64–1.44–1.47–1.43–1.32, respectively.

The illustrative signature curves shown in Figs. 6(a) and 7(a) concern steel ($E=210\text{GPa}$, $\nu=0.3$) (i) RLC columns with $b_w=100\text{mm}$, $b_f=60\text{mm}$, $b_l=10\text{mm}$, $b_s=10\text{mm}$ and (ii) WSC columns with $b_w=100\text{mm}$, $b_f=60\text{mm}$, $b_l=10\text{mm}$, respectively, and provide the variation of f_{cr} (elastic critical buckling stress) with the column length L (logarithmic scale) – in both cases, four thickness values are considered ($t=2\text{-}3\text{-}4\text{-}5\text{ mm}$). Each solid was obtained through GBT bifurcation analyses carried out in the code GBTUL and including the following deformation modes: 4 global (1–4), 4 distortional (5–8), 11 local (9–19) (RLC columns), and or 4 global (1–4), 2 distortional (5–6) and 11 local (7–17) (WSC columns) and (ii) 4 global (1–4), 2 distortional (5–6) and 11 local (7–17)³. The dashed curves provide the variation of the minor-axis flexural buckling stress $f_{b,Fm}$ with L (logarithmic scale) and are the same for the four cross-section geometries only differing in the wall thickness. Figs. 6(b) and 7(b) display the GBT modal participation diagrams associated with each f_{cr} vs. L curve, providing the contributions of each GBT deformation mode to the RLC and WSC column buckling modes – *e.g.*, columns with $t=3\text{ mm}$ and $L=500\text{ cm}$ buckle in modes combining contributions from modes 2 and 4: 12.8% + 87.2%, in the RLC column, and 12.6% + 87.4%, in the WSC column. Lastly, Figs. 6(c) and 7(c) show, for the RLC and WSC columns, the in-plane shapes of the GBT deformation modes 2–6 and the critical buckling modes of columns with $t=3\text{ mm}$ and lengths $L=200, 600, 1200\text{ cm}$. These buckling results prompt the following comments:

- Each f_{cr} vs. L curve has three zones (length intervals), the first one concerning distortional buckling in modes with various half-waves (only p_5 exists and f_{cr} remains fairly constant) – the only exception are the RLC columns with $t=2\text{ mm}$, which buckle in local modes (only p_9 exists and f_{cr} also remains

³ At this stage, note that, as done by Landesmann *et al.* (2016), all the WCS and WFSC columns buckling modes involving dominant contributions from deformation modes with numbers higher than 6 are viewed as locals. In other words, the “false distortional deformation modes”, stemming from motions of the stiffener nodes, are treated as local deformation modes.

Table 2: Selected CFS fixed-ended columns: cross-section mid-line dimensions geometries, geometrical properties (b_w , b_f , b_s , b_l , t , A , L , I_I , I_{II} , I_w – values in mm, mm^2 , mm^4 , mm^6), β_{FT} values and lengths

Column	b_w	b_f	b_s	b_l	t	A	I_I ($\times 10^4$)	I_{II} ($\times 10^4$)	I_w ($\times 10^6$)	β_{FT}	L_1	L_2	L_3	L_4	L_5	L_6
H ₁	60	55	11	-	4	7.68	58.04	33.67	173.14	2.39	5500	6000	6200	6500	7000	7200
H ₂	100	60	10	-	3	7.2	133.23	36.03	553.98	5.83	5750	6000	6500	7000	7500	8000
H ₃	120	60	15	-	5	13.5	356.75	72.16	1485.31	6.47	3200	3500	4000	4200	4500	5000
H ₄	140	70	10	-	4	12	411.01	77.83	2447.41	7.90	3750	4000	5000	5500	6000	7000
H ₅	100	50	10	-	3	6.6	118.22	23.32	352.34	7.36	3000	3500	4000	4500	5000	5200
H ₆	90	40	10	-	2	3.8	54.59	8.88	104.69	9.25	3000	3300	3500	4000	4500	5000
H ₇	130	70	20	-	4.5	13.95	450.52	105.16	2403.62	5.92	6000	6500	7000	7500	8000	8200
H ₈	130	65	15	-	4	11.6	356.30	71.42	1761.64	7.11	4500	5000	5500	6000	6500	7000
R ₁	110	55	10	15	3	8.1	166.41	46.78	1345.29	7.11	5000	6000	6500	7000	7500	8500
R ₂	100	60	11	20	4	11.28	195.27	83.74	2232.63	4.70	6500	7000	7500	8000	8500	9000
R ₃	120	60	15	25	5	16	380.43	131.60	5316.94	5.42	4500	5000	6000	7000	7500	8000
R ₄	140	70	10	20	5	17	571.85	159.45	6958.06	6.15	5500	6000	6500	7000	7500	8000
R ₅	100	50	10	15	3	7.5	126.63	37.19	921.92	6.71	4000	4500	5000	5500	6000	7000
R ₆	90	50	10	15	3	7.2	99.68	35.82	759.98	5.73	5000	5500	6000	7000	7500	8000
R ₇	130	60	15	20	5	16	445.08	119.77	5315.58	6.49	3500	4000	4500	5000	5500	6200
R ₈	120	70	10	15	5	15.5	392.01	133.87	4433.07	5.06	5500	6000	6500	7000	7500	8500
RLC ₁	80	55	10	15	4	9.60	108.21	44.58	817.50	4.34	4500	4750	5000	5500	6000	6500
RLC ₂	100	60	15	15	4	11.20	190.01	64.67	1984.29	5.68	4500	5000	5500	6000	6500	7000
RLC ₃	120	70	20	20	5	17.00	406.85	135.15	6565.70	5.87	5000	5500	6000	6500	7000	7500
RLC ₄	140	70	15	20	5	17.50	576.90	134.45	6717.71	7.15	3500	4000	5000	5500	6000	6500
RLC ₅	100	70	15	20	5	15.50	268.73	118.12	3833.30	4.37	6000	6500	7000	7500	8000	8500
RLC ₆	90	50	15	20	3	7.80	102.63	30.94	904.78	7.07	3000	3500	4000	4500	5000	6000
RLC ₇	130	70	15	20	5	17.00	487.35	130.73	5888.04	6.38	4000	4500	5000	5500	6000	7000
RLC ₈	120	60	10	15	4	11.60	284.75	63.72	2091.53	7.30	3500	4000	4500	5000	5500	6000
WSC ₁	110	60	15	-	3	8.05	162.76	41.58	1140.82	7.32	3500	4000	5000	6000	6500	7000
WSC ₂	100	50	10	-	2	4.57	74.86	15.25	320.85	9.52	3000	3500	4000	4500	5000	6000
WSC ₃	120	70	12	-	4	11.69	287.50	77.13	2276.39	6.25	4000	4500	5000	6000	6500	7200
WSC ₄	140	70	20	-	4	13.13	424.19	95.42	4296.33	7.87	3500	4000	5000	5500	6000	7000
WSC ₅	140	80	15	-	4	13.53	452.37	119.26	4841.92	6.79	6000	6500	7000	7500	8500	9000
WSC ₆	130	70	15	-	3	9.25	262.48	63.39	2280.07	8.03	5000	6000	7000	7500	8000	9000
WSC ₇	120	60	15	-	3	8.35	197.89	42.81	1359.33	8.43	3500	4000	4500	5000	6000	6500
WSC ₈	110	50	20	-	2	5.17	99.21	20.18	642.55	11.08	3500	4000	4500	5000	6000	6500
WFSC ₁	110	60	15	-	3	8.55	169.03	42.16	1022.96	6.85	4500	5000	5500	6000	6500	7000
WFSC ₂	100	60	10	-	3	7.95	131.82	36.25	658.20	5.92	4500	5000	5500	6000	6500	7000
WFSC ₃	100	50	10	-	2	4.90	77.87	15.61	280.70	8.66	3500	4500	5000	5500	6000	6500
WFSC ₄	90	50	10	-	2	4.70	61.14	15.04	221.21	7.20	4500	5000	5500	6000	6500	7000
WFSC ₅	100	60	15	-	3	8.25	136.04	40.76	838.12	5.83	5000	5500	6000	6500	7000	7500
WFSC ₆	120	60	20	-	3	9.15	211.59	48.00	1530.60	7.90	3500	4500	5500	6000	6500	7000
WFSC ₇	110	50	15	-	2	5.30	100.57	18.38	442.80	10.02	3500	4000	4500	5500	6000	6500
WFSC ₈	120	50	15	-	2	5.50	123.03	18.95	534.05	11.62	3000	3500	4000	4500	5500	6000

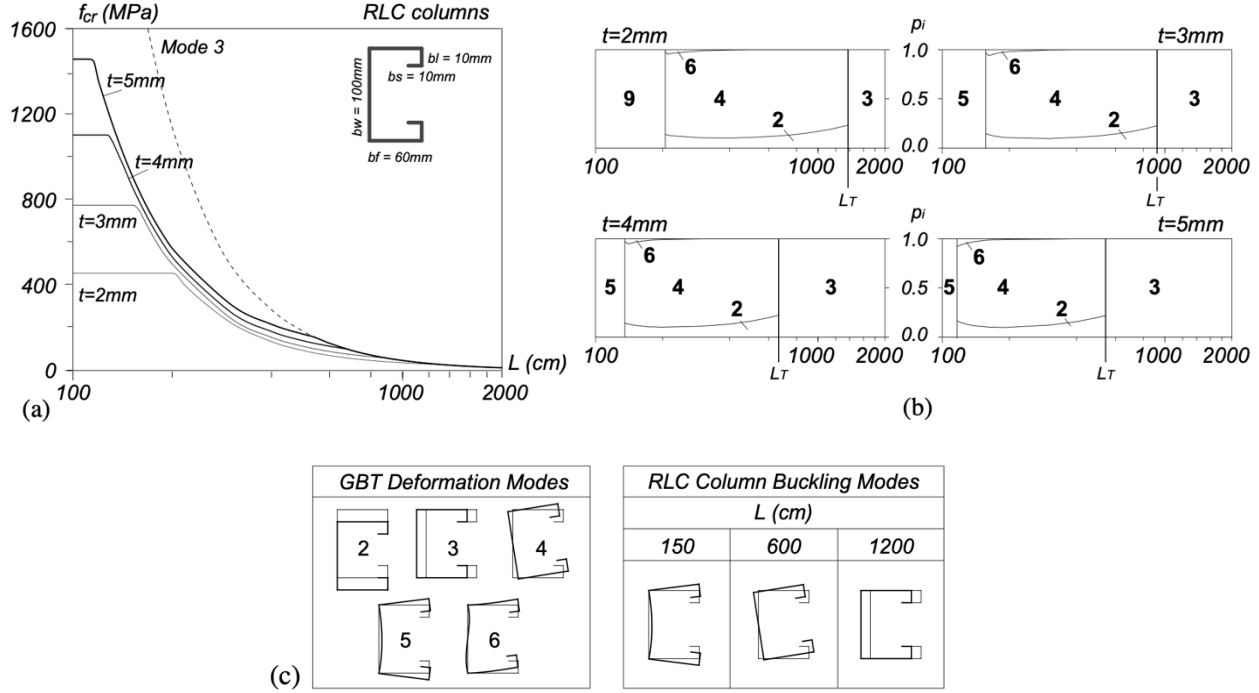


Figure 6: (a) f_{cr} vs. L curves and (b) GBT modal participation diagrams of RLC columns with $b_w=100\text{mm}$, $b_f=60\text{mm}$, $b_s=10\text{mm}$, $t=2-3-4.5\text{ mm}$, and (c) in-plane shapes of deformation modes 2-6 and $t=3\text{ mm}$ critical buckling modes

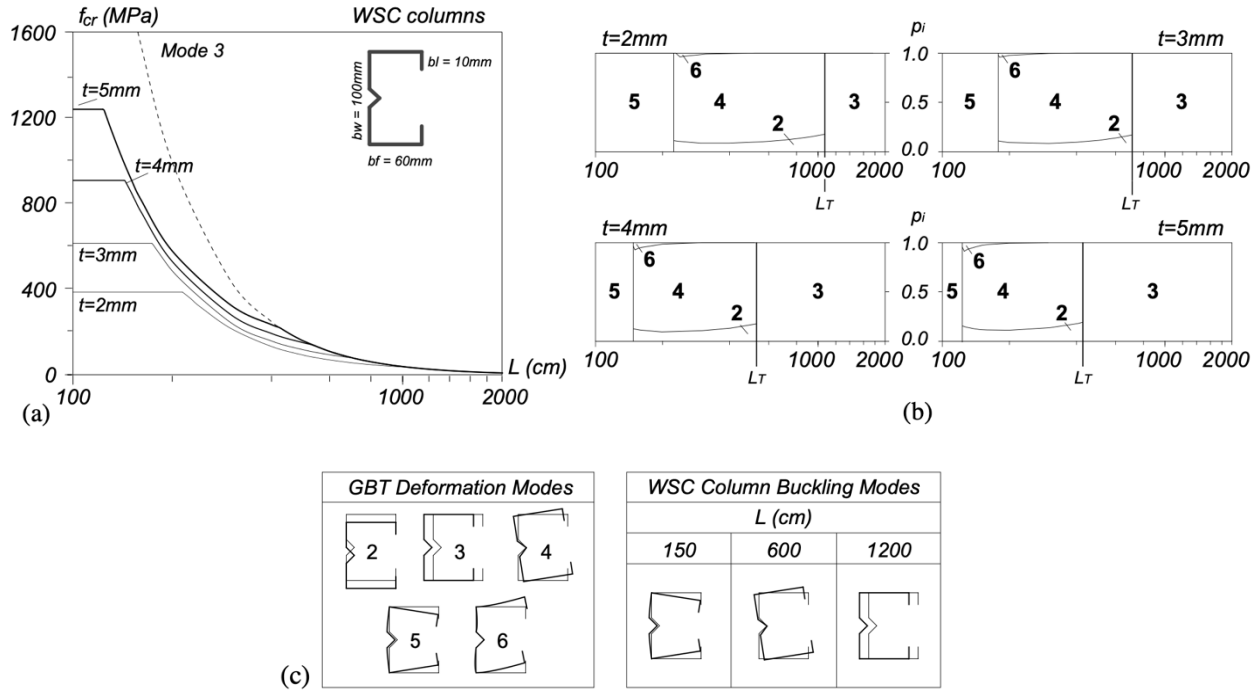


Figure 7: (a) f_{cr} vs. L curves and (b) GBT modal participation diagrams of WSC columns with $b_w=100\text{mm}$, $b_f=60\text{mm}$, $b_s=10\text{mm}$, $t=2-3-4-5\text{ mm}$, and (c) in-plane shapes of deformation modes 2-6 and $t=3\text{ mm}$ critical buckling modes

practically constant). The second zone concerns single half-wave global buckling and f_{cr} decreases monotonically with L and the columns buckle in global FMT (2+4) modes with dominant torsional

deformations. The third zone also concerns single half-wave global buckling and f_{cr} still decreases monotonically with L , but the columns buckle in global F_m (3) modes – the global buckling mode nature change occurs quite suddenly, at a “transition length” $L=L_T$. In between the first two zones, there is a small length interval inside which f_{cr} decreases monotonically with L and the column buckling modes include small contributions from the anti-symmetric distortional mode (6) – the size of this small length interval increases slightly with t .

- (ii) Because the column F_m buckling stresses are practically independent of t , the four F_{MT} signature curve branches, each associated with a given t value, end in a common F_m signature curve branch.
- (iii) Columns with $L=L_T$ have identical F_{MT} and F_m buckling stresses and, therefore, their post-buckling behaviors, strengths and failure stresses are expected to be influenced by the coupling between these two buckling modes (F_{MT} - F_m interaction). However, the interaction effects should also influence the post-buckling behavior, strength and failure stress/load of columns with lengths not too much below L_T , *i.e.*, such that R_G is not substantially larger than 1.0. On the other hand, such interaction effects are either absent or negligible in columns with lengths above L_T , which have R_G values below 1.0 and always fail in F_m modes – this is why such columns are not dealt with in this work.

3. Post-Buckling Behavior and Strength under Global-Global Interaction

A fundamental issue in mode coupling studies is to know how the initial geometrical imperfection shape influences the post-buckling behavior and strength of the member (or structural system) under scrutiny – to acquire this knowledge, it is necessary to carry out an imperfection-sensitivity study. In particular, it is essential to identify the most detrimental initial imperfection shape, in the sense that it leads to the lowest strengths. In this specific case, the purpose is to find which initial imperfection shape, combining arbitrarily F_{MT} and F_m components, leads to the maximum column strength and failure load erosion – naturally, all the initial geometrical imperfections considered share a common amplitude. Then, the identified most detrimental initial geometrical imperfection shapes are adopted (i) to carry out the elastic-plastic analyses whose results are presented in Section 3.2 and (i) to perform the parametric study aimed at assembling failure load data concerning CFS fixed-ended columns buckling in F_{MT} modes and exhibiting various R_G values, addressed in Section 4. It should be noted that the elastic and elastic-plastic results presented in this work were obtained by means of ANSYS (SAS 2009) non-linear shell finite element analyses (SFEA), using the models previously employed by Dinis *et al.* (2022) – rounded corner and residual stress effects were disregarded, since they are known to practically cancel each other in CFS members (*e.g.*, Ellobody & Young 2005).

3.1 Elastic Post-Buckling Strength – Most Detrimental Initial Geometrical Imperfections

Due to the presence of two competing buckling modes in columns affected by global-global interaction (critical F_{MT} and non-critical F_m modes), the commonly used approach of considering critical-mode initial imperfections ceases to be adequate. Indeed, in order to identify the most detrimental initial imperfection shape, it is necessary to determine and compare equilibrium paths of otherwise identical columns with initial geometrical imperfections that (i) span the whole critical-mode shape range and (ii) share a common amplitude. A systematic approach to identify the most detrimental initial geometrical imperfection shape was devised by Camotim & Dinis (2011) and accounts for the fact that the two competing buckling modes exhibit a single half-wave – it involves the performance of the following procedures:

- (i) Determine “pure” critical buckling mode shapes, normalized to exhibit unit mid-span displacements:
 - (i₁) a F_{MT} mode with a flange-lip corner downward vertical displacement equal to $v_{FT}=1$ mm and (i₂)

- two F_m modes with uniform horizontal displacements equal to $w_{Fm}=1$ mm (moving to the right) and $w_{Fm}=-1$ mm (moving to the left) – the need to consider the two F_m modes stems from the fact that they correspond to different post-buckling behaviors, as will be shown a bit ahead in the paper.
- (ii) To scale the three “pure” modes, so that their amplitudes equal $L/1000$ (value commonly prescribed in cold-formed steel specifications).
 - (iii) A given initial geometrical imperfection shape is obtained by linearly combining the scaled buckling modes shapes, with coefficients $C_{FT,0}$ and $C_{Fm,0}$ satisfying the condition $(C_{FT,0})^2+(C_{Fm,0})^2=1$. A better visualization and “feel” of the initial imperfection shapes considered can be obtained by considering the unit radius half circle drawn on the $C_{FT,0}$ - $C_{Fm,0}$ plane, as shown in Fig. 8(a)⁴. Each possible critical-mode imperfection shape corresponds to a point lying on this half circle, associated with an angle θ , measured from the horizontal ($C_{FT,0}$) axis and positive when counterclockwise – it defines a $C_{Fm,0}/C_{FT,0}$ ratio, where $C_{FT,0}=\cos\theta$ and $D_{Fm,0}=\sin\theta$. Fig. 8(b) shows the pure FT and F_m initial imperfection shapes ($\theta=0^\circ$; $\theta=90^\circ$; $\theta=-90^\circ$) of an illustrative WFS column.

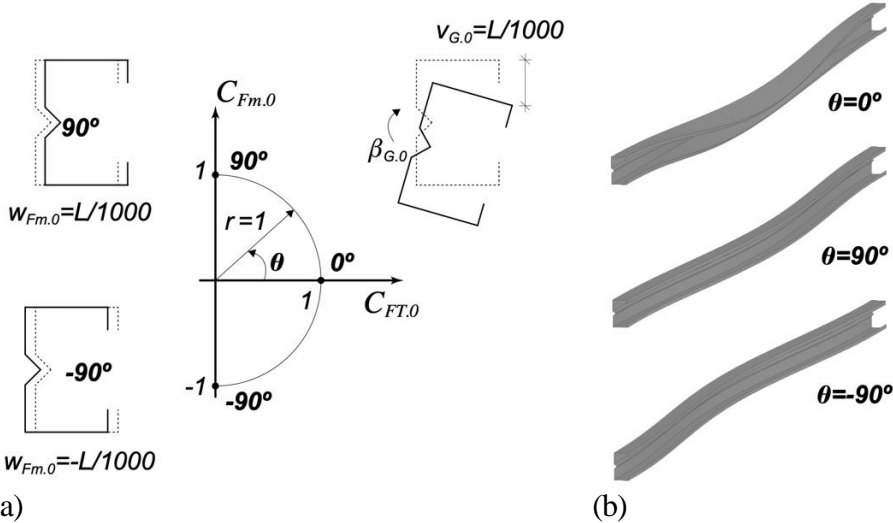


Figure 8: (a) Initial imperfection representation in the $C_{FT,0}$ - $C_{Fm,0}$ plane and (b) initial imperfection shapes for $\theta=0^\circ, \pm 90^\circ$

After having defined the full set of possible critical-mode initial geometrical imperfections shapes, it becomes possible to compare the elastic post-buckling behaviors of columns containing them, in order to (i) obtain numerical evidence of the occurrence of $F_M T$ - F_m interaction and (ii) identify the most detrimental initial imperfection shape – this study considers initial imperfections corresponding to 15° θ intervals: $\theta=0\pm 15\pm 30\pm 45\pm 60\pm 75\pm 90^\circ$. The P/P_{cr} vs. $\gamma_0+\gamma$ and P/P_{cr} vs. $(d_{m0}+d_m)/t$ equilibrium paths (γ and d_m are the mid-span torsional rotation translation due to minor-axis bending, respectively – γ_0 and d_{m0} are their initial values) displayed in Figs. 9(a₁)-(b₃) concern WSC₁ columns ($\beta_{FT}=7.32$) with lengths L_2 , L_4 and L_6 (corresponding to $R_G=1.47-1.19-1.01$) and containing the 13 distinct initial geometrical imperfections dealt with in this work. As for Figs. 10(a)-(b), they show (i) four post-buckling equilibrium paths P/P_{cr} vs. $\gamma_0+\gamma$ and P/P_{cr} vs. $(d_{m0}+d_m)/t$, already displayed in Fig. 9(a₁)-(b₁) and 9(a₃)-(b₃), concerning columns with lengths L_2 or L_6 and $\theta=60^\circ$ initial geometrical imperfections, and also (ii) the evolution of the column mid-span cross-section deformed configuration as loading progresses. The close observation of these post-buckling results prompts the following remarks:

⁴ Since the column $F_M T$ post-buckling behavior is symmetric, it suffices to consider the half-circle displayed in Fig. 8(a).

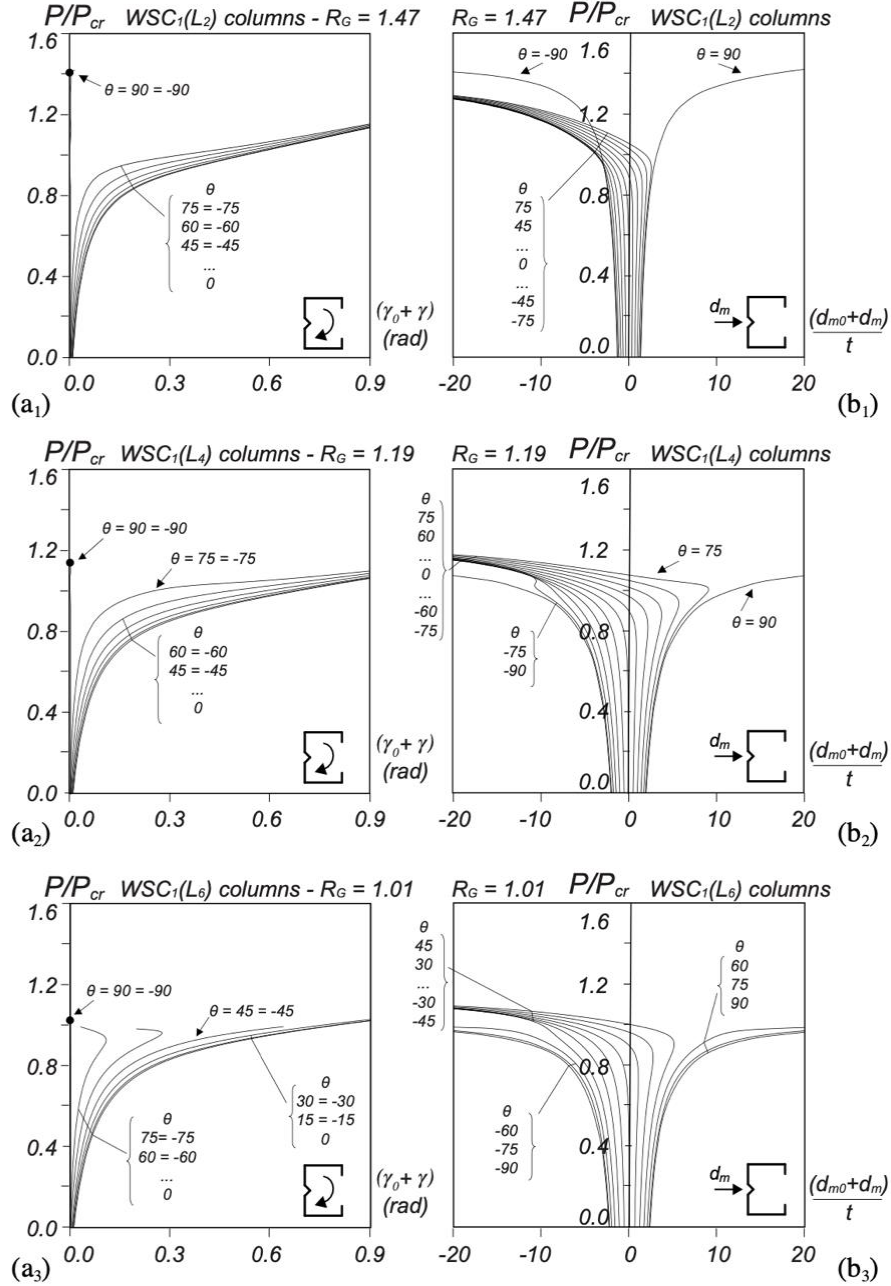


Figure 9: Elastic equilibrium paths (a) P/P_{cr} vs. $\gamma_0 + \gamma$ and (b) P/P_{cr} vs. $(d_{m0} + d_m)/t$ of WSC₁ columns with (1) L_2 , (2) L_4 and (3) L_6

- (i) Firstly, it should be noted that the WSC column post-buckling results presented here are qualitatively very similar to those concerning the remaining columns, which means that the comments made below are valid for all the columns analyzed in this work.
- (ii) The L_2 column equilibrium paths P/P_{cr} vs. $\gamma_0 + \gamma$ concerning $\theta = 0 \pm 15 \pm 30 \pm 45 \pm 60 \pm 75^\circ$ exhibit the expected stable behavior and merge into a common curve, associated with clockwise mid-span torsional rotations. Their post-critical strengths are ordered according to the amplitude of the F_m initial imperfection component, *i.e.*, the lowest and highest post-critical strengths correspond to the $\theta = 0^\circ$ and $\theta = \pm 75^\circ$ initial imperfections – naturally, the most detrimental initial imperfection shape is the pure

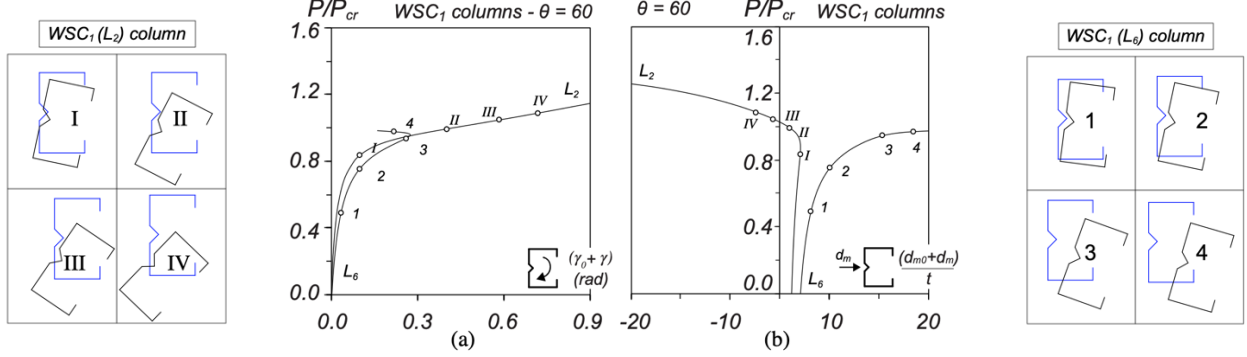


Figure 10: WSC₁ columns with lengths L_2 or L_6 and $\theta=60^\circ$ initial imperfections: elastic equilibrium paths (a) P/P_{cr} vs. $\gamma_0+\gamma$ and (b) P/P_{cr} vs. $(d_{m0}+d_m)/t$, and mid-span cross-section deformed configuration evolution along those equilibrium paths

F_{MT} one ($\theta=0^\circ$). Moreover, the equilibrium paths P/P_{cr} vs. $(d_{m0}+d_m)/t$ of the five columns with positive θ values exhibit a d_m reversal (from positive to negative) that occurs for $P/P_{cr} \approx 0.85$ – this does not happen for the five columns with negative θ values (d_m is always negative).

- (iii) The P/P_{cr} vs. $\gamma_0+\gamma$ and P/P_{cr} vs. $(d_{m0}+d_m)/t$ equilibrium paths of L_2 columns with $\theta=90^\circ$ and $\theta=-90^\circ$ (pure F_m initial geometrical imperfections) are identical and differ clearly from the remaining ones. They correspond to a “singular” post-buckling behavior. Indeed, these columns exhibit virtually no F_{MT} deformations (only F_m ones) and their common post-critical strength is always the highest one – note that no effective centroid shift effects occur, due to the absence of F_{MT} deformations.
- (iv) The post-buckling behaviors of the L_4 and L_6 columns are markedly different from their L_2 column counterpart, due to the fact that the R_G values are significantly lower (1.19 or 1.01 vs. 1.47). First of all, the post-critical strength is visibly smaller, which stems from the larger d_m values and reflects the presence of F_{MT}-F_m interaction, naturally more relevant in the L_6 columns – this interaction amplifies the d_m values due to the initial geometrical imperfections and effective centroid shifts. As before, the P/P_{cr} vs. $\gamma_0+\gamma$ and P/P_{cr} vs. $(d_{m0}+d_m)/t$ equilibrium paths concerning $\theta=90^\circ$ and $\theta=-90^\circ$ are identical and differ clearly from the remaining ones. However, reflecting the strength erosion due to the F_{MT}-F_m interaction, their common post-critical strength is no longer the highest one – in fact, it is the lowest one for the L_6 columns (even if this cannot be very clearly observed in Figs. 9(a₃) and 9(b₃)).
- (v) In the L_4 columns with $\theta=\pm 75^\circ$ and L_6 columns with $\theta=\pm 30\pm 45\pm 60\pm 75^\circ$, the mid-span cross-section F_{MT} deformations cease to grow, rather abruptly, at a given applied load level, while the F_m deformations continue to grow – this means that this cross-section deformed configuration becomes progressively “more akin” to the F_m buckling mode shape. This feature is illustrated in Figs. 10(a)-(b), which compare the equilibrium paths and mid-span cross-section deformed configurations of the L_2 and L_6 columns with $\theta=60^\circ$. In the L_6 column, note the difference between the mid-span cross-section deformed configurations corresponding to the equilibrium states 3 and 4: while the F_{MT} deformations are practically the same, the F_m translations are quite different (the latter is much larger).
- (vi) It can be concluded that, depending on the column R_G value, the most detrimental initial geometrical imperfection shape may be either the pure F_{MT} buckling mode ($\theta=0^\circ$) or the “pure” F_m buckling mode ($\theta=90^\circ$ or $\theta=-90^\circ$). Since it is often impossible to know, beforehand, which is the most detrimental initial imperfection shape, it was decided to consider both of them in the parametric study presented in Section 5, intended to gather failure load data of columns buckling in F_{MT} modes.

3.2 Elastic-Plastic Post-Buckling and Strength

As mentioned earlier, failure loads concerning all the CFS columns with both pure F_{MT} ($\theta=0^\circ$) and pure F_m ($\theta=90^\circ$) initial geometrical imperfections (amplitude L/1000) are evaluated – depending on the particular column, either failure load can be the lowest one. Figs. 11 and 12 illustrate the results obtained – they depict the elastic-plastic equilibrium paths P/P_{cr} vs. d_m/t of (i) H₅ columns with lengths L_3 or L_6 , pure F_{MT} or F_m initial imperfections and three yield stresses ($f_y/f_{cr,FT} \approx 1.1; 2.2; 3.3$ – the elastic equilibrium paths correspond to $f_y/f_{cr,FT} = \infty$), and (ii) R₈ columns with lengths L_4 or L_6 , pure F_{MT} or F_m initial imperfections and also 3 yield stresses ($f_y/f_{cr,FT} \approx 1.1; 2.2; 3.3$) – the failure loads are identified by the white circles. Moreover, these figures also include the failure modes and plastic strains at collapse of the columns with $f_y/f_{cr,FT} \approx 2.2$ – the failure modes corresponding to F_{MT} and F_m initial imperfections are identified by letters “A” and “B”, respectively, and have clearly different features: while the former failure modes exhibit plastic strains at top and bottom web-flange corner regions of the mid-span and end cross-sections, the latter ones involve the full yielding of those cross-sections. The observation of these figures shows that:

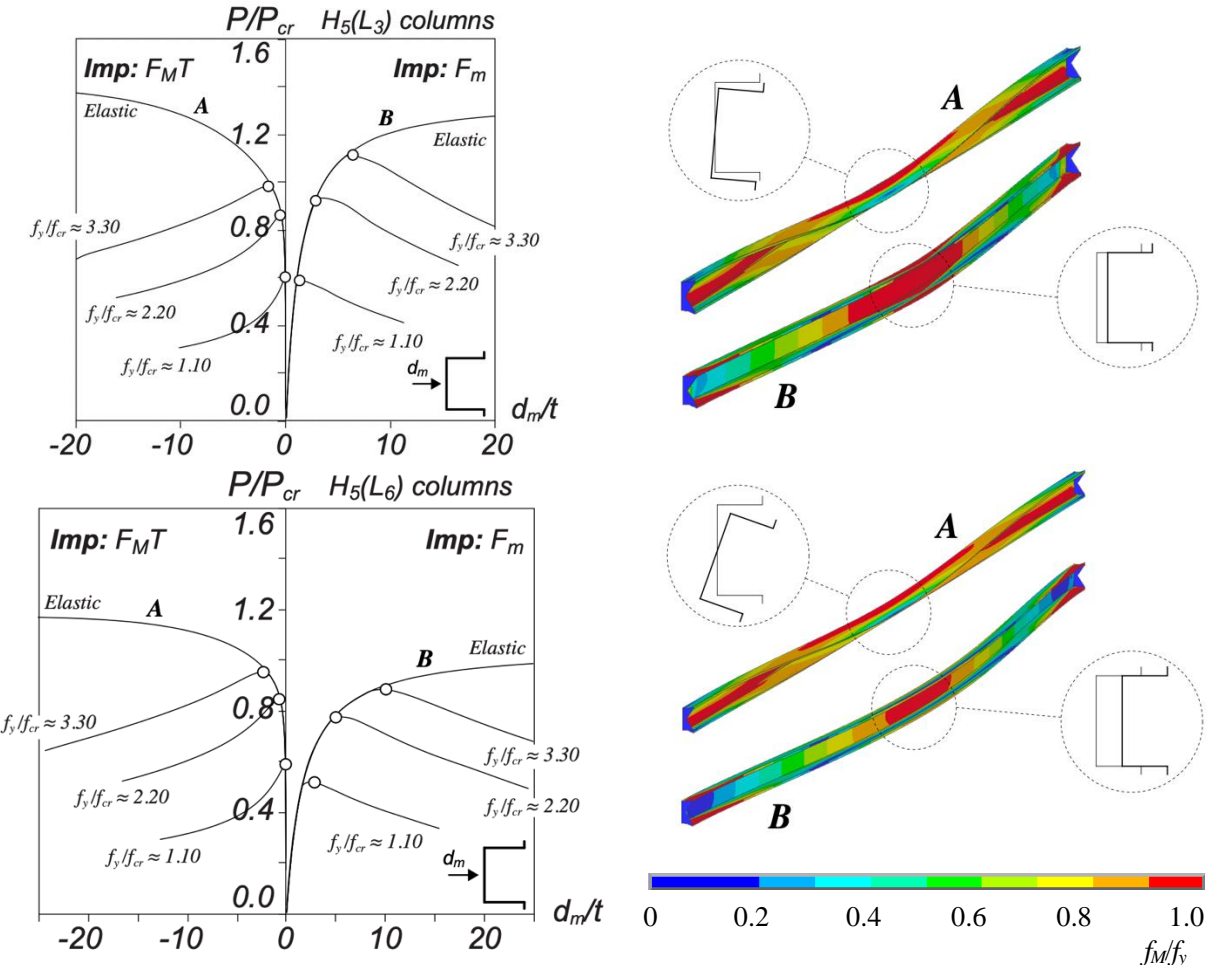


Figure 11: Elastic-plastic P/P_{cr} vs. d_m/t equilibrium paths and failure modes plus von Mises stresses at collapse (for $f_y/f_{cr,FT} \approx 2.2$) of H₅ columns with F_{MT} or F_m initial imperfections, lengths L_3 or L_6 and yield stresses such that $f_y/f_{cr,FT} \approx 1.1-2.2-3.3-\infty$

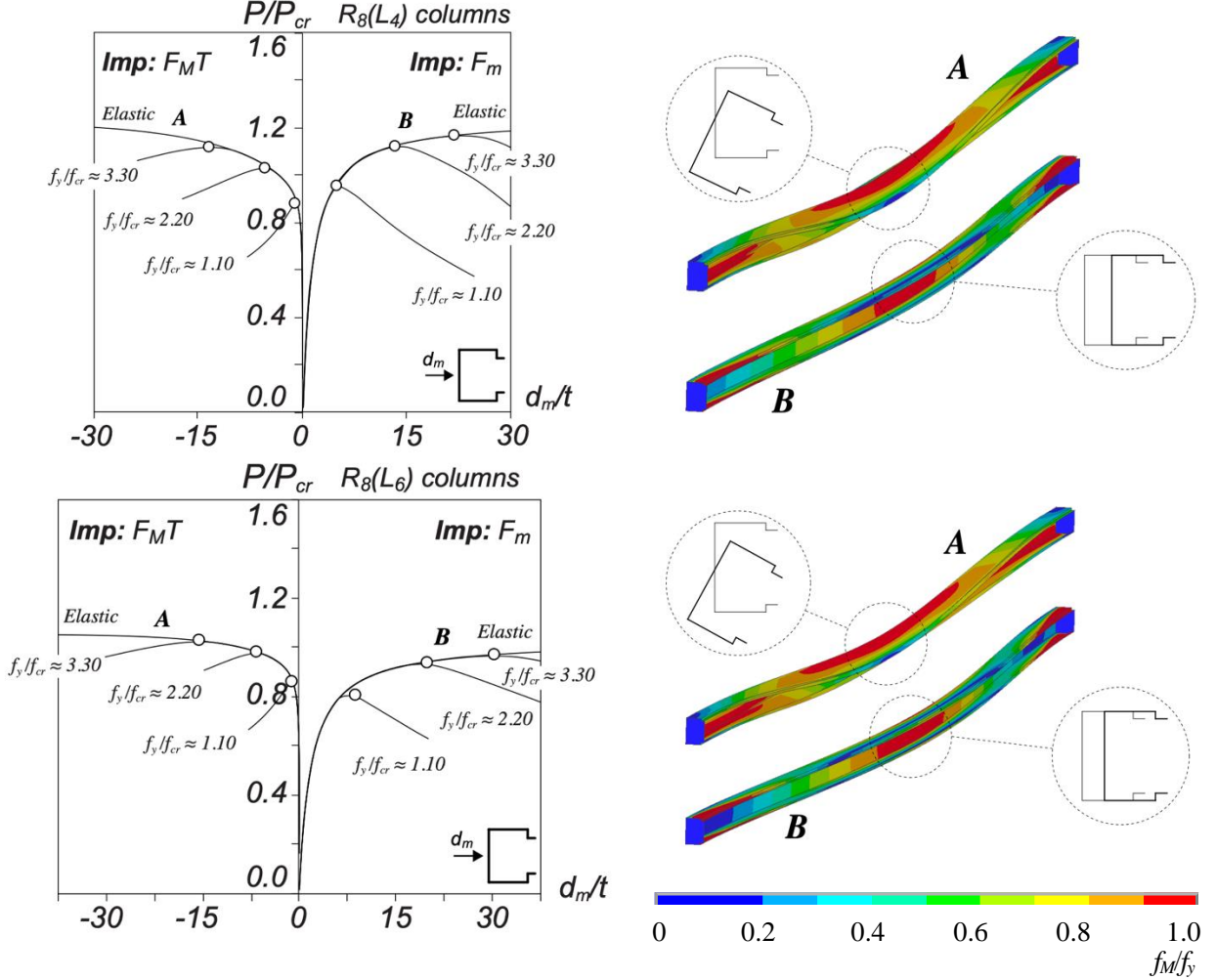


Figure 12: Elastic-plastic P/P_{cr} vs. d_m/t equilibrium paths and failure modes plus von Mises stresses at collapse (for $f_y/f_{cr,FT} \approx 2.2$) of R_8 columns with F_{MT} or F_m initial imperfections, lengths L_4 or L_6 and yield stresses such that $f_y/f_{cr,FT} \approx 1.1-2.2-3.3-\infty$

- (i) In the H_5-L_3 and H_5-L_4 columns, the failure loads obtained for F_{MT} initial imperfections are either a bit smaller ($f_y/f_{cr,FT} \approx 2.2; 3.3$) or practically identical ($f_y/f_{cr,FT} \approx 1.1$) to those obtained for F_m initial imperfections.
- (ii) In the L_6 columns, conversely, the failure loads obtained for F_m initial imperfections are always visibly smaller than those obtained for F_{MT} initial imperfections. Unlike in the H_5-L_3 and R_8-L_4 columns, the difference is highest for $f_y/f_{cr,FT} \approx 1.1$ and then decreases as the yield stress grows.

4. Failure Load Data for Columns Undergoing Global-Global Interaction

In order to be able to address the DSM-based design of fixed-ended CFS columns undergoing F_{MT} - F_m interaction, it is necessary to assemble fairly extensive failure load data involving columns affected by various levels of this coupling phenomenon. The failure loads obtained in this work concern columns with (i) the 48 geometries (combinations of b_w , b_f , b_l , b_s , t and L) for each of the five cross-section shapes considered ($H+R+RLC+WSC+WFSC$), all given in Table 2 and associated with critical F_{MT} buckling, and (iii) five yield stresses ($f_y = 150-300-450-600-750$ MPa), making it possible to cover wide critical slenderness ranges λ_{FT} . Although this equals a total of 1200 different columns, 2400 failure loads were

determined, as each column was analyzed with two initial geometrical imperfections: pure F_MT and pure F_m imperfections – naturally, only the lowest one is retained for design purposes. The whole failure load data gathered are presented, in tabular form, in Annex I: tables I.1 (H columns), I.2 (R columns), I.3 (RLC columns), I.4 (WSC columns) and I.5 (WFSC columns). These tables also provide several values related to the DSM-based prediction of the numerical F_MT failure loads, which are addressed in Section 5.

Figs. 13(a)-(g) shows plots P_u/P_y vs. λ_{FT} (P_u and $P_y = f_y \cdot A$ are the column failure and squash loads, respectively), for each cross-section shape considered in the current study, which include (i) the 475 numerical failure loads reported by Dinis *et al.* (2022) (235-U and 240-C columns – Figs. 13(a)-(b)) and (ii) the 2400 failure loads obtained in this work (Figs. 13(c)-(g) – see Table 2). The joint observation of these plots leads to the following comments:

- (i) Regardless of the cross-section shape, the P_u/P_y vs. λ_{FT} “clouds” follow the trends of quite similar “Winter-type” strength curves – in particular, note that there is no distinction between the “clouds”

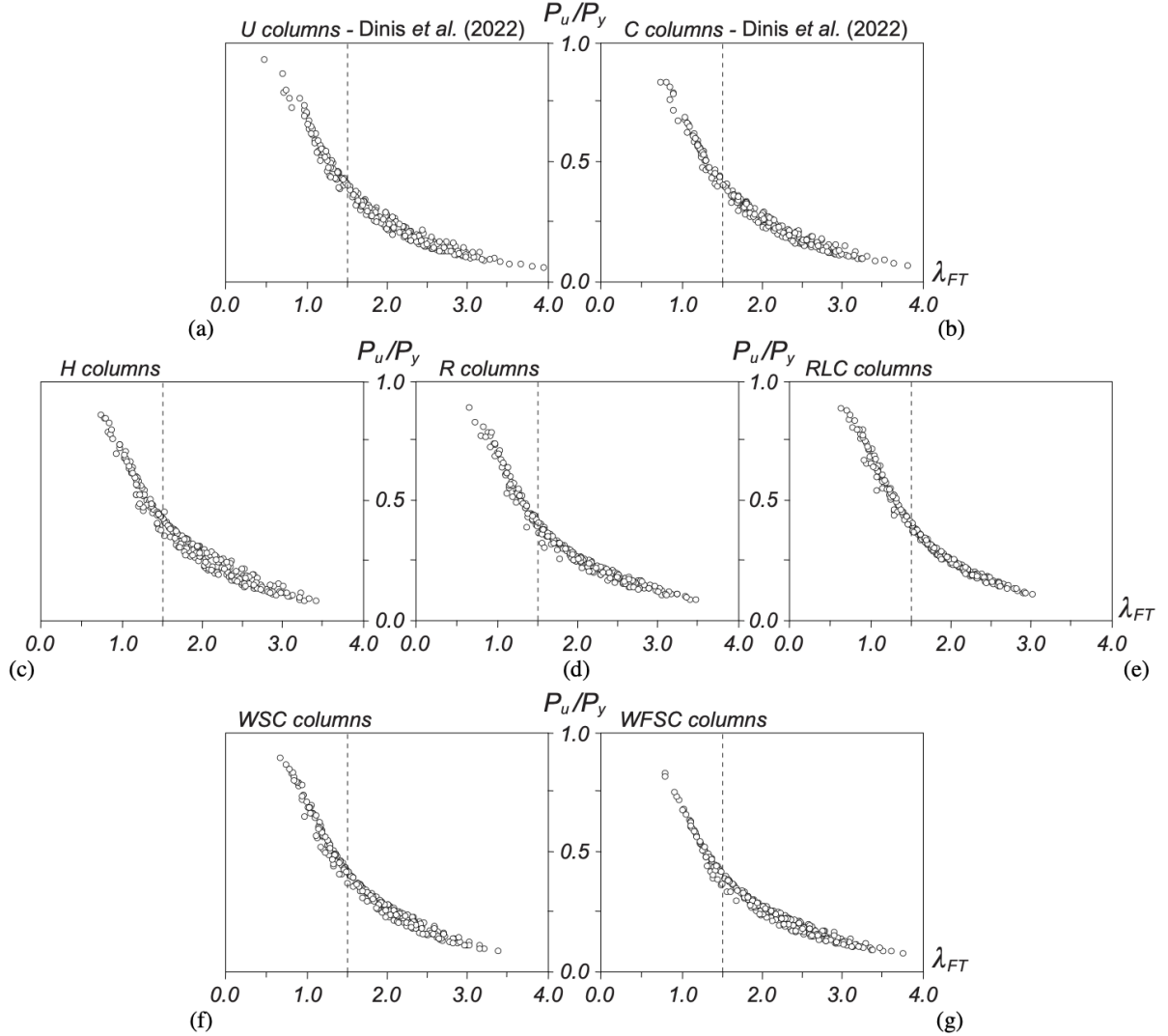


Figure 13: Plots P_u/P_y vs. λ_{FT} for the (a)-(b) U+C columns reported by Dinis *et al.* (2022) and (c)-(g) H+R+RLC+WSC+WFSC columns analyzed in this work

- (i₁) concerning the U and C columns, reported by Dinis *et al.* (2022), and (i₂) those concerning the columns with the remaining cross-section shapes, analyzed in this work.
- (ii) The content of the previous suggest is quite promising, in the sense that it suggests that the DSM-based design approach developed by Dinis *et al.* (2022) to handle F_{MT} and F_{MT}-F_m interactive failures of CFS fixed-ended U and C columns buckling in F_{MT} modes may also apply to similar CFS columns with other cross-section shapes, namely those analyzed considered in this work – if this is the case, it seems fair to argue that the above DSM-based design approach provides high-quality failure load predictions regardless of the fixed-ended columns cross-section shape. This issue is addressed in the next section.

5. DSM Design Considerations

The plots P_u/P_{nFT} vs. λ_{FT} shown in Figs. 14(a₁)-(a₇) plots concern the CFS fixed-ended (i) U+C columns analyzed by Dinis *et al.* (2022), and (ii) H+R+RLC+WSC+WFSC columns analyzed in this work – the latter set of P_u/P_{nFT} values are also provided, in tabular form, in Annex I. As for Figs. 14(b₁)-(b₇), they plot part of the above P_u/P_{nFT} values (those concerning columns with moderate and high slenderness – $\lambda_{FT} > 1.5$) against the buckling load ratio R_G (values obtained in this work also given in the tables of Annex I). All figures provide the associated P_u/P_{nFT} statistical indicators (averages, standard deviations and maximum/minimum values). The observation of the above plots and statistical indicators prompts the following remarks:

- (i) As it would now be fair to expect, the P_u/P_{nFT} plots and statistical indicators are qualitatively identical and quantitatively very similar for all the CFS fixed-ended column sets, which means that the contents of the items below apply to all of them.
- (ii) The P_{nFT} failure load estimates (see Eqs. (3)-(4)) are not capable of predicting adequately the failure loads of the CFS fixed-ended columns undergoing F_{MT}-F_m interaction. Indeed, the P_u/P_{nFT} averages (0.881 (C) to 0.961 (WSC)), standard deviations (0.123 (WSC) to 0.175 (H)) and minimum values (0.434 (H) to 0.604 (WSC)), combined with very large overestimation percentages (49.6% (C) to 67.5% (WFSC)), indicate a very poor failure load prediction quality. If only columns with $\lambda_{FT} > 1.5$ are considered (see Figs. 14(b₁)-(b₇)), this quality drops even lower: the above indicators become 0.829 (C) to 0.917 (WSC), 0.123 (WSC) to 0.183 (H), 0.434 (H) to 0.604 (WSC), and 63.5% (H) to 89.47% (R), respectively. It is also clear that the failure load overestimation grows with λ_{FT} .
- (iii) Naturally, Figs. 14(b₁)-(b₇) show that the amount of failure load overestimation is closely related to the R_G value – indeed, the overestimations are highest for $R_G \approx 1.0$, remain meaningful up to $R_G \approx 1.5$ and practically cease to occur for $R_G > 1.5$.

Since the plots concerning the columns analyzed in this work and in Dinis *et al.* (2022) are very similar, both qualitatively and quantitatively, it makes all the sense to begin by assessing whether the DSM-based design approach proposed by these authors, for U and C columns, also leads to efficient (safe, accurate and reliable) failure load predictions for H, R, RLC, WSC and WFSC columns buckling in F_{MT} modes and failing in F_{MT}-F_m interactive modes – recall that an overview of this design approach, cast in the form expressed by Eqs. (5)-(7), was presented in the introductory section of this paper.

In order to illustrate the failure load prediction quality achieved by Eqs. (5)-(7) for the columns analyzed in this work (the vast majority of which are affected by F_{MT}-F_m interaction), Figs. 15(a)-(f) and 16(a)-(f) (i) show plots P_u/P_y vs. λ_{FT} (recall that P_u is the lowest of $P_{u,FT}$ and $P_{u,Fm}$) for the RLC₆ columns ($\beta_{FT}=7.07$) with lengths L_I-L_6 ($R_G=1.49-1.42-1.34-1.26-1.19-1.05$) and (ii) WSC₃ columns ($\beta_{FT}=6.25$)

with lengths L_1-L_6 ($R_G=1.57-1.47-1.37-1.19-1.11-1.01$), respectively, and (ii) compare them with the corresponding DSM-based strength curves given by Eqs. (1), (2)-(4) and (5)-(7) (P_{nG} , P_{nFT} and P_{nFT-Fm} – solid red, dashed black and solid black lines, respectively) – note that one has always $P_{nG} \leq P_{nFT-Fm} \leq P_{nFT}$

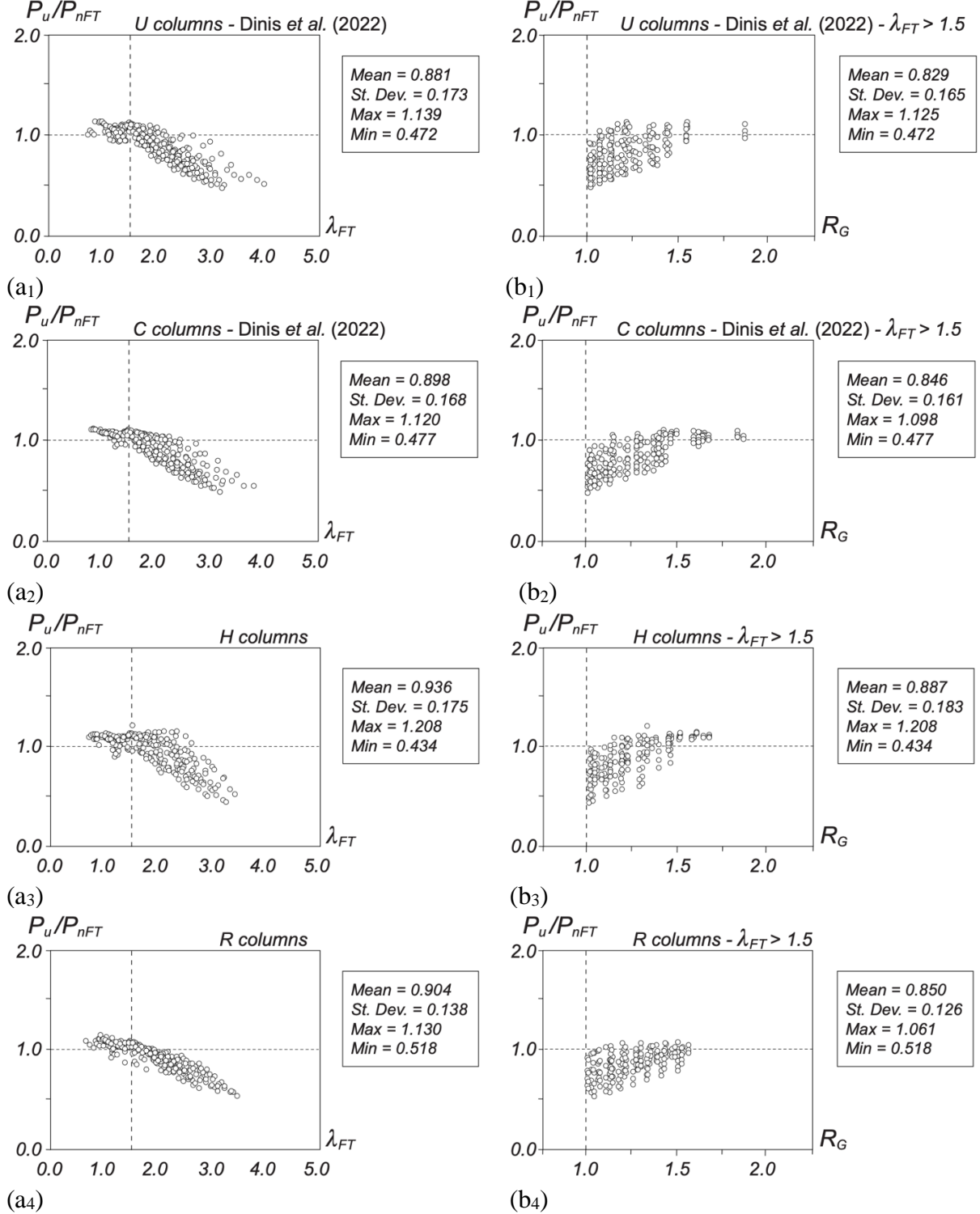


Figure 14 (to be continued): (a) P_u/P_{nFT} vs. λ_{FT} for the U, C, H, R, RLC, WSC and WFSC columns considered in this study, and (b) P_u/P_{nFT} vs. R_G plots for the columns with $\lambda_{FT}>1.5$

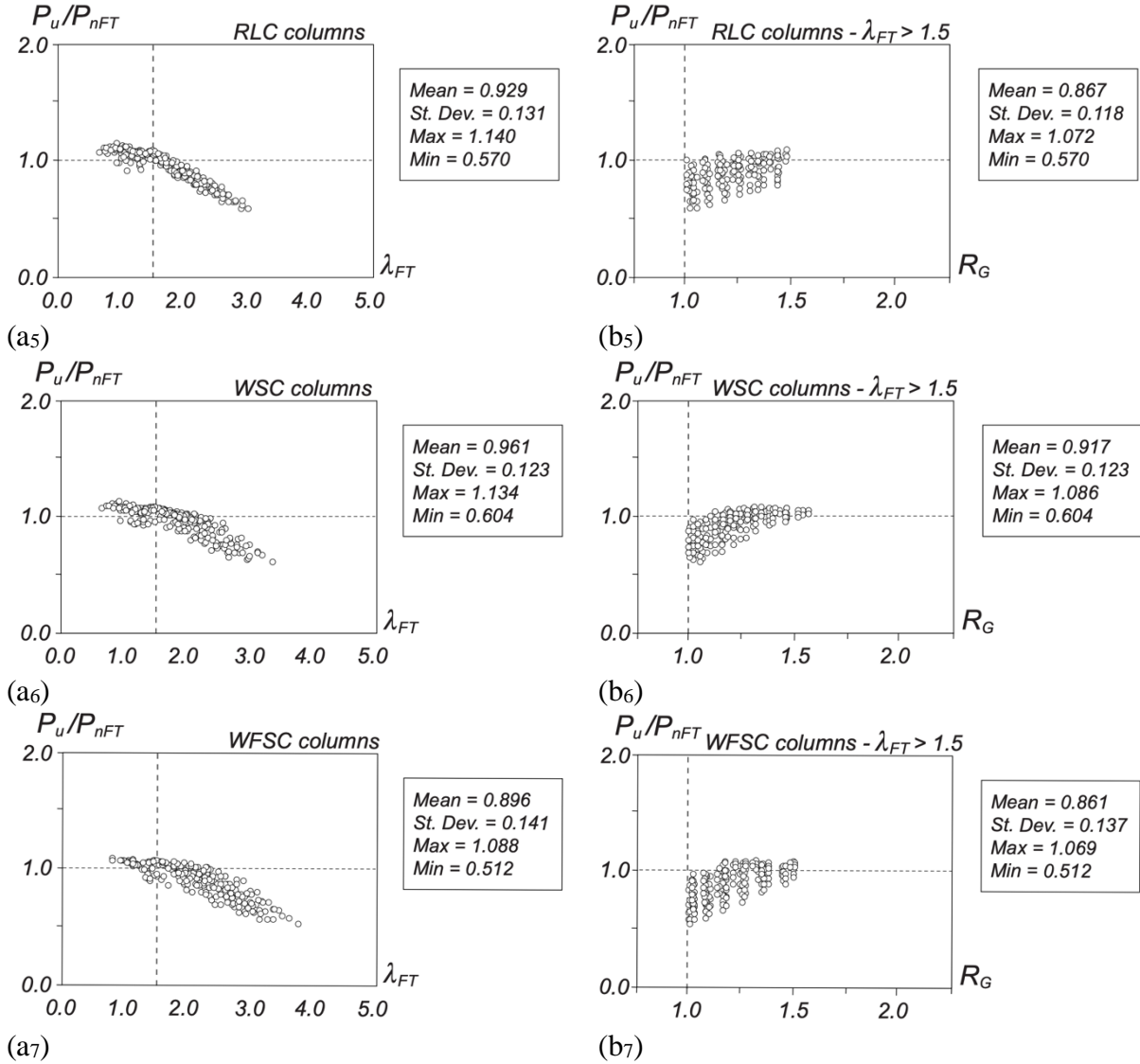


Figure 14 (continuation): (a) P_u/P_{nFT} vs. λ_{FT} for the U, C, H, R, RLC, WSC and WFSC columns considered in this study, and (b) P_u/P_{nFT} vs. R_G plots for the columns with $\lambda_{FT} > 1.5$

and that two consecutive curves may be practically coincident. It is clear that all P_u/P_y values are very well predicted by the P_{nFT-Fm}/P_y strength curves – indeed, they always provide quite accurate failure load underestimations, regardless of the R_G value (*i.e.*, F_MT-F_m interaction level). On the other hand, those same P_u/P_y values are consistently and progressively more (i) overestimated by the P_{nFT}/P_y strength curves as R_G approaches 1.0, and (ii) underestimated by the P_{nG}/P_y strength curve as R_G moves away from 1.0.

Tables I.1 to I.5, included in Annex I, provide the whole set of numerical failure-to-predicted failure load ratios P_u/P_{nG} , P_u/P_{nFT} and P_u/P_{nFT-Fm} concerning the CFS fixed-ended H, R, RLC, WSC and WFSC columns analyzed in this work, as well as the values of the relevant quantities involved in their calculation, namely the column buckling load ratios R_G . To assess the performance and merits of the proposed DSM-based design approach (Eqs. (5)-(7)), Figs. 17(a₁)-(a₇) show plots P_u/P_{nFT-Fm} vs. λ_{FT} for all CFS fixed-ended columns considered in this study, the overwhelming majority of which experience F_MT-F_m interaction – recall that the U and C column plots were reported earlier by Dinis *et al.* (2022). As for Figs. 17(b₁)-(b₇),

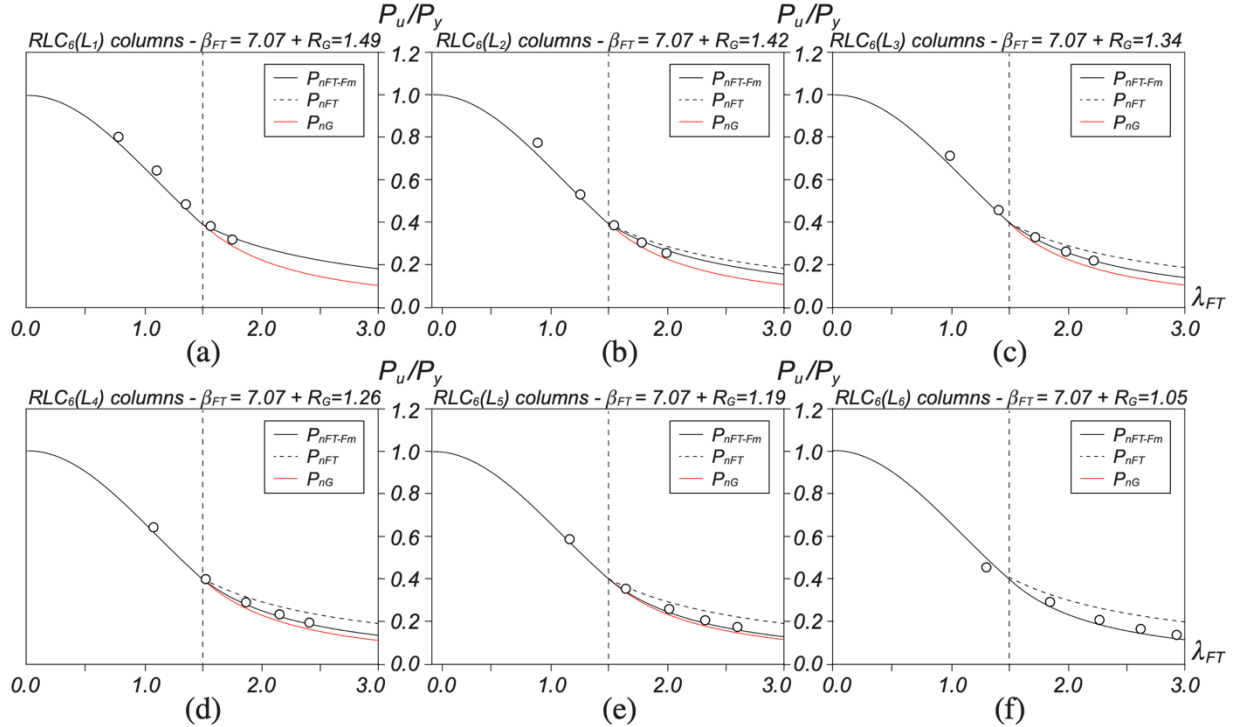


Figure 15: Comparison between the proposed (P_{nFT-Fm}/P_y) and existing (P_{nFT}/P_y and P_{nG}/P_y) DSM-based design curves and the P_u/P_y values of the RLC_6 columns with (a) L_1 , (b) L_2 , (c) L_3 , (d) L_4 , (e) L_5 and (f) L_6 lengths

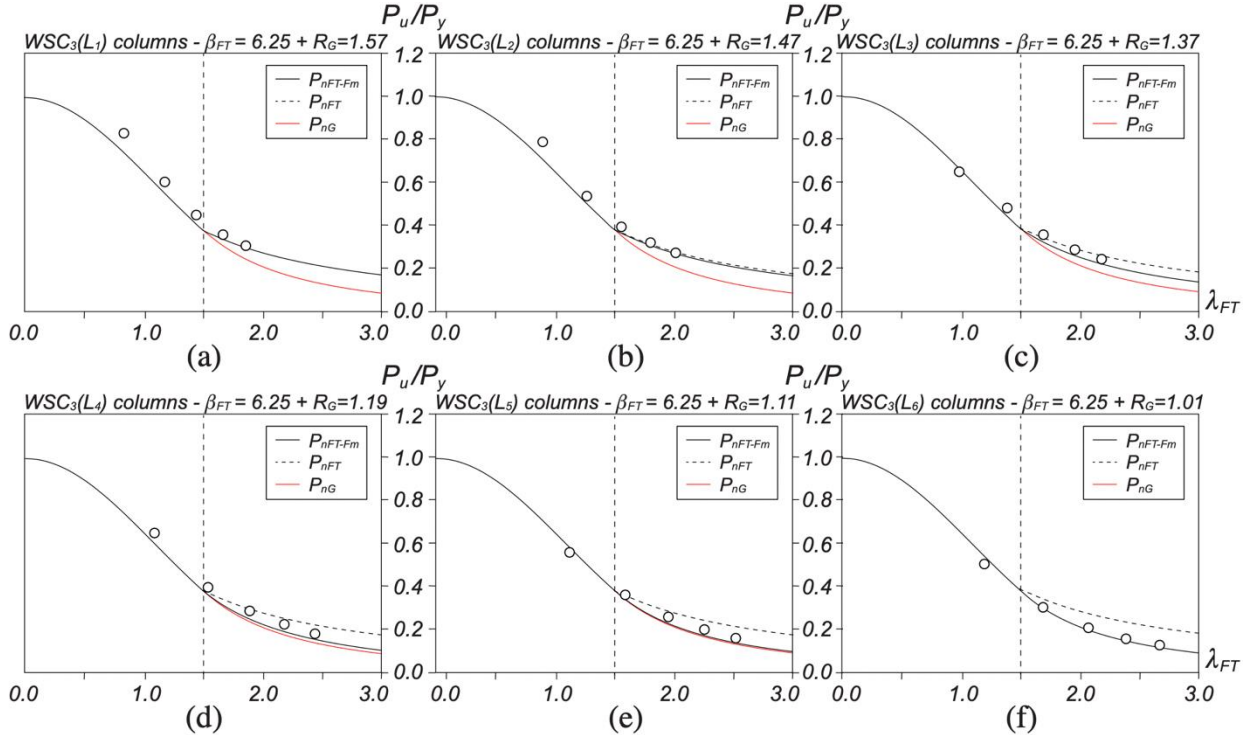


Figure 16: Comparison between the proposed (P_{nFT-Fm}/P_y) and existing (P_{nFT}/P_y and P_{nG}/P_y) DSM-based design curves and the P_u/P_y values of the WSC_3 columns with (a) L_1 , (b) L_2 , (c) L_3 , (d) L_4 , (e) L_5 and (f) L_6 lengths

they display similar plots (P_u/P_{nFT-Fm} vs. λ_{FT}) for the failure loads of the CFS fixed-ended columns analyzed by Dinis *et al.* (2019, 2020b), all failing in pure F_MT modes (the vast majority of their R_G values are much higher than $1.0 - R_G \geq 1.5$). All the above figures display also the associated P_u/P_{nFT-Fm}

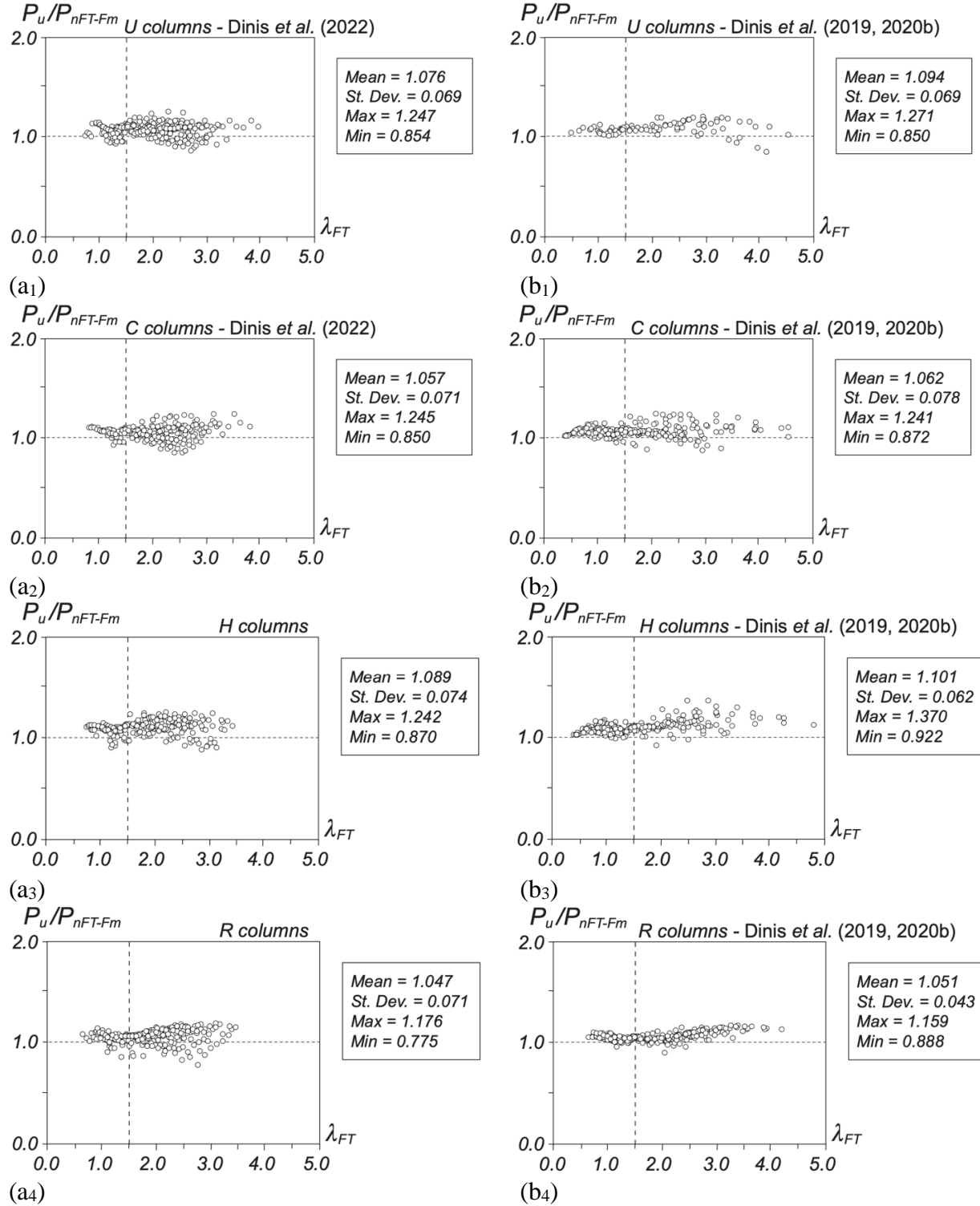


Figure 17 (to be continued): Plots P_u/P_{nFT-Fm} vs. λ_{FT} for the columns with a given cross-section shape (a) considered in this study (including those analyzed by Dinis *et al.* 2022) and (b) analyzed by Dinis *et al.* (2019, 2020b) (exhibiting no F_MT-F_m interaction)

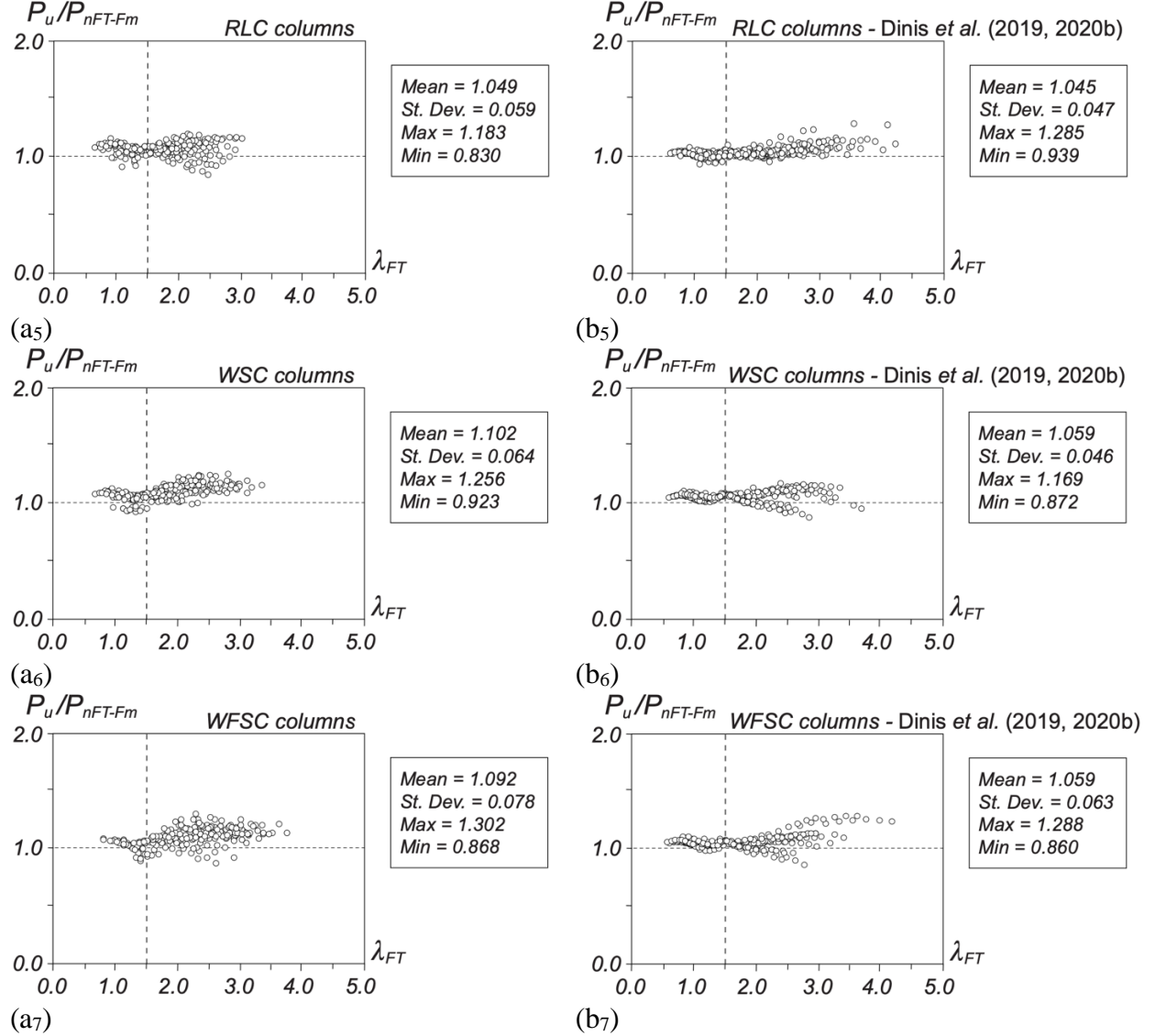


Figure 17 (continuation): Plots P_u/P_{nFT-Fm} vs. λ_{FT} for the columns with a given cross-section shape (a) considered in this study (including those analyzed by Dinis *et al.* 2022) and (b) analyzed by Dinis *et al.* (2019, 2020b) (exhibiting no $F_{MT}-F_m$ interaction)

statistical indicators (averages, standard deviations and maximum/minimum values). The comparisons within each pair of figures (same cross-section shape) and between the seven pairs of figures (different cross-section shapes) reveals a remarkable similarity between the P_u/P_{nFT-Fm} distributions, which is quantitatively attested by the closeness between the corresponding statistical indicators. Therefore, it can be concluded that the DSM-based design curve set defined by Eqs. (5)-(7) yields equally safe and accurate failure load estimates for CFS fixed-ended columns buckling in F_{MT} modes regardless of (i) their cross-section shape and (ii) whether they fail in pure F_{MT} modes or $F_{MT}-F_m$ interactive ones – its performance and merits will be assessed in the next section.

Finally, in order to provide a visualization of the benefits of replacing the currently codified design curve (P_{nG}) with the proposed strength curve set (P_{nFT-Fm}), Figs. 18(a₁)-(b₂) show the P_u/P_{nG} vs. λ_{FT} ($=\lambda_G$) and P_u/P_{nFT-Fm} vs. λ_{FT} plots of all the CFS columns analyzed (i) in the current study (including those reported by Dinis *et al.* 2022), and (ii) by Dinis *et al.* (2019, 2020b). As expected, Figs. 18(a₁)-(a₂) show that the

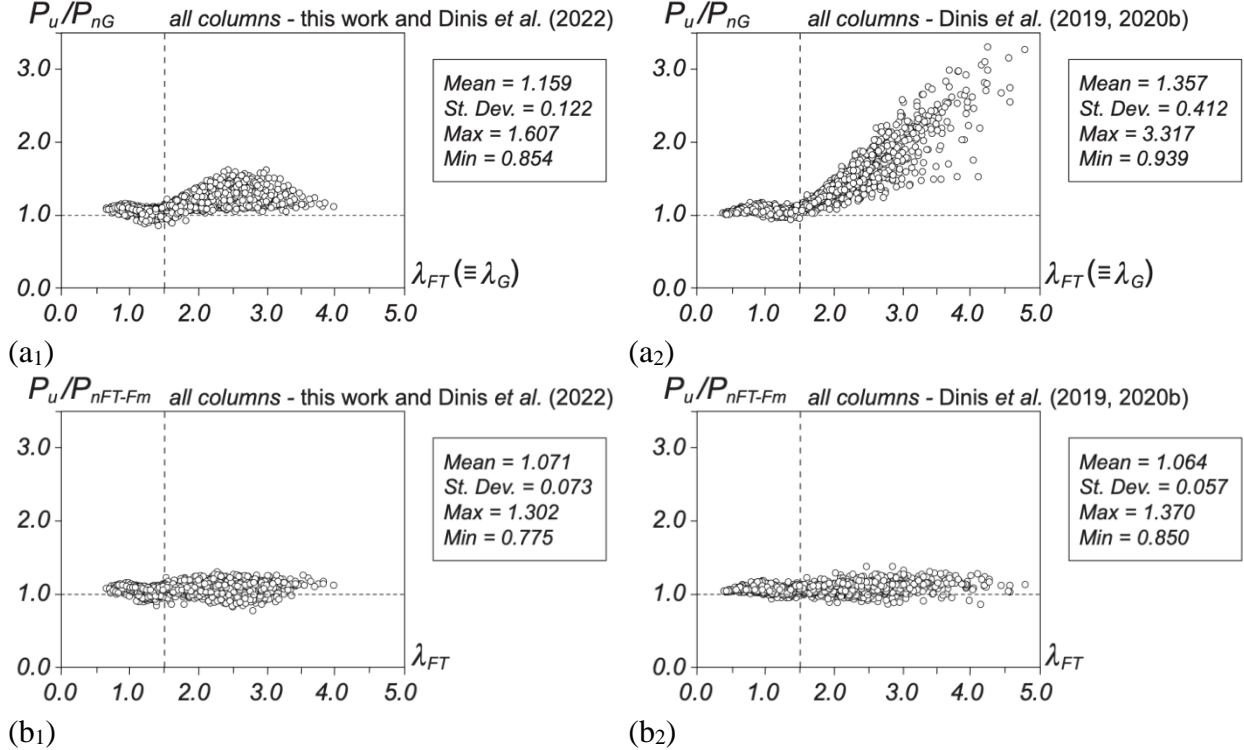


Figure 18: Plots (a) P_u/P_{nG} and (b) P_u/P_{nFT-Fm} vs. λ_{FT} for the U, C, H, R, RLC, WSC and WFSC columns analyzed (1) in the current study (including those reported by Dinis *et al.* 2022) and (2) by Dinis *et al.* (2019, 2020b)

improvement of the failure load prediction quality, between the P_{nFT-Fm} and P_{nG} values, is substantially higher more for the latter (almost all columns not affected by F_MT-F_m interaction, *i.e.*, failing in pure F_MT modes) than for the former (almost all columns affected by F_MT-F_m interaction, *i.e.*, failing mostly in F_MT-F_m interactive modes, even if some pure F_MT failures also occur). Nonetheless, the improvement in failure load prediction quality is visible also for the columns affected by F_MT-F_m interaction, as attested by the fact that (i) the P_u/P_{nG} and P_u/P_{nFT-Fm} averages equal 1.159 and 1.071, respectively, (ii) the P_u/P_{nFT-Fm} values are much closer to 1.0 than their P_u/P_{nG} counterparts (for $\lambda_{FT}>1.5$, of course). Thus, it can be concluded that the proposed design curves (P_{nFT-Fm}), which are able to handle columns with any R_G value, lead to more economical designs than the codified one (P_{nG}) – naturally, the amount of economy decreases as (i) β_{FT} increases, indicating a lower FT post-critical strength (Dinis *et al.* 2020b), and (ii) R_G approaches 1.0, indicating a higher F_MT-F_m interaction. It is worth noting that the failure loads of all the column with $\lambda_{FT}>1.5$ are overestimated by their current (P_{nG}) predictions.

5.1 Merit and Reliability Assessment

Tables 3 to 5 provides, for all the CFS fixed-ended columns analyzed in this work and in previous studies (Dinis *et al.* 2019, 2020a, 2022) – all buckling in F_MT modes and failing in either pure F_MT or F_MT-F_m interactive modes –, the failure load numbers (n) and P_u/P_{nG} , P_u/P_{nFT} and P_u/P_{nFT-Fm} statistical indicators, making a distinction between the columns with $\lambda_{FT}\leq 1.5$ (those whose failure loads are estimated by the currently codified DSM global design curve – Eq. (1)) and with $\lambda_{FT}>1.5$ (those whose failure loads are predicted by the proposed DSM-based design approach – Eqs. (5)-(7)). The observation of the values presented in these tables prompts the following remarks:

Table 3: P_u/P_{nFT-Fm} , P_u/P_{nFT} and P_u/P_{nFT-Fm} statistical indicators concerning the CFS fixed-ended columns reported by Dinis *et al.* (2019, 2020b) – almost all columns failing in pure F_MT modes

CFS		U		C		H		R		RLC		WSC		WFSC		All Columns	
λ_{FT}		≤ 1.5	> 1.5	≤ 1.5	> 1.5												
n		29	61	128	142	134	136	96	174	96	174	108	162	107	163	624	1411
P_u/P_{nG}	Avr	1.064	1.850	1.056	1.553	1.073	1.644	1.036	1.490	1.024	1.436	1.054	1.510	1.046	1.537	1.051	1.543
	SD	0.029	0.547	0.037	0.423	0.037	0.503	0.025	0.362	0.027	0.356	0.019	0.312	0.024	0.378	0.033	0.411
	Max	1.125	3.146	1.146	2.752	1.172	3.317	1.092	2.814	1.086	2.791	1.105	2.279	1.108	2.700	1.172	3.317
	Min	1.017	1.116	0.952	1.027	0.991	1.071	0.953	1.039	0.939	1.022	1.010	1.081	0.982	1.067	0.939	1.022
P_u/P_{nFT}	Avr	1.064	1.073	1.056	1.050	1.073	1.112	1.036	1.062	1.024	1.043	1.054	1.060	1.046	1.067	1.051	1.065
	SD	0.029	0.091	0.037	0.067	0.037	0.063	0.025	0.048	0.027	0.041	0.019	0.059	0.024	0.078	0.033	0.066
	Max	1.125	1.202	1.146	1.236	1.172	1.306	1.092	1.159	1.086	1.149	1.105	1.157	1.108	1.288	1.172	1.306
	Min	1.017	0.792	0.952	0.807	0.991	0.904	0.953	0.888	0.939	0.965	1.010	0.872	0.982	0.860	0.939	0.792
P_u/P_{nFT-Fm}	Avr	1.064	1.101	1.056	1.067	1.073	1.128	1.036	1.059	1.024	1.057	1.054	1.063	1.046	1.110	1.051	1.073
	SD	0.029	0.071	0.037	0.071	0.037	0.069	0.025	0.048	0.027	0.052	0.019	0.057	0.024	0.075	0.033	0.067
	Max	1.125	1.202	1.146	1.241	1.172	1.370	1.092	1.159	1.086	1.285	1.105	1.169	1.108	1.302	1.172	1.370
	Min	1.017	0.850	0.952	0.872	0.991	0.922	0.953	0.888	0.939	0.965	1.010	0.872	0.982	0.868	0.939	0.850

Table 4: P_u/P_{nFT-Fm} , P_u/P_{nFT} and P_u/P_{nFT-Fm} statistical indicators concerning the CFS fixed-ended columns analyzed in this work and reported by Dinis *et al.* (2022) – almost all columns undergoing F_MT-F_m interaction

CFS		U		C		H		R		RLC		WSC		WFSC		All Columns	
λ_{FT}		≤ 1.5	> 1.5	≤ 1.5	> 1.5												
n		56	179	59	181	70	170	69	171	83	157	78	162	52	188	624	1411
P_u/P_{nG}	Avr	1.046	1.203	1.057	1.217	1.057	1.235	1.036	1.198	1.046	1.144	1.054	1.194	1.024	1.217	1.047	1.202
	SD	0.055	0.118	0.042	0.112	0.056	0.139	0.047	0.111	0.045	0.062	0.049	0.096	0.045	0.117	0.050	0.113
	Max	1.139	1.607	1.120	1.542	1.128	1.602	1.130	1.446	1.140	1.294	1.134	1.460	1.088	1.565	1.140	1.607
	Min	0.933	1.010	0.933	0.986	0.888	0.961	0.854	0.879	0.898	1.011	0.923	0.955	0.892	0.929	0.854	0.879
P_u/P_{nFT}	Avr	1.046	0.829	1.057	0.846	1.057	0.887	1.036	0.850	1.046	0.867	1.054	0.917	1.024	0.861	1.047	0.864
	SD	0.055	0.165	0.042	0.161	0.056	0.183	0.047	0.126	0.045	0.118	0.049	0.123	0.045	0.137	0.050	0.149
	Max	1.139	1.125	1.120	1.098	1.128	1.208	1.130	1.061	1.140	1.072	1.134	1.086	1.088	1.069	1.140	1.208
	Min	0.933	0.472	0.933	0.477	0.888	0.434	0.854	0.518	0.898	0.570	0.923	0.604	0.892	0.512	0.854	0.434
P_u/P_{nFT-Fm}	Avr	1.046	1.065	1.057	1.057	1.057	1.104	1.036	1.052	1.046	1.050	1.054	1.125	1.024	1.110	1.047	1.081
	SD	0.055	0.072	0.042	0.079	0.056	0.075	0.047	0.078	0.045	0.066	0.049	0.058	0.045	0.075	0.050	0.078
	Max	1.139	1.247	1.120	1.245	1.128	1.242	1.130	1.176	1.140	1.183	1.134	1.256	1.088	1.302	1.140	1.302
	Min	0.933	0.854	0.933	0.850	0.888	0.870	0.854	0.775	0.898	0.830	0.923	0.954	0.892	0.868	0.854	0.775

- (i) First of all, it should be emphasized again that the P_{nFT} and P_{nFT-Fm} values only differ from the P_{nG} ones for columns with $\lambda_{FT} > 1.5$ and, therefore, the differences between the three DSM-based design approaches are restricted to such columns – they are addressed in the next items. Concerning the columns with $\lambda_{FT} \leq 1.5$, the failure load prediction quality provided by the P_{nG} values is very good, as attested by the corresponding P_u/P_{nG} statistical indicators (naturally, very similar): 1.051-0.033-1.172-0.939 (Table 3), 1.047-0.050-1.140-0.854 (Table 4) and 1.049-0.041-1.172-0.854 (Table 5).

Table 5: P_u/P_{nFT-Fm} , P_u/P_{nFT} and P_u/P_{nFT-Fm} statistical indicators concerning the CFS fixed-ended columns analyzed in this work and reported by Dinis *et al.* (2019, 2020a, 2022) – columns failing in either pure F_MT or F_MT-F_m interactive modes

CFS		U		C		H		R		RLC		WSC		WFSC		All Columns	
λ_{FT}		≤ 1.5		> 1.5		≤ 1.5		> 1.5		≤ 1.5		> 1.5		≤ 1.5		> 1.5	
n		85	240	187	323	204	306	165	345	179	331	186	324	159	351	1165	2220
P_u/P_{nG}	Avr	1.052	1.368	1.056	1.365	1.068	1.417	1.036	1.345	1.034	1.298	1.054	1.352	1.039	1.366	1.049	1.358
	SD	0.048	0.395	0.038	0.336	0.045	0.405	0.036	0.305	0.038	0.299	0.035	0.280	0.034	0.315	0.041	0.336
	Max	1.139	3.146	1.146	2.752	1.172	3.317	1.130	2.814	1.140	2.791	1.134	2.279	1.108	2.700	1.172	3.317
	Min	0.933	1.010	0.933	0.986	0.888	0.961	0.854	0.879	0.898	1.011	0.923	0.955	0.892	0.929	0.854	0.879
P_u/P_{nFT}	Avr	1.052	0.891	1.056	0.936	1.068	0.994	1.036	0.955	1.034	0.967	1.054	0.989	1.039	0.957	1.049	0.958
	SD	0.048	0.184	0.038	0.164	0.045	0.187	0.036	0.142	0.038	0.131	0.035	0.120	0.034	0.153	0.041	0.157
	Max	1.139	1.202	1.146	1.236	1.172	1.370	1.130	1.159	1.140	1.285	1.134	1.157	1.108	1.288	1.172	1.370
	Min	0.933	0.472	0.933	0.477	0.888	0.434	0.854	0.518	0.898	0.570	0.923	0.604	0.892	0.512	0.854	0.434
P_u/P_{nFT-Fm}	Avr	1.052	1.074	1.056	1.062	1.068	1.114	1.036	1.055	1.034	1.054	1.054	1.094	1.039	1.090	1.049	1.077
	SD	0.048	0.073	0.038	0.075	0.045	0.074	0.036	0.065	0.038	0.059	0.035	0.065	0.034	0.079	0.041	0.073
	Max	1.139	1.247	1.146	1.245	1.172	1.370	1.130	1.176	1.140	1.285	1.134	1.256	1.108	1.302	1.172	1.370
	Min	0.933	0.850	0.933	0.850	0.888	0.870	0.854	0.775	0.898	0.830	0.923	0.872	0.892	0.860	0.854	0.775

- (ii) The P_{nG} values clearly underestimate all the failure loads of the columns with $\lambda_{FT}>1.5$, as attested by the P_u/P_{nG} statistical indicators: 1.543-0.411-3.317-1.022 (columns rarely affected by F_MT-F_m interaction – see Table 3) and 1.202-0.113-1.607-0.879 (columns rarely unaffected by F_MT-F_m interaction – see Table 4). Naturally, the underestimation is much higher in the former case, since it has been shown that the presence of F_MT-F_m interaction may cause significant failure load erosion.
- (iii) The P_{nFT} values provide high-quality failure estimates for the columns with $\lambda_{FT}>1.5$ analyzed by Dinis *et al.* (2019, 2020b), which are rarely affected by F_MT-F_m interaction – the corresponding P_u/P_{nFT} statistical indicators are 1.065-0.066-1.306-0.792 (see Table 3). However, the same is not true for the columns with $\lambda_{FT}>1.5$ analyzed in this work and by Dinis *et al.* (2022), which are rarely unaffected by F_MT-F_m interaction – there is a very clear failure load underestimation, as attested by the corresponding P_u/P_{nFT} statistical indicators are 0.864-0.149-1.208-0.434 (see Table 4).
- (iv) The P_{nFT-Fm} values provide equally high-quality failure estimates for the columns with $\lambda_{FT}>1.5$ that are unaffected or affected by F_MT-F_m interaction – indeed, the P_u/P_{nFT-Fm} statistical indicators concerning the columns analyzed (iv₁) by Dinis *et al.* (2019, 2020b) and (iv₂) in this work and by Dinis *et al.* (2022) read 1.073-0.067-1.370-0.850 (see Table 3) and 1.081-0.078-1.302-0.775 (see Table 4), respectively. Naturally, similar P_u/P_{nFT-Fm} statistical indicators are obtained when the two sets of columns with $\lambda_{FT}>1.5$ are considered together: 1.077-0.073-1.370-0.775 (see Table 5).
- (v) Regardless of the β_{FT} and R_G combination, the P_{nFT-Fm} values provide high-quality failure load predictions for both the columns with $\lambda_{FT}\leq 1.5$ (P_u/P_{nFT-Fm} statistical indicators equal to 1.049-0.041-1.172-0.854) and with $\lambda_{FT}>1.5$ (P_u/P_{nFT-Fm} statistical indicators equal to 1.077-0.073-1.370-0.775). Fig. 19 plots P_u/P_{nFT-Fm} vs. λ_{FT} for the whole set of columns considered (all slenderness values) and indicates the corresponding P_u/P_{nFT-Fm} statistical indicators: 1.068-0.065-1.370-0.775.
- (vi) The contents of the previous items are qualitatively identical and quantitatively very similar for the columns with the seven cross-section shapes considered in this study, which provides very strong evidence that the findings reported in this work do not depend on the column cross-section shape.

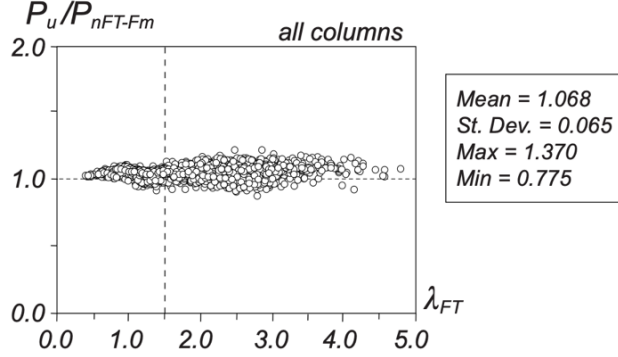


Figure 19: Plot P_u/P_{nFT-Fm} vs. λ_{FT} for all the whole set of columns analyzed in this work and by Dinis *et al.* (2019, 2020b, 2022)

(vii) The content of the previous item makes it possible to conclude that the DSM-based design approach developed and proposed by Dinis *et al.* (2022), in the context of CFS fixed-ended U and C columns, in this work, which is expressed by Eqs. (5)-(7), provides a high estimation quality for the numerical failure loads of CFS fixed-ended columns buckling in F_MT modes and failing in either pure F_MT or F_MT-F_m interactive modes, regardless of their cross-section shape.

Next, the reliability of the failure load predictions provided by the proposed DSM-based design approach is assessed, through the determination of the LRFD (Load and Resistance Factor Design) resistance factors ϕ associated with the numerical failure loads obtained for the CFS fixed-ended columns analyzed in this work and by Dinis *et al.* (2019, 2020a, 2022). In particular, it is intended to check whether values equal or higher than $\phi=0.85$ are achieved – this is the value recommended by the current North American Specification (AISI 2020) for compression members. According to this specification (Chapter K – Section K2.1.1), ϕ can be determined using the expression

$$\phi = C_\phi (M_m F_m P_m) e^{-\beta_0 \sqrt{V_M^2 + V_F^2 + C_P V_P^2 + V_Q^2}} \quad \text{with} \quad C_P = \left(1 + \frac{1}{n}\right) \frac{m}{m-2} \quad , \quad (8)$$

where (i) C_ϕ is a calibration coefficient ($C_\phi=1.52$ for LRFD), (ii) $M_m=1.10$ and $F_m=1.00$ are the mean values of the material and fabrication factors, respectively, (iii) β_0 is the target reliability index ($\beta_0=2.5$ for structural members in LRFD), (iv) $V_M=0.10$, $V_F=0.05$ and $V_Q=0.21$ are the coefficients of variation of the material factor, fabrication factor and load effect, respectively, (v) C_P is a correction factor depending on the numbers of tests (n) and degrees of freedom ($m=n-1$), and (vi) P_m and V_P are the mean and coefficient of variation of the “exact”-to-predicted failure load ratios P_u/P_{nFT-Fm} .

Table 6 to 8 show the n , C_P , P_m , V_P and ϕ values obtained from the P_u/P_{nFT-Fm} values concerning the numerical failure loads obtained in this investigation, namely from the (i) columns analyzed by Dinis *et al.* (2019, 2020b), almost all unaffected by F_MT-F_m interaction (*i.e.*, exhibiting pure F_MT failures), (ii) columns analyzed in this work and by Dinis *et al.* (2022), almost all affected by F_MT-F_m interaction (*i.e.*, exhibiting pure F_MT or F_MT-F_m interactive failures), and (iii) the whole set of columns. From the observation of the ϕ values presented in these table, it can be concluded that:

- (i) The ϕ values obtained from the P_{nFT-Fm} failure load estimates concerning all columns belonging to each of the two first sets are very similar (0.965 vs. 0.961 – see Tables 6 and 7). Moreover, the ϕ values concerning the columns with the same cross-section shape, in each set, are not far apart (0.952-0.994 vs. 0.941-0.995 – see Tables 6 and 7). Note that all these values are well above the value prescribed by AISI (2020) for compression members ($\phi=0.85$).

Table 6: LRFD ϕ values obtained from the P_{nFT-Fm} column failure load predictions reported by Dinis *et al.* (2019, 2020b)

Columns	U	C	H	R	RLC	WSC	$WFSC$	All
n	90	270	270	270	270	279	270	1710
m	89	269	269	269	269	269	269	1709
C_P	1.034	1.011	1.011	1.011	1.011	1.011	1.011	1.002
P_m	1.089	1.062	1.101	1.052	1.045	1.059	1.059	1.064
V_P	0.063	0.059	0.063	0.044	0.049	0.041	0.065	0.057
ϕ	0.984	0.962	0.994	0.960	0.952	0.969	0.955	0.965

Table 7: LRFD ϕ values obtained from the P_{nFT-Fm} column failure load predictions reported in this work and by Dinis *et al.* (2022)

Columns	U	C	H	R	RLC	WSC	$WFSC$	All
n	235	240	240	240	240	240	240	1675
m	234	239	239	239	239	239	239	2034
C_P	1.013	1.013	1.013	1.013	1.013	1.013	1.013	1.002
P_m	1.061	1.057	1.089	1.047	1.049	1.102	1.092	1.071
V_P	0.069	0.071	0.074	0.071	0.059	0.064	0.078	0.073
ϕ	0.955	0.950	0.977	0.941	0.950	0.995	0.976	0.961

Table 8: LRFD ϕ values obtained from all P_{nFT-Fm} column failure load predictions (this work and Dinis *et al.* 2019, 2020b, 2022)

Columns	U	C	H	R	RLC	WSC	$WFSC$	All
n	325	510	510	510	510	510	510	3385
m	324	509	509	509	509	509	509	3384
C_P	1.009	1.006	1.006	1.006	1.006	1.006	1.006	1.001
P_m	1.068	1.060	1.095	1.049	1.047	1.079	1.074	1.068
V_P	0.068	0.064	0.068	0.058	0.053	0.059	0.072	0.065
ϕ	0.962	0.957	0.987	0.951	0.951	0.977	0.965	0.963

- (ii) Naturally, the ϕ values obtained from the P_{nFT-Fm} estimates concerning the whole set of columns are comprised between the previous pairs. For all the columns, $\phi=0.963$ is obtained (see Table 8).
- (iii) In view of the content of the previous two items, it can be concluded that the proposed DSM-based design approach provides very reliable failure load predictions for CFS fixed-ended columns buckling in F_MT modes and failing in either pure F_MT or F_MT-F_m interactive modes, regardless of their cross-section shape.

6. Concluding Remarks

This work reported the available numerical results of an ongoing investigation dealing with the post-buckling behavior, strength and DSM design of cold-formed steel columns buckling in major-axis

flexural-torsional (F_{MT}) modes and experiencing global-global (G-G) interaction or, to be more precise, interaction between major-axis flexural/torsional and minor-axis flexural buckling ($F_{MT}-F_m$ interaction) – the results presented and discussed in the paper deal with CFS fixed-ended columns exhibiting various cross-section shapes, namely plain (U) and lipped (C), return (RLC), web-stiffened lipped (WSC) and web-flange-stiffened lipped (WFSC) channels, (ii) hat-sections (H) and rack-sections (R) – note that the U and C column results had been previously reported by Dinis *et al.* (2022). After providing an overview of the DSM-based design approach developed by Dinis *et al.* (2022), in the sole context of CFS fixed-ended U and C columns undergoing $F_{MT}-F_m$ interaction, the paper addressed the selection of the H, R, RLC, WSC and WFSC column geometries ensuring critical buckling in F_{MT} modes and a variable closeness between the F_{MT} and F_m buckling loads. Then, ANSYS shell finite element models were used to (i) investigate the column elastic and elastic-plastic post-buckling behavior, including the identification of the most detrimental initial geometrical imperfection shape (*i.e.*, that leading to the lowest failure load), and (ii) obtain the failure loads of the selected 1200 CFS fixed-ended columns, which exhibit various cross-section dimensions, lengths and yield stresses, chosen to enable covering wide buckling load ratio (R_G) and F_{MT} flexural-torsional slenderness ranges (λ_{FT}). On the basis of these failure load data, combined with the 475 fixed-ended U and C column failure loads reported by Dinis *et al.* (2022), it was possible to show that the DSM-based design approach developed and proposed by Dinis *et al.* (2022) also predicts efficiently (safely, accurately and reliably) the failure loads of CFS fixed-ended H, R, RLC, WSC and WFSC columns failing in pure F_{MT} or $F_{MT}-F_m$ interactive modes. In other words, it was shown that the above DSM-based design approach provides high-quality failure load predictions for CFS fixed-ended columns, regardless of their cross-section shape. Indeed, the P_{nFT-Fm} column failure load predictions reported in this work and by Dinis *et al.* (2019, 2020b, 2022) lead to LRFD resistance factors higher than 0.96, *i.e.*, well above the value prescribed in AISI (2020) for compression members – $\phi_c=0.85$.

The findings reported provided encouragement to extend the methodology adopted to columns with other end support conditions, so that a general and unified DSM-based approach for the design of CFS columns buckling in F_{MT} modes and failing in F_{MT} (pure) or $F_{MT}-F_m$ (interactive) modes is reached. The authors are currently working towards achieving this goal, namely by (i) widening the scope of this numerical investigation and (ii) seeking experimental validation for the results obtained – although the fruits of this research effort will only be reported in the near future, it should be pointed out that the results obtained so far confirm that a general and unified DSM-based approach is possible.

Acknowledgments

The second author gratefully acknowledges the financial support of the following Brazilian institutions: (i) CAPES (*Coordenação de Aperfeiçoamento de Pessoal de Nível Superior*) – Finance Code 001, (ii) CNPq (*Conselho Nacional de Desenvolvimento Científico e Tecnológico*) – Finance Code 313197/2020-2 and (iii) FAPERJ (*Fundação Carlos Chagas Filho de Amparo à Pesquisa do Estado do Rio de Janeiro*) – Finance Code E-26/202.758/2017.

References

- AISI (American Iron and Steel Institute) (2020). *North American Specification (NAS) for the Design of Cold-Formed Steel Structural Members* (2016 edition reaffirmed in 2020), AISI-S100-16 w/S2-20, Washington DC.
- Bebiano R, Camotim D, Gonçalves R (2018). GBTUL 2.0 – a second-generation code for the GBT-based buckling and vibration analysis of thin-walled members, *Thin-Walled Structures*, **124**(March), 235-257.
- Camotim D, Dinis PB (2011). Coupled instabilities with distortional buckling in cold-formed steel lipped channel columns, *Thin-Walled Structures*, **49**(5), 562-575.

- Camotim D, Dinis PB, Martins AD (2016). Direct Strength Method (DSM) – a general approach for the design of cold-formed steel structures, *Recent Trends in Cold-Formed Steel Construction*, C. Yu (ed.), Woodhead Publishing (Amsterdam – Series in Civil and Structural Engineering), 69-105.
- Camotim D, Dinis PB, Landesmann A (2020). Behavior, failure and Direct Strength Method design of steel angle columns: geometrical simplicity vs. structural complexity, *Journal of Structural Engineering*, **146**(11), paper 04020226 (25 pages).
- Cerqueira E, Dinis PB, Camotim D, Landesmann A, Martins AD (2021). Behavior, strength and DSM design of CFS lipped channel columns failing in global-global interactive modes, *Website Proceedings of Structural Stability Research Council (SSRC) Annual Stability Conference* (Kentucky, 13-16/4).
- Dinis PB, Camotim D, Landesmann A, Martins AD (2019). On the Direct Strength Method design of columns against global failure, *Thin-Walled Structures*, **139**(June), 242-270.
- Dinis PB, Camotim D, Martins AD, Landesmann A (2020a). Global-global interaction in cold-formed steel channel columns: relevance, post-buckling behavior, strength and DSM design, *Website Proceedings of Structural Stability Research Council (SSRC) Annual Stability Conference* (Georgia, 21-24/4).
- Dinis PB, Camotim D, Landesmann A, Martins AD (2020b). Improving the Direct Strength Method prediction of column flexural-torsional failure loads, *Thin-Walled Structures*, **148**(March), paper 106461 (18 pages).
- Dinis PB, Camotim D, Landesmann A, Martins AD, Cerqueira E (2022). Global-global interaction in cold-formed steel plain and lipped channel columns, *Thin-Walled Structures*, in press.
- Ellobody E, Young B (2005). Behavior of cold-formed steel plain angle columns, *Journal of Structural Engineering (ASCE)*, **131**(3), 469-478.
- Hancock GJ, Kwon YB, Bernard ES (1994). Strength design curves for thin-walled sections undergoing distortional buckling, *Journal of Construction Steel Research*, **31**(2-3), 169-186.
- Landesmann A, Camotim D, Garcia R (2016). On the strength and DSM design of cold-formed steel web/flange-stiffened lipped channel columns buckling and failing in distortional modes, *Thin-Walled Structures*, **105**(August), 248-265.
- SAS (Swanson Analysis Systems Inc.) (2009). *ANSYS Reference Manual* (vrs. 12).
- Schafer BW (2008). Review: the direct strength method of cold-formed steel member design, *Journal of Constructional Steel Research*, **64**(7-8), 766-778.
- Schafer BW (2019). Advances in the Direct Strength Method of cold-formed steel design, *Thin-Walled Structures*, **140**(July), 533-541.
- Schafer BW, Peköz T (1998). Direct strength prediction of cold-formed steel members using numerical elastic buckling solutions, *Proceedings of 14th International Specialty Conference on Cold-Formed Steel Structures* (St. Louis, 15-16/10), W.W. Yu, R. LaBoube (eds.), 69-76.
- Torabian S, Schafer BW (2018). Development and experimental validation of the Direct Strength Method for cold-formed steel beam-columns, *Journal of Structural Engineering (ASCE)*, **144**(10), paper 04018175 (21 pages).

ANNEX I: Data Concerning the CFS Fixed-Ended Columns Analyzed in this Work

Table I.1: H column (i) geometries, (ii) β_{FT} values, (iii) yield stresses, (iv) buckling load values and ratios, (v) numerical failure loads, (vi) failure load predictions estimates P_{nG} , P_{nFT} and P_{nFT-Fm} , and (vii) numerical-to-predicted failure loads ratios (mm, kN)

Column	Geometry				SFEA				DSM Design													
	$b_w \times b_f \times b_s \times t$	β_{FT}	L	f_y	$P_{u,FT}$	$P_{u,Fm}$	P_u	$P_{cr,FT}$	$P_{b,Fm}$	$\frac{P_u}{P_{c,G}}$	λ_{FT}	b	a	P_{nFT}	$\frac{P_u}{P_{nFT}}$	R_G	R_{DL}	c	b	a	P_{nFT-Fm}	$\frac{P_u}{P_{nFT-Fm}}$
H1_L1	60x55x11x4	2.39	5500	150	60.4	66.4	60.4	70.9	92.3	1.04	1.28	0.85	0.55	58.34	1.04	1.30	11.74	1.21	1.35	0.67	58.34	1.04
		2.39	5500	300	70.0	81.6	70.0	70.9	92.3	1.13	1.80	0.85	0.55	76.79	0.91	1.30	11.74	1.21	1.35	0.67	70.06	1.00
		2.39	5500	450	75.6	85.9	75.6	70.9	92.3	1.22	2.21	0.85	0.55	96.88	0.78	1.30	11.74	1.21	1.35	0.67	79.89	0.95
		2.39	5500	600	79.5	87.7	79.5	70.9	92.3	1.28	2.55	0.85	0.55	114.25	0.70	1.30	11.74	1.21	1.35	0.67	87.70	0.91
		2.39	5500	750	82.0	87.4	82.0	70.9	92.3	1.32	2.85	0.85	0.55	129.84	0.63	1.30	11.74	1.21	1.35	0.67	94.27	0.87
H1_L2	60x55x11x4	2.39	6000	150	56.4	59.6	56.4	65.2	77.6	1.02	1.33	0.85	0.55	55.01	1.02	1.19	14.30	1.39	1.53	0.73	55.01	1.02
		2.39	6000	300	63.9	69.9	63.9	65.2	77.6	1.12	1.88	0.85	0.55	74.12	0.86	1.19	14.30	1.39	1.53	0.73	63.63	1.00
		2.39	6000	450	67.9	72.8	67.9	65.2	77.6	1.19	2.30	0.85	0.55	93.52	0.73	1.19	14.30	1.39	1.53	0.73	69.97	0.97
		2.39	6000	600	70.3	74.1	70.3	65.2	77.6	1.23	2.66	0.85	0.55	110.28	0.64	1.19	14.30	1.39	1.53	0.73	74.86	0.94
H1_L3	60x55x11x4	2.39	6200	150	54.9	56.9	54.9	63.1	72.6	1.02	1.35	0.85	0.55	53.68	1.02	1.15	15.49	1.46	1.61	0.75	53.68	1.02
		2.39	6200	300	61.5	65.7	61.5	63.1	72.6	1.11	1.91	0.85	0.55	73.10	0.84	1.15	15.49	1.46	1.61	0.75	60.93	1.01
		2.39	6200	450	65.0	68.4	65.0	63.1	72.6	1.17	2.34	0.85	0.55	92.22	0.70	1.15	15.49	1.46	1.61	0.75	65.99	0.98
		2.39	6200	600	66.9	69.5	66.9	63.1	72.6	1.21	2.70	0.85	0.55	108.76	0.62	1.15	15.49	1.46	1.61	0.75	69.83	0.96
		2.39	6200	750	68.1	70.2	68.1	63.1	72.6	1.23	3.02	0.85	0.55	123.60	0.55	1.15	15.49	1.46	1.61	0.75	72.96	0.93
H1_L4	60x55x11x4	2.39	6500	150	52.5	53.0	52.5	60.2	66.1	1.02	1.38	0.85	0.55	51.68	1.02	1.10	17.47	1.60	1.74	0.79	51.68	1.02
		2.39	6500	300	58.3	59.5	58.3	60.2	66.1	1.10	1.96	0.85	0.55	71.60	0.81	1.10	17.47	1.60	1.74	0.79	56.57	1.03
		2.39	6500	450	60.9	59.7	59.7	60.2	66.1	1.13	2.40	0.85	0.55	90.34	0.66	1.10	17.47	1.60	1.74	0.79	59.64	1.00
		2.39	6500	600	62.3	59.8	59.8	60.2	66.1	1.13	2.77	0.85	0.55	106.53	0.56	1.10	17.47	1.60	1.74	0.79	61.92	0.97
		2.39	6500	750	63.0	59.9	59.9	60.2	66.1	1.14	3.09	0.85	0.55	121.07	0.49	1.10	17.47	1.60	1.74	0.79	63.75	0.94
H1_L5	60x55x11x4	2.39	7000	150	48.7	46.9	46.9	55.5	57.0	0.97	1.44	0.85	0.55	48.35	0.97	1.03	21.34	1.87	2.00	0.88	48.35	0.97
		2.39	7000	300	53.1	52.5	52.5	55.5	57.0	1.08	2.04	0.85	0.55	69.21	0.76	1.03	21.34	1.87	2.00	0.88	48.73	1.08
		2.39	7000	450	54.7	52.9	52.9	55.5	57.0	1.09	2.49	0.85	0.55	87.31	0.61	1.03	21.34	1.87	2.00	0.88	48.73	1.09
		2.39	7000	600	55.4	52.4	52.4	55.5	57.0	1.08	2.88	0.85	0.55	102.96	0.51	1.03	21.34	1.87	2.00	0.88	48.73	1.08
		2.39	7000	750	55.7	52.4	52.4	55.5	57.0	1.08	3.22	0.85	0.55	117.01	0.45	1.03	21.34	1.87	2.00	0.88	48.73	1.08
H1_L6	60x55x11x4	2.39	7200	150	47.3	44.8	44.8	53.8	53.9	0.95	1.46	0.85	0.55	47.02	0.95	1.00	23.11	2.00	2.00	0.88	47.02	0.95
		2.39	7200	300	51.2	49.8	49.8	53.8	53.9	1.05	2.07	0.85	0.55	68.28	0.73	1.00	23.11	2.00	2.00	0.88	47.22	1.05
		2.39	7200	450	52.5	50.1	50.1	53.8	53.9	1.06	2.53	0.85	0.55	86.14	0.58	1.00	23.11	2.00	2.00	0.88	47.22	1.06
		2.39	7200	600	52.9	50.1	50.1	53.8	53.9	1.06	2.93	0.85	0.55	101.59	0.49	1.00	23.11	2.00	2.00	0.88	47.22	1.06
		2.39	7200	750	52.8	50.1	50.1	53.8	53.9	1.06	3.27	0.85	0.55	115.45	0.43	1.00	23.11	2.00	2.00	0.88	47.22	1.06
H2_L1	100x60x10x3	5.83	5750	150	54.9	63.6	54.9	62.0	90.4	1.05	1.32	1.06	0.60	52.11	1.05	1.46	5.29	0.82	1.17	0.63	52.11	1.05
		5.83	5750	300	69.0	78.6	69.0	62.0	90.4	1.27	1.87	1.06	0.60	66.83	1.03	1.46	5.29	0.82	1.17	0.63	65.17	1.06
		5.83	5750	450	78.9	83.0	78.9	62.0	90.4	1.45	2.29	1.06	0.60	80.86	0.98	1.46	5.29	0.82	1.17	0.63	77.04	1.02
		5.83	5750	600	84.7	84.9	84.7	62.0	90.4	1.56	2.64	1.06	0.60	92.56	0.91	1.46	5.29	0.82	1.17	0.63	86.74	0.98
		5.83	5750	750	87.7	85.8	85.8	62.0	90.4	1.58	2.95	1.06	0.60	102.80	0.83	1.46	5.29	0.82	1.17	0.63	95.11	0.90
H2_L2	100x60x10x3	5.83	6000	150	54.0	58.8	54.0	59.5	83.0	1.07	1.35	1.06	0.60	50.49	1.07	1.40	5.76	1.02	1.37	0.68	50.49	1.07
		5.83	6000	300	66.6	73.2	66.6	59.5	83.0	1.28	1.91	1.06	0.60	65.35	1.02	1.40	5.76	1.02	1.37	0.68	60.68	1.10
		5.83	6000	450	75.2	76.8	75.2	59.5	83.0	1.44	2.33	1.06	0.60	79.07	0.95	1.40	5.76	1.02	1.37	0.68	68.96	1.09
		5.83	6000	600	79.9	78.2	78.2	59.5	83.0	1.50	2.70	1.06	0.60	90.51	0.86	1.40	5.76	1.02	1.37	0.68	75.51	1.04
		5.83	6000	750	82.1	79.0	79.0	59.5	83.0	1.52	3.01	1.06	0.60	100.52	0.79	1.40	5.76	1.02	1.37	0.68	81.02	0.98
H2_L3	100x60x10x3	5.83	6500	150	50.8	53.4	50.8	55.1	70.7	1.07	1.40	1.06	0.60	47.55	1.07	1.28	6.73	1.24	1.59	0.74	47.55	1.07
		5.83	6500	300	61.7	58.3	58.3	55.1	70.7	1.21	1.98	1.06	0.60	62.77	0.93	1.28	6.73	1.24	1.59	0.74	54.20	1.08
		5.83	6500	450	68.0	58.1	58.1	55.1	70.7	1.20	2.42	1.06	0.60	75.94	0.77	1.28	6.73	1.24	1.59	0.74	58.91	0.99
		5.83	6500	600	70.8	58.1	58.1	55.1	70.7	1.20	2.80	1.06	0.60	86.94	0.67	1.28	6.73	1.24	1.59	0.74	62.50	0.93
		5.83	6500	750	71.8	58.1	58.1	55.1	70.7	1.20	3.13	1.06	0.60	96.55	0.60	1.28	6.73	1.24	1.59	0.74	65.44	0.89
H2_L4	100x60x10x3	5.83	7000	150	47.8	54.2	47.8	51.5	61.0	1.06	1.45	1.06	0.60	44.93	1.06	1.18	7.87	1.40	1.75	0.79	44.93	1.06
		5.83	7000	300	57.0	63.4	57.0	51.5	61.0	1.26	2.05	1.06	0.60	60.58	0.94	1.18	7.87	1.40	1.75	0.79	48.91	1.17
		5.83	7000	450	61.3	65.9	61.3	51.5	61.0	1.36	2.51	1.06	0.60	73.30	0.84	1.18</td						

Column	Geometry			SFEA					DSM Design													
	$b_w \times b_f \times b_s \times t$	β_{FT}	L	f_y	$P_{u,FT}$	$P_{u,Fm}$	P_u	$P_{cr,FT}$	$P_{b,Fm}$	$\frac{P_u}{P_{nG}}$	λ_{FT}	b	a	P_{nFT}	$\frac{P_u}{P_{nFT}}$	R_G	R_{DL}	c	b	a	P_{nFT-Fm}	$\frac{P_u}{P_{nFT-Fm}}$
H3_L1	120x60x15x5	6.47	3200	150	180.5	175.3	175.3	369.6	584.0	1.09	0.74	1.10	0.61	161.00	1.09	1.58	3.16	0.71	1.10	0.61	161.00	1.09
		6.47	3200	300	288.7	310.7	288.7	369.6	584.0	1.13	1.05	1.10	0.61	256.01	1.13	1.58	3.16	0.71	1.10	0.61	256.01	1.13
		6.47	3200	450	334.0	402.2	334.0	369.6	584.0	1.09	1.28	1.10	0.61	305.31	1.09	1.58	3.16	0.71	1.10	0.61	305.31	1.09
		6.47	3200	600	362.9	469.9	362.9	369.6	584.0	1.12	1.48	1.10	0.61	323.65	1.12	1.58	3.16	0.71	1.10	0.61	323.65	1.12
		6.47	3200	750	390.1	508.6	390.1	369.6	584.0	1.20	1.66	1.10	0.61	354.41	1.10	1.58	3.16	0.71	1.10	0.61	354.41	1.10
H3_L2	120x60x15x6	6.47	3500	150	177.2	172.8	172.8	333.3	488.3	1.10	0.78	1.10	0.61	157.04	1.10	1.46	3.84	0.794	1.18	0.63	157.04	1.10
		6.47	3500	300	271.4	291.0	271.4	333.3	488.3	1.11	1.10	1.10	0.61	243.56	1.11	1.46	3.84	0.794	1.18	0.63	243.56	1.11
		6.47	3500	450	309.3	379.1	309.3	333.3	488.3	1.09	1.35	1.10	0.61	283.32	1.09	1.46	3.84	0.794	1.18	0.63	283.32	1.09
		6.47	3500	600	336.5	409.2	336.5	333.3	488.3	1.15	1.56	1.10	0.61	302.84	1.11	1.46	3.84	0.794	1.18	0.63	301.86	1.11
		6.47	3500	750	362.4	434.0	362.4	333.3	488.3	1.24	1.74	1.10	0.61	334.89	1.08	1.46	3.84	0.794	1.18	0.63	330.71	1.10
H3_L3	120x60x15x7	6.47	4000	150	171.0	161.1	161.1	289.5	373.9	1.07	0.84	1.10	0.61	151.10	1.07	1.29	5.16	1.226	1.61	0.75	151.10	1.07
		6.47	4000	300	246.5	268.8	246.5	289.5	373.9	1.09	1.18	1.10	0.61	225.50	1.09	1.29	5.16	1.226	1.61	0.75	225.50	1.09
		6.47	4000	450	277.5	304.9	277.5	289.5	373.9	1.10	1.45	1.10	0.61	252.40	1.10	1.29	5.16	1.226	1.61	0.75	252.40	1.10
		6.47	4000	600	301.7	324.4	301.7	289.5	373.9	1.19	1.67	1.10	0.61	280.27	1.08	1.29	5.16	1.226	1.61	0.75	264.95	1.14
		6.47	4000	750	323.2	336.6	323.2	289.5	373.9	1.27	1.87	1.10	0.61	309.94	1.04	1.29	5.16	1.226	1.61	0.75	276.62	1.17
H3_L4	120x60x15x8	6.47	4200	150	168.9	158.9	158.9	276.0	339.2	1.07	0.86	1.10	0.61	148.95	1.07	1.23	5.75	1.321	1.71	0.78	148.95	1.07
		6.47	4200	300	238.2	248.9	238.2	276.0	339.2	1.09	1.21	1.10	0.61	219.12	1.09	1.23	5.75	1.321	1.71	0.78	219.12	1.09
		6.47	4200	450	267.0	289.0	267.0	276.0	339.2	1.10	1.48	1.10	0.61	241.76	1.10	1.23	5.75	1.321	1.71	0.78	241.76	1.10
		6.47	4200	600	289.4	305.1	289.4	276.0	339.2	1.20	1.71	1.10	0.61	272.99	1.06	1.23	5.75	1.321	1.71	0.78	251.70	1.15
		6.47	4200	750	308.7	312.8	308.7	276.0	339.2	1.28	1.92	1.10	0.61	301.89	1.02	1.23	5.75	1.321	1.71	0.78	260.01	1.19
H3_L5	120x60x15x9	6.47	4500	150	165.0	155.4	155.4	258.7	295.5	1.07	0.88	1.10	0.61	145.93	1.07	1.14	6.66	1.481	1.87	0.83	145.93	1.07
		6.47	4500	300	226.9	230.8	226.9	258.7	295.5	1.08	1.25	1.10	0.61	210.32	1.08	1.14	6.66	1.481	1.87	0.83	210.32	1.08
		6.47	4500	450	252.6	257.3	252.6	258.7	295.5	1.11	1.53	1.10	0.61	231.43	1.09	1.14	6.66	1.481	1.87	0.83	227.65	1.11
		6.47	4500	600	272.4	268.6	268.6	258.7	295.5	1.18	1.77	1.10	0.61	263.49	1.02	1.14	6.66	1.481	1.87	0.83	231.96	1.16
		6.47	4500	750	287.8	273.9	273.9	258.7	295.5	1.21	1.98	1.10	0.61	291.38	0.94	1.14	6.66	1.481	1.87	0.83	235.36	1.16
H3_L6	120x60x15x10	6.47	5000	150	159.6	142.7	142.7	236.0	239.4	1.01	0.93	1.10	0.61	141.40	1.01	1.01	8.37	1.926	2.00	0.88	141.40	1.01
		6.47	5000	300	210.7	197.3	197.3	236.0	239.4	1.00	1.31	1.10	0.61	197.46	1.00	1.01	8.37	1.926	2.00	0.88	197.46	1.00
		6.47	5000	450	231.5	213.9	213.9	236.0	239.4	1.03	1.60	1.10	0.61	220.03	0.97	1.01	8.37	1.926	2.00	0.88	207.07	1.03
		6.47	5000	600	245.6	220.7	220.7	236.0	239.4	1.07	1.85	1.10	0.61	250.51	0.88	1.01	8.37	1.926	2.00	0.88	207.07	1.07
		6.47	5000	750	254.9	224.8	224.8	236.0	239.4	1.09	2.07	1.10	0.61	277.03	0.81	1.01	8.37	1.926	2.00	0.88	207.07	1.09
H4_L1	140x70x10x4	7.90	3750	150	153.0	155.0	153.0	279.2	457.9	1.11	0.80	1.18	0.63	137.42	1.11	1.64	1.61	0.71	1.18	0.63	137.42	1.11
		7.90	3750	300	231.9	263.1	231.9	279.2	457.9	1.11	1.14	1.18	0.63	209.84	1.11	1.64	1.61	0.71	1.18	0.63	209.84	1.11
		7.90	3750	450	263.4	346.3	263.4	279.2	457.9	1.10	1.39	1.18	0.63	240.31	1.10	1.64	1.61	0.71	1.18	0.63	240.31	1.10
		7.90	3750	600	286.9	386.7	286.9	279.2	457.9	1.17	1.61	1.18	0.63	258.99	1.11	1.64	1.61	0.71	1.18	0.63	258.99	1.11
		7.90	3750	750	310.2	402.4	310.2	279.2	457.9	1.27	1.80	1.18	0.63	283.68	1.09	1.64	1.61	0.71	1.18	0.63	283.68	1.09
H4_L2	140x70x10x4	7.90	4000	150	149.4	153.1	149.4	253.9	402.7	1.12	0.84	1.18	0.63	133.79	1.12	1.59	1.85	0.71	1.18	0.63	133.79	1.12
		7.90	4000	300	217.5	260.8	217.5	253.9	402.7	1.09	1.19	1.18	0.63	198.88	1.09	1.59	1.85	0.71	1.18	0.63	198.88	1.09
		7.90	4000	450	245.9	317.7	245.9	253.9	402.7	1.11	1.46	1.18	0.63	221.73	1.11	1.59	1.85	0.71	1.18	0.63	221.73	1.11
		7.90	4000	600	269.6	345.8	269.6	253.9	402.7	1.21	1.68	1.18	0.63	244.86	1.10	1.59	1.85	0.71	1.18	0.63	244.86	1.10
		7.90	4000	750	292.7	359.1	292.7	253.9	402.7	1.31	1.88	1.18	0.63	268.20	1.09	1.59	1.85	0.71	1.18	0.63	268.20	1.09
H4_L3	140x70x10x4	7.90	5000	150	133.2	130.7	130.7	187.5	258.0	1.09	0.98	1.18	0.63	120.43	1.09	1.38	2.98	1.067	1.54	0.73	120.43	1.09
		7.90	5000	300	174.8	199.3	174.8	187.5	258.0	1.08	1.39	1.18	0.63	161.15	1.08	1.38	2.98	1.067	1.54	0.73	161.15	1.08
		7.90	5000	450	198.5	223.5	198.5	187.5	258.0	1.21	1.70	1.18	0.63	181.95	1.09	1.38	2.98	1.067	1.54	0.73	174.10	1.14
		7.90	5000	600	219.1	233.6	219.1	187.5	258.0	1.33	1.96	1.18	0.63	204.60	1.07	1.38	2.98	1.067	1.54	0.73	185.98	1.18
		7.90	5000	750	234.9	238.4	234.9	187.5	258.0	1.43	2.19	1.18	0.63	224.10	1.05	1.38	2.98	1.067	1.54	0.73	195.76	1.20
H4_L4	140x70x10x4	7.90	5500	150	125.3	122.8	122.8	166.7	213.3	1.07	1.04	1.18	0.63	114.56	1.07	1.28	3.65	1.245	1.72	0.78	114.56	1.07
		7.90	550																			

Column	Geometry			SFEA				DSM Design														
	$b_w \times b_f \times b_s \times t$	β_{FT}	L	f_y	$P_{u,FT}$	$P_{u,Fm}$	P_u	$P_{cr,FT}$	$P_{b,Fm}$	$\frac{P_u}{P_{cG}}$	λ_{FT}	b	a	P_{nFT}	$\frac{P_u}{P_{nFT}}$	R_G	R_{DL}	c	b	a	P_{nFT-Fm}	$\frac{P_u}{P_{nFT-Fm}}$
H5_L1	100x50x10x3	7.36	3000	150	79.8	80.5	79.8	128.0	214.7	1.11	0.88	1.15	0.62	71.63	1.11	1.68	2.41	0.71	1.15	0.62	71.63	1.11
		7.36	3000	300	112.4	137.1	112.4	128.0	214.7	1.08	1.24	1.15	0.62	103.64	1.08	1.68	2.41	0.71	1.15	0.62	103.64	1.08
		7.36	3000	450	127.5	173.7	127.5	128.0	214.7	1.14	1.52	1.15	0.62	113.81	1.12	1.68	2.41	0.71	1.15	0.62	113.81	1.12
		7.36	3000	600	141.4	185.8	141.4	128.0	214.7	1.26	1.76	1.15	0.62	128.58	1.10	1.68	2.41	0.71	1.15	0.62	128.58	1.10
H5_L2	100x50x10x3	7.36	3500	150	73.4	77.7	73.4	104.6	157.8	1.10	0.97	1.15	0.62	66.63	1.10	1.51	3.40	0.71	1.15	0.62	66.63	1.10
		7.36	3500	300	97.3	118.0	97.3	104.6	157.8	1.09	1.38	1.15	0.62	89.68	1.09	1.51	3.40	0.71	1.15	0.62	89.68	1.09
		7.36	3500	450	111.2	135.3	111.2	104.6	157.8	1.21	1.68	1.15	0.62	101.33	1.10	1.51	3.40	0.71	1.15	0.62	101.33	1.10
		7.36	3500	600	123.9	142.0	123.9	104.6	157.8	1.35	1.95	1.15	0.62	114.49	1.08	1.51	3.40	0.71	1.15	0.62	114.49	1.08
H5_L3	100x50x10x3	7.36	4000	150	67.8	69.8	67.8	89.3	120.9	1.09	1.05	1.15	0.62	62.24	1.09	1.35	4.53	1.117	1.56	0.73	62.24	1.09
		7.36	4000	300	86.7	98.4	86.7	89.3	120.9	1.11	1.49	1.15	0.62	78.27	1.11	1.35	4.53	1.117	1.56	0.73	78.27	1.11
		7.36	4000	450	99.1	106.6	99.1	89.3	120.9	1.27	1.82	1.15	0.62	92.49	1.07	1.35	4.53	1.117	1.56	0.73	85.42	1.16
		7.36	4000	600	109.0	110.0	109.0	89.3	120.9	1.39	2.11	1.15	0.62	104.49	1.04	1.35	4.53	1.117	1.56	0.73	91.03	1.20
H5_L4	100x50x10x3	7.36	4500	150	62.8	62.5	62.5	78.6	95.5	1.07	1.12	1.15	0.62	58.44	1.07	1.21	5.84	1.344	1.79	0.80	58.44	1.07
		7.36	4500	300	78.6	77.5	77.5	78.6	95.5	1.12	1.59	1.15	0.62	72.37	1.07	1.21	5.84	1.344	1.79	0.80	69.83	1.11
		7.36	4500	450	88.7	85.6	85.6	78.6	95.5	1.24	1.94	1.15	0.62	85.95	1.00	1.21	5.84	1.344	1.79	0.80	72.94	1.17
		7.36	4500	600	95.4	89.0	89.0	78.6	95.5	1.29	2.24	1.15	0.62	97.11	0.92	1.21	5.84	1.344	1.79	0.80	75.23	1.18
H5_L5	100x50x10x3	7.36	5000	150	58.6	52.5	52.5	70.8	77.4	0.95	1.18	1.15	0.62	55.15	0.95	1.09	7.30	1.615	2.00	0.88	55.15	0.95
		7.36	5000	300	71.7	67.6	67.6	70.8	77.4	1.09	1.67	1.15	0.62	68.15	0.99	1.09	7.30	1.615	2.00	0.88	62.15	1.09
		7.36	5000	450	79.1	71.2	71.2	70.8	77.4	1.15	2.05	1.15	0.62	80.94	0.88	1.09	7.30	1.615	2.00	0.88	62.15	1.15
		7.36	5000	600	82.9	72.7	72.7	70.8	77.4	1.17	2.36	1.15	0.62	91.45	0.79	1.09	7.30	1.615	2.00	0.88	62.15	1.17
H5_L6	100x50x10x3	7.36	5200	150	57.1	47.9	47.9	68.3	71.5	0.89	1.20	1.15	0.62	53.96	0.89	1.05	7.92	1.775	2.00	0.88	53.96	0.89
		7.36	5200	300	69.2	61.8	61.8	68.3	71.5	1.03	1.70	1.15	0.62	66.72	0.93	1.05	7.92	1.775	2.00	0.88	59.92	1.03
		7.36	5200	450	75.5	65.3	65.3	68.3	71.5	1.09	2.09	1.15	0.62	79.25	0.82	1.05	7.92	1.775	2.00	0.88	59.92	1.09
		7.36	5200	600	78.2	67.4	67.4	68.3	71.5	1.13	2.41	1.15	0.62	89.54	0.75	1.05	7.92	1.775	2.00	0.88	59.92	1.12
H6_L1	90x40x10x2	9.25	3000	150	38.3	43.2	38.3	51.0	81.7	1.07	1.06	1.27	0.65	35.69	1.07	1.60	3.02	0.71	1.27	0.65	35.69	1.07
		9.25	3000	300	49.9	63.8	49.9	51.0	81.7	1.12	1.50	1.27	0.65	44.70	1.12	1.60	3.02	0.71	1.27	0.65	44.70	1.12
		9.25	3000	450	58.6	70.8	58.6	51.0	81.7	1.31	1.83	1.27	0.65	51.80	1.13	1.60	3.02	0.71	1.27	0.65	51.80	1.13
		9.25	3000	600	66.1	73.8	66.1	51.0	81.7	1.48	2.12	1.27	0.65	57.57	1.15	1.60	3.02	0.71	1.27	0.65	57.57	1.15
H6_L2	90x40x10x2	9.25	3300	150	35.4	38.5	35.4	44.7	67.6	1.06	1.13	1.27	0.65	33.41	1.06	1.51	3.74	0.71	1.27	0.65	33.41	1.06
		9.25	3300	300	45.8	55.3	45.8	44.7	67.6	1.17	1.60	1.27	0.65	41.05	1.12	1.51	3.74	0.71	1.27	0.65	41.05	1.12
		9.25	3300	450	54.0	60.0	54.0	44.7	67.6	1.38	1.96	1.27	0.65	47.64	1.13	1.51	3.74	0.71	1.27	0.65	47.64	1.13
		9.25	3300	600	60.2	61.7	60.2	44.7	67.6	1.54	2.26	1.27	0.65	52.95	1.14	1.51	3.74	0.71	1.27	0.65	52.95	1.14
H6_L3	90x40x10x2	9.25	3500	150	33.8	37.6	33.8	41.3	60.1	1.06	1.17	1.27	0.65	31.99	1.06	1.45	4.27	0.835	1.39	0.69	31.99	1.06
		9.25	3500	300	43.6	50.3	43.6	41.3	60.1	1.20	1.66	1.27	0.65	39.07	1.12	1.45	4.27	0.835	1.39	0.69	38.57	1.13
		9.25	3500	450	51.3	53.9	51.3	41.3	60.1	1.42	2.03	1.27	0.65	45.35	1.13	1.45	4.27	0.835	1.39	0.69	43.65	1.18
		9.25	3500	600	56.6	55.4	55.4	41.3	60.1	1.53	2.35	1.27	0.65	50.40	1.10	1.45	4.27	0.835	1.39	0.69	47.65	1.16
H6_L4	90x40x10x2	9.25	4000	150	30.3	32.2	30.3	35.0	46.0	1.05	1.28	1.27	0.65	28.83	1.05	1.31	5.71	1.189	1.74	0.79	28.83	1.05
		9.25	4000	300	39.0	39.4	39.0	35.0	46.0	1.27	1.80	1.27	0.65	35.18	1.11	1.31	5.71	1.189	1.74	0.79	32.20	1.21
		9.25	4000	450	44.8	42.1	42.1	35.0	46.0	1.37	2.21	1.27	0.65	40.83	1.03	1.31	5.71	1.189	1.74	0.79	33.92	1.24
		9.25	4000	600	47.8	43.0	43.0	35.0	46.0	1.40	2.55	1.27	0.65	45.38	0.95	1.31	5.71	1.189	1.74	0.79	35.19	1.22
H6_L5	90x40x10x2	9.25	4500	150	27.7	27.5	27.5	30.6	36.4	1.05	1.36	1.27	0.65	26.16	1.05	1.19	7.37	1.391	1.95	0.86	26.16	1.05
		9.25	4500	300	35.0	32.4	32.4	30.6	36.4	1.21	1.93	1.27	0.65	32.33	1.00	1.19	7.37	1.391	1.95	0.86	27.24	1.19
		9.25	4500	450	38.8	33.7	33.7	30.6	36.4	1.26	2.36	1.27	0.65	37.53	0.90	1.19	7.37	1.391	1.95	0.86	27.54	1.22
		9.25	4500	600	40.1	34.3	34.3	30.6	36.4	1.28	2.73	1.27	0.65	41.71	0.82	1.19	7.37	1.391	1.95	0.86	27.76	1.23
H6_L6	90x40x10x2	9.25	5000	150	25.5	23.5	23.5	27.5	29.4	0.98	1.44	1.27	0.65	23.91	0.98	1.07	9.25	1.682	2.00	0.88	23.91	0.98
		9.25	5000	300	31.2	26.7	26.7	27.5	29.4	1.11	2.04	1.27	0.65	30.18	0.88	1.07	9.25	1.682	2.00	0.88	24.10	1.11
		9.25	5000	450	33.3	27.6	27.6	27.5	29.4	1.15	2.50	1.27	0.65	35.03	0.79	1.07	9.25	1.682	2.00	0.88	24.10	1.14
		9.25	5000	600	33.6																	

Column	Geometry			SFEA					DSM Design													
	$b_w \times b_f \times b_s \times t$	β_{FT}	L	f_y	$P_{u,FT}$	$P_{u,Fm}$	P_u	$P_{cr,FT}$	$P_{b,Fm}$	$\frac{P_u}{P_{u,G}}$	λ_{FT}	b	a	P_{nFT}	$\frac{P_u}{P_{nFT}}$	R_G	R_{DL}	c	b	a	P_{nFT-Fm}	$\frac{P_u}{P_{nFT-Fm}}$
H7_L1	130x70x20x4.5	5.92	6000	150	133.2	142.8	133.2	167.5	242.2	1.07	1.12	1.07	0.60	124.03	1.07	1.45	6.65	0.864	1.22	0.64	124.03	1.07
		5.92	6000	300	168.5	189.4	168.5	167.5	242.2	1.15	1.58	1.07	0.60	154.33	1.09	1.45	6.65	0.864	1.22	0.64	153.09	1.10
		5.92	6000	450	194.3	217.9	194.3	167.5	242.2	1.32	1.94	1.07	0.60	186.53	1.04	1.45	6.65	0.864	1.22	0.64	179.36	1.08
		5.92	6000	600	213.9	224.5	213.9	167.5	242.2	1.46	2.24	1.07	0.60	213.37	1.00	1.45	6.65	0.864	1.22	0.64	200.69	1.07
		5.92	6000	750	226.8	227.5	226.8	167.5	242.2	1.54	2.50	1.07	0.60	236.83	0.96	1.45	6.65	0.864	1.22	0.64	218.96	1.04
H7_L2	130x70x20x4.5	5.92	6500	150	127.1	125.6	125.6	155.7	206.4	1.05	1.16	1.07	0.60	119.21	1.05	1.33	7.91	1.169	1.52	0.72	119.21	1.05
		5.92	6500	300	158.8	172.5	158.8	155.7	206.4	1.16	1.64	1.07	0.60	148.44	1.07	1.33	7.91	1.169	1.52	0.72	142.50	1.11
		5.92	6500	450	180.7	188.2	180.7	155.7	206.4	1.32	2.01	1.07	0.60	179.41	1.01	1.33	7.91	1.169	1.52	0.72	156.93	1.15
		5.92	6500	600	195.4	193.1	193.1	155.7	206.4	1.41	2.32	1.07	0.60	205.23	0.94	1.33	7.91	1.169	1.52	0.72	168.05	1.15
		5.92	6500	750	203.9	195.0	195.0	155.7	206.4	1.43	2.59	1.07	0.60	227.78	0.86	1.33	7.91	1.169	1.52	0.72	177.21	1.10
H7_L3	130x70x20x4.5	5.92	7000	150	121.6	118.6	118.6	146.0	178.0	1.03	1.20	1.07	0.60	114.88	1.03	1.22	9.29	1.338	1.69	0.77	114.88	1.03
		5.92	7000	300	167.5	154.5	154.5	146.0	178.0	1.21	1.69	1.07	0.60	143.49	1.08	1.22	9.29	1.338	1.69	0.77	133.01	1.16
		5.92	7000	450	149.9	163.1	149.9	146.0	178.0	1.17	2.07	1.07	0.60	173.42	0.86	1.22	9.29	1.338	1.69	0.77	141.55	1.06
		5.92	7000	600	177.7	167.1	167.1	146.0	178.0	1.30	2.39	1.07	0.60	198.38	0.84	1.22	9.29	1.338	1.69	0.77	147.94	1.13
		5.92	7000	750	182.7	169.1	169.1	146.0	178.0	1.32	2.68	1.07	0.60	220.18	0.77	1.22	9.29	1.338	1.69	0.77	153.10	1.10
H7_L4	130x70x20x4.5	5.92	7500	150	116.7	111.2	111.2	138.1	155.0	1.00	1.23	1.07	0.60	110.96	1.00	1.12	10.80	1.53	1.88	0.84	110.96	1.00
		5.92	7500	300	141.4	135.2	135.2	138.1	155.0	1.12	1.74	1.07	0.60	139.25	0.97	1.12	10.80	1.53	1.88	0.84	123.27	1.10
		5.92	7500	450	154.8	142.3	142.3	138.1	155.0	1.18	2.13	1.07	0.60	168.30	0.85	1.12	10.80	1.53	1.88	0.84	126.22	1.13
		5.92	7500	600	161.2	146.7	146.7	138.1	155.0	1.21	2.46	1.07	0.60	192.52	0.76	1.12	10.80	1.53	1.88	0.84	128.35	1.14
		5.92	7500	750	163.6	148.1	148.1	138.1	155.0	1.22	2.75	1.07	0.60	213.68	0.69	1.12	10.80	1.53	1.88	0.84	130.03	1.14
H7_L5	130x70x20x4.5	5.92	8000	150	112.1	97.2	97.2	131.3	136.3	0.90	1.26	1.07	0.60	107.38	0.90	1.04	12.42	1.816	2.00	0.88	107.38	0.90
		5.92	8000	300	133.2	121.5	121.5	131.3	136.3	1.06	1.79	1.07	0.60	135.57	0.90	1.04	12.42	1.816	2.00	0.88	115.20	1.05
		5.92	8000	450	142.6	127.4	127.4	131.3	136.3	1.11	2.19	1.07	0.60	163.85	0.78	1.04	12.42	1.816	2.00	0.88	115.20	1.11
		5.92	8000	600	146.1	129.5	129.5	131.3	136.3	1.12	2.53	1.07	0.60	187.43	0.69	1.04	12.42	1.816	2.00	0.88	115.20	1.12
		5.92	8000	750	146.6	130.6	130.6	131.3	136.3	1.13	2.82	1.07	0.60	208.03	0.63	1.04	12.42	1.816	2.00	0.88	115.20	1.13
H7_L6	130x70x20x4.5	5.92	8200	150	110.4	99.9	99.9	128.8	129.7	0.94	1.27	1.07	0.60	106.03	0.94	1.01	13.09	1.965	2.00	0.88	106.03	0.94
		5.92	8200	300	129.9	116.7	116.7	128.8	129.7	1.03	1.80	1.07	0.60	134.22	0.87	1.01	13.09	1.965	2.00	0.88	113.06	1.03
		5.92	8200	450	138.0	121.5	121.5	128.8	129.7	1.08	2.21	1.07	0.60	162.22	0.75	1.01	13.09	1.965	2.00	0.88	113.06	1.07
		5.92	8200	600	140.6	122.8	122.8	128.8	129.7	1.09	2.55	1.07	0.60	185.57	0.66	1.01	13.09	1.965	2.00	0.88	113.06	1.09
		5.92	8200	750	140.4	124.3	124.3	128.8	129.7	1.10	2.85	1.07	0.60	205.96	0.60	1.01	13.09	1.965	2.00	0.88	113.06	1.10
H8_L1	130x65x15x4	7.11	4500	150	129.3	133.5	129.3	185.1	292.4	1.10	0.97	1.14	0.62	117.40	1.10	1.58	3.57	0.71	1.14	0.62	117.40	1.10
		7.11	4500	300	171.6	213.9	171.6	185.1	292.4	1.08	1.37	1.14	0.62	158.42	1.08	1.58	3.57	0.71	1.14	0.62	158.42	1.08
		7.11	4500	450	196.8	248.0	196.8	185.1	292.4	1.21	1.68	1.14	0.62	179.05	1.10	1.58	3.57	0.71	1.14	0.62	179.05	1.10
		7.11	4500	600	220.8	261.9	220.8	185.1	292.4	1.36	1.94	1.14	0.62	202.71	1.09	1.58	3.57	0.71	1.14	0.62	202.71	1.09
		7.11	4500	750	238.7	268.6	238.7	185.1	292.4	1.47	2.17	1.14	0.62	223.21	1.07	1.58	3.57	0.71	1.14	0.62	223.21	1.07
H8_L2	130x65x15x4	7.11	5000	150	121.5	130.0	121.5	163.4	236.9	1.09	1.03	1.14	0.62	111.42	1.09	1.45	4.51	0.852	1.28	0.65	111.42	1.09
		7.11	5000	300	156.9	186.7	156.9	163.4	236.9	1.10	1.46	1.14	0.62	142.70	1.10	1.45	4.51	0.852	1.28	0.65	142.70	1.10
		7.11	5000	450	180.5	206.6	180.5	163.4	236.9	1.26	1.79	1.14	0.62	166.79	1.08	1.45	4.51	0.852	1.28	0.65	162.70	1.11
		7.11	5000	600	200.5	216.1	200.5	163.4	236.9	1.40	2.06	1.14	0.62	188.84	1.06	1.45	4.51	0.852	1.28	0.65	180.49	1.11
		7.11	5000	750	214.8	220.0	214.8	163.4	236.9	1.50	2.31	1.14	0.62	207.93	1.03	1.45	4.51	0.852	1.28	0.65	195.62	1.10
H8_L3	130x65x15x4	7.11	5500	150	114.5	113.3	113.3	147.2	195.8	1.07	1.09	1.14	0.62	106.08	1.07	1.33	5.54	1.161	1.59	0.74	106.08	1.07
		7.11	5500	300	166.2	159.4	159.4	147.2	195.8	1.24	1.54	1.14	0.62	131.93	1.21	1.33	5.54	1.161	1.59	0.74	130.46	1.22
		7.11	5500	450	145.3	174.3	145.3	147.2	195.8	1.13	1.88	1.14	0.62	157.16	0.92	1.33	5.54	1.161	1.59	0.74	141.83	1.02
		7.11	5500	600	181.9	180.7	180.7	147.2	195.8	1.40	2.17	1.14	0.62	177.94	1.02	1.33	5.54	1.161	1.59	0.74	150.50	1.20
		7.11	5500	750	192.0	183.7	183.7	147.2	195.8	1.42	2.43	1.14	0.62	195.92	0.94	1.33	5.54	1.161	1.59	0.74	157.58	1.17
H8_L4	130x65x15x4	7.11	6000	150	108.3	109.4	108.3	134.6	164.5	1.07	1.14	1.14	0.62	101.31	1.07	1.22	6.69	1				

Table I.2: R column (i) geometries, (ii) β_{FT} values, (iii) yield stresses, (iv) buckling load values and ratios, (v) numerical failure loads, (vi) failure load predictions estimates P_{nG} , P_{nFT} and P_{nFT-Fm} , and (vii) numerical-to-predicted failure loads ratios (mm, kN)

Column	Geometry			SFEA					DSM Design													
	$b_w \times b_f \times b_l \times b_s \times t$	β_{FT}	L	f_y	$P_{u,FT}$	$P_{u,Fm}$	P_u	$P_{cr,FT}$	$P_{b,Fm}$	$\frac{P_u}{P_{cr}}$	λ_{FT}	b	a	P_{nFT}	$\frac{P_u}{P_{nFT}}$	R_G	R_{DL}	c	b	a	P_{nFT-Fm}	$\frac{P_u}{P_{nFT-Fm}}$
R1_L1	110x55x10x15x3	7.11	5000	150	78.4	89.0	78.4	103.0	154.9	1.06	1.09	1.14	0.62	74.15	1.06	1.50	2.91	0.71	1.14	0.62	74.15	1.06
		7.11	5000	300	97.9	126.1	97.9	103.0	154.9	1.08	1.54	1.14	0.62	92.24	1.06	1.50	2.91	0.71	1.14	0.62	92.24	1.06
		7.11	5000	450	109.6	137.4	109.6	103.0	154.9	1.21	1.88	1.14	0.62	109.89	1.00	1.50	2.91	0.71	1.14	0.62	109.89	1.00
		7.11	5000	600	119.6	142.4	119.6	103.0	154.9	1.32	2.17	1.14	0.62	124.42	0.96	1.50	2.91	0.71	1.14	0.62	124.42	0.96
		7.11	5000	750	127.4	145.0	127.4	103.0	154.9	1.41	2.43	1.14	0.62	137.01	0.93	1.50	2.91	0.71	1.14	0.62	137.01	0.93
R1_L2	110x55x10x15x3	7.11	6000	150	66.1	71.8	66.1	79.9	107.7	1.03	1.23	1.14	0.62	64.28	1.03	1.35	4.31	1.127	1.55	0.73	64.28	1.03
		7.11	6000	300	80.1	93.5	80.1	79.9	107.7	1.14	1.74	1.14	0.62	79.84	1.00	1.35	4.31	1.127	1.55	0.73	74.96	1.07
		7.11	6000	450	89.5	98.6	89.5	79.9	107.7	1.28	2.14	1.14	0.62	95.11	0.94	1.35	4.31	1.127	1.55	0.73	82.06	1.09
		7.11	6000	600	96.0	101.0	96.0	79.9	107.7	1.37	2.47	1.14	0.62	107.69	0.89	1.35	4.31	1.127	1.55	0.73	87.50	1.10
		7.11	6000	750	100.1	102.3	100.1	79.9	107.7	1.43	2.76	1.14	0.62	118.58	0.84	1.35	4.31	1.127	1.55	0.73	91.97	1.09
R1_L3	110x55x10x15x3	7.11	6500	150	61.2	67.3	61.2	72.0	91.8	1.02	1.30	1.14	0.62	59.95	1.02	1.27	5.13	1.252	1.68	0.77	59.95	1.02
		7.11	6500	300	73.5	81.1	73.5	72.0	91.8	1.16	1.84	1.14	0.62	75.26	0.98	1.27	5.13	1.252	1.68	0.77	67.43	1.09
		7.11	6500	450	81.3	84.9	81.3	72.0	91.8	1.29	2.25	1.14	0.62	89.66	0.91	1.27	5.13	1.252	1.68	0.77	71.98	1.13
		7.11	6500	600	86.1	86.6	86.1	72.0	91.8	1.36	2.60	1.14	0.62	101.52	0.85	1.27	5.13	1.252	1.68	0.77	75.39	1.14
		7.11	6500	750	88.7	87.6	87.6	72.0	91.8	1.39	2.91	1.14	0.62	111.78	0.78	1.27	5.13	1.252	1.68	0.77	78.14	1.12
R1_L4	110x55x10x15x3	7.11	7000	150	57.0	58.9	57.0	65.7	79.1	1.02	1.36	1.14	0.62	56.00	1.02	1.21	5.99	1.359	1.79	0.80	56.00	1.02
		7.11	7000	300	67.7	70.9	67.7	65.7	79.1	1.18	1.92	1.14	0.62	71.43	0.95	1.21	5.99	1.359	1.79	0.80	60.77	1.11
		7.11	7000	450	73.9	73.7	73.7	65.7	79.1	1.28	2.36	1.14	0.62	85.09	0.87	1.21	5.99	1.359	1.79	0.80	63.48	1.16
		7.11	7000	600	77.2	75.1	75.1	65.7	79.1	1.30	2.72	1.14	0.62	96.34	0.78	1.21	5.99	1.359	1.79	0.80	65.47	1.15
		7.11	7000	750	78.6	75.8	75.8	65.7	79.1	1.32	3.04	1.14	0.62	106.09	0.71	1.21	5.99	1.359	1.79	0.80	67.05	1.13
R1_L5	110x55x10x15x3	7.11	7500	150	53.3	54.0	53.3	60.5	68.9	1.02	1.42	1.14	0.62	52.41	1.02	1.14	6.87	1.486	1.91	0.85	52.41	1.02
		7.11	7500	300	62.5	62.4	62.4	60.5	68.9	1.18	2.00	1.14	0.62	68.17	0.92	1.14	6.87	1.486	1.91	0.85	54.43	1.15
		7.11	7500	450	67.2	64.7	64.7	60.5	68.9	1.22	2.46	1.14	0.62	81.21	0.80	1.14	6.87	1.486	1.91	0.85	55.40	1.17
		7.11	7500	600	69.2	65.7	65.7	60.5	68.9	1.24	2.83	1.14	0.62	91.95	0.71	1.14	6.87	1.486	1.91	0.85	56.10	1.17
		7.11	7500	750	69.9	66.3	66.3	60.5	68.9	1.25	3.17	1.14	0.62	101.25	0.65	1.14	6.87	1.486	1.91	0.85	56.65	1.17
R1_L6	110x55x10x15x3	7.11	8000	150	47.2	44.1	44.1	52.5	53.7	0.96	1.52	1.14	0.62	46.64	0.95	1.02	8.85	1.887	2.00	0.88	46.08	0.96
		7.11	8000	300	53.4	49.4	49.4	52.5	53.7	1.07	2.15	1.14	0.62	62.91	0.78	1.02	8.85	1.887	2.00	0.88	46.08	1.07
		7.11	8000	450	55.5	50.8	50.8	52.5	53.7	1.10	2.63	1.14	0.62	74.95	0.68	1.02	8.85	1.887	2.00	0.88	46.08	1.10
		7.11	8000	600	55.9	51.5	51.5	52.5	53.7	1.12	3.04	1.14	0.62	84.86	0.61	1.02	8.85	1.887	2.00	0.88	46.08	1.12
		7.11	8000	750	55.9	51.9	51.9	52.5	53.7	1.13	3.40	1.14	0.62	93.45	0.56	1.02	8.85	1.887	2.00	0.88	46.08	1.13
R2_L1	110x60x11x20x4	4.70	6500	150	90.3	101.2	90.3	109.3	164.3	1.02	1.24	0.99	0.58	88.53	1.02	1.50	5.22	0.71	0.99	0.58	88.53	1.02
		4.70	6500	300	108.5	140.0	108.5	109.3	164.3	1.13	1.76	0.99	0.58	112.67	0.96	1.50	5.22	0.71	0.99	0.58	112.67	0.96
		4.70	6500	450	121.2	150.1	121.2	109.3	164.3	1.26	2.15	0.99	0.58	138.22	0.88	1.50	5.22	0.71	0.99	0.58	138.22	0.88
		4.70	6500	600	131.2	154.0	131.2	109.3	164.3	1.37	2.49	0.99	0.58	159.80	0.82	1.50	5.22	0.71	0.99	0.58	159.80	0.82
		4.70	6500	750	138.5	156.1	138.5	109.3	164.3	1.44	2.78	0.99	0.58	178.82	0.77	1.50	5.22	0.71	0.99	0.58	178.82	0.77
R2_L2	110x60x11x20x4	4.70	7000	150	84.6	99.7	84.6	100.3	141.7	1.01	1.30	0.99	0.58	83.53	1.01	1.41	6.08	0.973	1.26	0.65	83.53	1.01
		4.70	7000	300	100.6	124.4	100.6	100.3	141.7	1.14	1.84	0.99	0.58	107.97	0.93	1.41	6.08	0.973	1.26	0.65	102.36	0.98
		4.70	7000	450	111.5	130.6	111.5	100.3	141.7	1.27	2.25	0.99	0.58	132.45	0.84	1.41	6.08	0.973	1.26	0.65	119.05	0.94
		4.70	7000	600	119.5	133.6	119.5	100.3	141.7	1.36	2.60	0.99	0.58	153.13	0.78	1.41	6.08	0.973	1.26	0.65	132.52	0.90
		4.70	7000	750	125.0	135.3	125.0	100.3	141.7	1.42	2.90	0.99	0.58	171.36	0.73	1.41	6.08	0.973	1.26	0.65	144.00	0.87
R2_L3	110x60x11x20x4	4.70	7500	150	79.5	89.0	79.5	92.8	123.4	1.01	1.35	0.99	0.58	78.90	1.01	1.33	6.94	1.162	1.44	0.70	78.90	1.01
		4.70	7500	300	93.6	109.8	93.6	92.8	123.4	1.15	1.91	0.99	0.58	103.89	0.90	1.33	6.94	1.162	1.44	0.70	93.16	1.00
		4.70	7500	450	102.7	114.7	102.7	92.8	123.4	1.26	2.34	0.99	0.58	127.45	0.81	1.33	6.94	1.162	1.44	0.70	104.28	0.98
		4.70	7500	600	108.9	117.0	108.9	92.8	123.4	1.34	2.70	0.99	0.58	147.34	0.74	1.33	6.94	1.162	1.44	0.70	112.97	0.96
		4.70	7500	750	112.8	118.4	112.8	92.8	123.4	1.39	3.02	0.99	0.58	164.88	0.68	1.33	6.94	1.162	1.44	0.70	120.21	0.94
R2_L4	110x60x11x20x4	4.70	8000	150	75.0	82.6	75.0	86.5	108.5	1.01	1.40	0.99	0.58	74.59	1.01	1.25	7.91	1.282	1.56	0.74	74.59	1.01
		4.70	8000	300	87.2																	

Column	Geometry			SFEA					DSM Design													
	$b_w \times b_f \times b_l \times b_s \times t$	β_{FT}	L	f_y	$P_{u,FT}$	$P_{u,Fm}$	P_u	$P_{cr,FT}$	$P_{b,Fm}$	$\frac{P_u}{P_{nG}}$	λ_{FT}	b	a	P_{nFT}	$\frac{P_u}{P_{nFT}}$	R_G	R_{DL}	c	b	a	P_{nFT-Fm}	$\frac{P_u}{P_{nFT-Fm}}$
R3_L1	120x60x15x25x5	5.42	4500	150	198.3	194.6	194.6	351.3	537.2	1.08	0.83	1.03	0.59	180.32	1.08	1.53	2.63	0.71	1.03	0.59	180.32	1.08
		5.42	4500	300	289.6	356.1	289.6	351.3	537.2	1.07	1.17	1.03	0.59	270.96	1.07	1.53	2.63	0.71	1.03	0.59	270.96	1.07
		5.42	4500	450	322.3	427.5	322.3	351.3	537.2	1.06	1.43	1.03	0.59	305.37	1.06	1.53	2.63	0.71	1.03	0.59	305.37	1.06
		5.42	4500	600	343.2	465.9	343.2	351.3	537.2	1.11	1.65	1.03	0.59	338.59	1.01	1.53	2.63	0.71	1.03	0.59	338.59	1.01
		5.42	4500	750	361.3	483.7	361.3	351.3	537.2	1.17	1.85	1.03	0.59	377.09	0.96	1.53	2.63	0.71	1.03	0.59	377.09	0.96
R3_L2	120x60x15x25x5	5.42	5000	150	188.6	199.4	188.6	302.9	435.7	1.09	0.89	1.03	0.59	172.27	1.09	1.44	3.32	0.892	1.22	0.64	172.27	1.09
		5.42	5000	300	259.3	315.4	259.3	302.9	435.7	1.05	1.26	1.03	0.59	247.30	1.05	1.44	3.32	0.892	1.22	0.64	247.30	1.05
		5.42	5000	450	285.3	367.6	285.3	302.9	435.7	1.07	1.54	1.03	0.59	272.95	1.05	1.44	3.32	0.892	1.22	0.64	271.59	1.05
		5.42	5000	600	303.7	389.3	303.7	302.9	435.7	1.14	1.78	1.03	0.59	313.59	0.97	1.44	3.32	0.892	1.22	0.64	303.96	1.00
		5.42	5000	750	320.1	400.2	320.1	302.9	435.7	1.20	1.99	1.03	0.59	349.24	0.92	1.44	3.32	0.892	1.22	0.64	331.70	0.97
R3_L3	120x60x15x25x5	5.42	6000	150	168.6	175.1	168.6	238.5	302.9	1.07	1.00	1.03	0.59	157.52	1.07	1.27	4.91	1.259	1.58	0.74	157.52	1.07
		5.42	6000	300	213.5	248.6	213.5	238.5	302.9	1.03	1.42	1.03	0.59	206.76	1.03	1.27	4.91	1.259	1.58	0.74	206.76	1.03
		5.42	6000	450	232.0	269.6	232.0	238.5	302.9	1.11	1.74	1.03	0.59	241.20	0.96	1.27	4.91	1.259	1.58	0.74	222.50	1.04
		5.42	6000	600	246.0	279.0	246.0	238.5	302.9	1.18	2.01	1.03	0.59	277.11	0.89	1.27	4.91	1.259	1.58	0.74	236.22	1.04
		5.42	6000	750	257.6	284.2	257.6	238.5	302.9	1.23	2.24	1.03	0.59	308.62	0.83	1.27	4.91	1.259	1.58	0.74	247.44	1.04
R3_L4	120x60x15x25x5	5.42	7000	150	150.7	147.3	147.3	198.1	222.6	1.02	1.10	1.03	0.59	144.53	1.02	1.12	6.84	1.525	1.85	0.83	144.53	1.02
		5.42	7000	300	181.3	192.0	181.3	198.1	222.6	1.04	1.56	1.03	0.59	180.15	1.01	1.12	6.84	1.525	1.85	0.83	174.79	1.04
		5.42	7000	450	194.3	203.5	194.3	198.1	222.6	1.12	1.91	1.03	0.59	219.08	0.89	1.12	6.84	1.525	1.85	0.83	180.17	1.08
		5.42	7000	600	203.4	208.5	203.4	198.1	222.6	1.17	2.20	1.03	0.59	251.70	0.81	1.12	6.84	1.525	1.85	0.83	184.09	1.10
		5.42	7000	750	209.7	211.5	209.7	198.1	222.6	1.21	2.46	1.03	0.59	280.32	0.75	1.12	6.84	1.525	1.85	0.83	187.19	1.12
R3_L5	120x60x15x25x5	5.42	7500	150	142.6	132.9	132.9	183.0	194.0	0.96	1.15	1.03	0.59	138.62	0.96	1.06	7.90	1.727	2.00	0.88	138.62	0.96
		5.42	7500	300	168.2	169.9	168.2	183.0	194.0	1.05	1.62	1.03	0.59	172.92	0.97	1.06	7.90	1.727	2.00	0.88	160.60	1.05
		5.42	7500	450	178.8	178.8	178.8	183.0	194.0	1.11	1.98	1.03	0.59	210.29	0.85	1.06	7.90	1.727	2.00	0.88	160.60	1.11
		5.42	7500	600	185.3	182.8	182.8	183.0	194.0	1.14	2.29	1.03	0.59	241.61	0.76	1.06	7.90	1.727	2.00	0.88	160.60	1.14
		5.42	7500	750	189.5	185.1	185.1	183.0	194.0	1.15	2.56	1.03	0.59	269.07	0.69	1.06	7.90	1.727	2.00	0.88	160.60	1.15
R3_L6	120x60x15x25x5	5.42	8000	150	135.2	124.6	124.6	170.3	170.5	0.94	1.19	1.03	0.59	133.05	0.94	1.00	8.97	1.993	2.00	0.88	133.05	0.94
		5.42	8000	300	156.7	151.7	151.7	170.3	170.5	1.02	1.68	1.03	0.59	166.59	0.91	1.00	8.97	1.993	2.00	0.88	149.41	1.02
		5.42	8000	450	164.8	158.3	158.3	170.3	170.5	1.06	2.06	1.03	0.59	202.58	0.78	1.00	8.97	1.993	2.00	0.88	149.41	1.06
		5.42	8000	600	169.1	161.5	161.5	170.3	170.5	1.08	2.37	1.03	0.59	232.75	0.69	1.00	8.97	1.993	2.00	0.88	149.41	1.08
		5.42	8000	750	171.4	163.3	163.3	170.3	170.5	1.09	2.65	1.03	0.59	259.21	0.63	1.00	8.97	1.993	2.00	0.88	149.41	1.09
R4_L1	140x70x10x20x5	6.15	5500	150	197.4	201.3	197.4	304.6	436.5	1.10	0.92	1.08	0.60	179.62	1.10	1.43	2.81	0.909	1.28	0.65	179.62	1.10
		6.15	5500	300	266.9	320.0	266.9	304.6	436.5	1.05	1.29	1.08	0.60	253.04	1.05	1.43	2.81	0.909	1.28	0.65	253.04	1.05
		6.15	5500	450	296.1	371.9	296.1	304.6	436.5	1.11	1.58	1.08	0.60	281.15	1.05	1.43	2.81	0.909	1.28	0.65	278.09	1.06
		6.15	5500	600	319.5	391.3	319.5	304.6	436.5	1.20	1.83	1.08	0.60	320.96	1.00	1.43	2.81	0.909	1.28	0.65	308.52	1.04
		6.15	5500	750	340.8	401.8	340.8	304.6	436.5	1.28	2.05	1.08	0.60	355.69	0.96	1.43	2.81	0.909	1.28	0.65	334.40	1.02
R4_L2	140x70x10x20x5	6.15	6000	150	187.8	196.5	187.8	271.8	367.0	1.09	0.97	1.08	0.60	172.19	1.09	1.35	3.39	1.124	1.49	0.71	172.19	1.09
		6.15	6000	300	244.3	285.5	244.3	271.8	367.0	1.05	1.37	1.08	0.60	232.55	1.05	1.35	3.39	1.124	1.49	0.71	232.55	1.05
		6.15	6000	450	270.1	321.0	270.1	271.8	367.0	1.13	1.68	1.08	0.60	264.41	1.02	1.35	3.39	1.124	1.49	0.71	252.46	1.07
		6.15	6000	600	291.2	333.8	291.2	271.8	367.0	1.22	1.94	1.08	0.60	301.86	0.96	1.35	3.39	1.124	1.49	0.71	271.56	1.07
		6.15	6000	750	308.9	341.3	308.9	271.8	367.0	1.30	2.17	1.08	0.60	334.52	0.92	1.35	3.39	1.124	1.49	0.71	287.38	1.07
R4_L3	140x70x10x20x5	6.15	6500	150	178.3	182.7	178.3	246.0	312.8	1.08	1.02	1.08	0.60	165.25	1.08	1.27	4.02	1.257	1.63	0.75	165.25	1.08
		6.15	6500	300	225.3	254.6	225.3	246.0	312.8	1.05	1.44	1.08	0.60	214.19	1.05	1.27	4.02	1.257	1.63	0.75	214.19	1.05
		6.15	6500	450	248.3	278.5	248.3	246.0	312.8	1.15	1.76	1.08	0.60	250.57	0.99	1.27	4.02	1.257	1.63	0.75	229.36	1.08
		6.15	6500	600	266.5	288.6	266.5	246.0	312.8	1.23	2.04	1.08	0.60	286.06	0.93	1.27	4.02	1.257	1.63	0.75	242.02	1.10
		6.15	6500	750	280.6	293.3	280.6	246.0	312.8	1.30	2.28	1.08	0.60	317.01	0.89	1.27	4.02	1.257	1.63	0.75	252.33	1.11
R4_L4	140x70x10x20x5	6.15	7000	150	169.3	162.9	162.9	225.3	269.8	1.03	1.06	1.08	0.60	158.78	1.03	1.20	4.69	1.373	1.74	0.79	158.7	

Column	Geometry		SFEA					DSM Design															
	$b_w \times b_f \times b_l \times b_s \times t$	β_{FT}	L	f_y	$P_{u,FT}$	$P_{u,Fm}$	P_u	$P_{cr,FT}$	$P_{b,Fm}$	$\frac{P_u}{P_{nG}}$	λ_{FT}	b	a	P_{nFT}	$\frac{P_u}{P_{nFT}}$	R_G	R_{DL}	c	b	a	P_{nFT-Fm}	$\frac{P_u}{P_{nFT-Fm}}$	
R5_L1	100x50x10x15x3		6.71	4000	150	83.2	91.7	83.2	122.7	192.2	1.09	0.96	1.11	0.61	76.65	1.09	1.57	2.40	0.71	1.11	0.61	76.65	1.09
			6.71	4000	300	109.8	144.1	109.8	122.7	192.2	1.05	1.35	1.11	0.61	104.44	1.05	1.57	2.40	0.71	1.11	0.61	104.44	1.05
			6.71	4000	450	121.6	164.2	121.6	122.7	192.2	1.13	1.66	1.11	0.61	117.71	1.03	1.57	2.40	0.71	1.11	0.61	117.71	1.03
			6.71	4000	600	131.6	172.5	131.6	122.7	192.2	1.22	1.92	1.11	0.61	133.74	0.98	1.57	2.40	0.71	1.11	0.61	133.74	0.98
R5_L2	100x50x10x15x3		6.71	4500	150	76.1	85.3	76.1	103.2	152.0	1.07	1.04	1.11	0.61	71.27	1.07	1.47	3.11	0.757	1.16	0.62	71.27	1.07
			6.71	4500	300	95.9	121.9	95.9	103.2	152.0	1.06	1.48	1.11	0.61	90.31	1.06	1.47	3.11	0.757	1.16	0.62	90.31	1.06
			6.71	4500	450	106.4	133.8	106.4	103.2	152.0	1.18	1.81	1.11	0.61	106.88	1.00	1.47	3.11	0.757	1.16	0.62	105.94	1.00
			6.71	4500	600	115.4	139.2	115.4	103.2	152.0	1.28	2.09	1.11	0.61	121.43	0.95	1.47	3.11	0.757	1.16	0.62	119.54	0.97
R5_L3	100x50x10x15x3		6.71	5000	150	69.4	76.9	69.4	89.1	123.2	1.05	1.12	1.11	0.61	66.30	1.05	1.38	3.90	1.049	1.45	0.70	66.30	1.05
			6.71	5000	300	85.2	103.6	85.2	89.1	123.2	1.09	1.59	1.11	0.61	82.27	1.04	1.38	3.90	1.049	1.45	0.70	80.67	1.06
			6.71	5000	450	94.6	111.1	94.6	89.1	123.2	1.21	1.95	1.11	0.61	98.49	0.96	1.38	3.90	1.049	1.45	0.70	90.15	1.05
			6.71	5000	600	102.2	114.3	102.2	89.1	123.2	1.31	2.25	1.11	0.61	111.89	0.91	1.38	3.90	1.049	1.45	0.70	97.54	1.05
R5_L4	100x50x10x15x3		6.71	5500	150	63.7	69.4	63.7	78.5	101.9	1.03	1.20	1.11	0.61	61.75	1.03	1.30	4.80	1.216	1.62	0.75	61.75	1.03
			6.71	5500	300	76.8	88.3	76.8	78.5	101.9	1.12	1.69	1.11	0.61	76.70	1.00	1.30	4.80	1.216	1.62	0.75	72.14	1.06
			6.71	5500	450	84.9	93.3	84.9	78.5	101.9	1.23	2.07	1.11	0.61	91.81	0.92	1.30	4.80	1.216	1.62	0.75	77.94	1.09
			6.71	5500	600	90.8	95.5	90.8	78.5	101.9	1.32	2.39	1.11	0.61	104.31	0.87	1.30	4.80	1.216	1.62	0.75	82.34	1.10
R5_L5	100x50x10x15x3		6.71	6000	150	58.7	63.2	58.7	70.4	85.6	1.02	1.26	1.11	0.61	57.61	1.02	1.22	5.79	1.34	1.74	0.79	57.61	1.02
			6.71	6000	300	69.9	75.6	69.9	70.4	85.6	1.13	1.79	1.11	0.61	72.16	0.97	1.22	5.79	1.34	1.74	0.79	64.60	1.08
			6.71	6000	450	76.5	79.2	76.5	70.4	85.6	1.24	2.19	1.11	0.61	86.39	0.89	1.22	5.79	1.34	1.74	0.79	68.06	1.12
			6.71	6000	600	80.7	80.9	80.7	70.4	85.6	1.31	2.53	1.11	0.61	98.15	0.82	1.22	5.79	1.34	1.74	0.79	70.63	1.14
R5_L6	100x50x10x15x3		6.71	7000	150	50.8	48.7	48.7	58.7	62.9	0.97	1.38	1.11	0.61	50.44	0.97	1.07	7.90	1.682	2.00	0.88	50.44	0.97
			6.71	7000	300	58.6	57.1	57.1	58.7	62.9	1.11	1.96	1.11	0.61	65.24	0.87	1.07	7.90	1.682	2.00	0.88	51.50	1.11
			6.71	7000	450	62.2	59.1	59.1	58.7	62.9	1.15	2.40	1.11	0.61	78.10	0.76	1.07	7.90	1.682	2.00	0.88	51.50	1.15
			6.71	7000	750	64.2	60.6	60.6	58.7	62.9	1.18	3.10	1.11	0.61	97.97	0.62	1.07	7.90	1.682	2.00	0.88	51.50	1.18
R6_L1	90x50x10x15x3		5.73	5000	150	62.5	75.1	62.5	77.7	118.7	1.03	1.18	1.05	0.60	60.38	1.03	1.53	4.13	0.71	1.05	0.60	60.38	1.03
			5.73	5000	300	76.1	99.7	76.1	77.7	118.7	1.12	1.67	1.05	0.60	75.38	1.01	1.53	4.13	0.71	1.05	0.60	75.38	1.01
			5.73	5000	450	85.2	107.4	85.2	77.7	118.7	1.25	2.04	1.05	0.60	91.32	0.93	1.53	4.13	0.71	1.05	0.60	91.32	0.93
			5.73	5000	600	92.8	110.5	92.8	77.7	118.7	1.36	2.36	1.05	0.60	104.64	0.89	1.53	4.13	0.71	1.05	0.60	104.64	0.89
R6_L2	90x50x10x15x3		5.73	5500	150	57.2	68.2	57.2	68.8	98.2	1.02	1.25	1.05	0.60	55.97	1.02	1.43	5.08	0.929	1.27	0.65	55.97	1.02
			5.73	5500	300	68.8	84.4	68.8	68.8	98.2	1.14	1.77	1.05	0.60	70.67	0.97	1.43	5.08	0.929	1.27	0.65	68.14	1.01
			5.73	5500	450	76.7	90.0	76.7	68.8	98.2	1.27	2.17	1.05	0.60	85.61	0.90	1.43	5.08	0.929	1.27	0.65	78.97	0.97
			5.73	5500	750	86.8	93.4	86.8	68.8	98.2	1.44	2.80	1.05	0.60	109.02	0.80	1.43	5.08	0.929	1.27	0.65	87.68	0.94
R6_L3	90x50x10x15x3		5.73	6000	150	52.8	60.0	52.8	61.8	82.5	1.02	1.32	1.05	0.60	51.98	1.02	1.33	6.12	1.153	1.50	0.72	51.98	1.02
			5.73	6000	300	62.7	73.1	62.7	61.8	82.5	1.16	1.87	1.05	0.60	66.80	0.94	1.33	6.12	1.153	1.50	0.72	60.59	1.04
			5.73	6000	450	69.3	76.4	69.3	61.8	82.5	1.28	2.29	1.05	0.60	80.93	0.86	1.33	6.12	1.153	1.50	0.72	67.10	1.03
			5.73	6000	600	73.7	78.0	73.7	61.8	82.5	1.36	2.64	1.05	0.60	92.73	0.79	1.33	6.12	1.153	1.50	0.72	72.13	1.02
R6_L4	90x50x10x15x3		5.73	7000	150	45.6	46.9	45.6	51.7	60.6	1.01	1.44	1.05	0.60	45.08	1.01	1.17	8.33	1.419	1.76	0.80	45.08	1.01
			5.73	7000	300	52.7	55.0	52.7	51.7	60.6	1.16	2.04	1.05	0.60	60.82	0.87	1.17	8.33	1.419	1.76	0.80	48.85	1.08
			5.73	7000	450	56.6	57.0	56.6	51.7	60.6	1.25	2.50	1.05	0.60	73.69	0.77	1.17	8.33	1.419	1.76	0.80	51.25	1.10
			5.73	7000	750	59.5	58.4	58.4	51.7	60.6	1.29	3.23	1.05	0.60	93.83	0.62	1.17	8.33	1.419	1.76	0.80	53.03	1.09
R6_L5	90x50x10x15x3		5.73	7500	150	42.6	43.5	42.6	48.0	52.8	1.01	1.50	1.05	0.60	42.10	1.01	1.10	9.59	1.588	1.93	0.85	42.08	1.01
			5.73	7500	300	48.5	48.4	48.4	48.0	52.8	1.15	2.12	1.05	0.60	58.44	0.83	1.10	9.59	1.588	1.93	0.85	43.09	1.12
			5.73	7500	450	51.2	49.9	49.9	48.0	52.8	1.19	2.60	1.05	0.60	70.80	0.71	1.10	9.59	1.588	1.93	0.85	43.69	1.14
			5.73	7500	600	52.3	50.6	50.6	48.0	52.8	1.20	3.00	1.05	0.60	81.12	0.62	1.10	9.59	1.588	1.93	0.85	44.12	1.15
R6_L6	90x50x10x15x3		5.73	8000	150	40.0	38.9																

Column	Geometry			SFEA					DSM Design															
	$b_w \times b_f \times b_l \times b_s \times t$	β_{FT}	L	f_y	$P_{u,FT}$	$P_{u,Fm}$	P_u	$P_{cr,FT}$	$P_{b,Fm}$	$\frac{P_u}{P_{nG}}$	λ_{FT}	b	a	P_{nFT}	$\frac{P_u}{P_{nFT}}$	R_G	R_{DL}	c	b	a	P_{nFT-Fm}	$\frac{P_u}{P_{nFT-Fm}}$		
R7_L1	130x60x15x20x5			6.49	3500	150	216.3	214.6	556.4	802.7	1.07	0.66	1.10	0.61	200.36	1.07	1.44	1.82	0.877	1.27	0.65	200.36	1.07	
				6.49	3500	300	377.9	408.5	377.9	556.4	802.7	1.13	0.93	1.10	0.61	334.52	1.13	1.44	1.82	0.877	1.27	0.65	334.52	1.13
				6.49	3500	450	461.1	550.0	461.1	556.4	802.7	1.10	1.14	1.10	0.61	418.90	1.10	1.44	1.82	0.877	1.27	0.65	418.90	1.10
				6.49	3500	600	500.3	633.6	500.3	556.4	802.7	1.07	1.31	1.10	0.61	466.28	1.07	1.44	1.82	0.877	1.27	0.65	466.28	1.07
				6.49	3500	750	522.6	679.1	522.6	556.4	802.7	1.07	1.47	1.10	0.61	486.57	1.07	1.44	1.82	0.877	1.27	0.65	486.57	1.07
R7_L2	130x60x15x20x5			6.49	4000	150	210.4	199.8	199.8	452.5	617.4	1.04	0.73	1.10	0.61	192.23	1.04	1.36	2.38	1.094	1.48	0.71	192.23	1.04
				6.49	4000	300	342.2	367.3	342.2	452.5	617.4	1.11	1.03	1.10	0.61	307.92	1.11	1.36	2.38	1.094	1.48	0.71	307.92	1.11
				6.49	4000	450	395.6	475.8	395.6	452.5	617.4	1.07	1.26	1.10	0.61	369.94	1.07	1.36	2.38	1.094	1.48	0.71	369.94	1.07
				6.49	4000	600	421.8	514.7	421.8	452.5	617.4	1.07	1.46	1.10	0.61	395.06	1.07	1.36	2.38	1.094	1.48	0.71	395.06	1.07
				6.49	4000	750	440.4	547.3	440.4	452.5	617.4	1.11	1.63	1.10	0.61	427.59	1.03	1.36	2.38	1.094	1.48	0.71	414.32	1.06
R7_L3	130x60x15x20x5			6.49	4500	150	187.9	185.4	185.4	380.8	488.9	1.01	0.79	1.10	0.61	184.35	1.01	1.28	3.07	1.238	1.63	0.75	184.35	1.01
				6.49	4500	300	255.3	261.2	255.3	380.8	488.9	0.90	1.12	1.10	0.61	283.20	0.90	1.28	3.07	1.238	1.63	0.75	283.20	0.90
				6.49	4500	450	278.5	298.5	278.5	380.8	488.9	0.85	1.38	1.10	0.61	326.30	0.85	1.28	3.07	1.238	1.63	0.75	326.30	0.85
				6.49	4500	600	293.6	310.6	293.6	380.8	488.9	0.88	1.59	1.10	0.61	351.70	0.83	1.28	3.07	1.238	1.63	0.75	341.30	0.86
				6.49	4500	750	305.4	316.9	305.4	380.8	488.9	0.91	1.78	1.10	0.61	388.87	0.79	1.28	3.07	1.238	1.63	0.75	355.80	0.86
R7_L4	130x60x15x20x5			6.49	5000	150	194.6	184.0	184.0	329.0	396.5	1.04	0.85	1.10	0.61	176.84	1.04	1.21	3.88	1.36	1.75	0.79	176.84	1.04
				6.49	5000	300	276.6	296.8	276.6	329.0	396.5	1.06	1.21	1.10	0.61	260.61	1.06	1.21	3.88	1.36	1.75	0.79	260.61	1.06
				6.49	5000	450	304.4	341.0	304.4	329.0	396.5	1.06	1.48	1.10	0.61	288.05	1.06	1.21	3.88	1.36	1.75	0.79	288.05	1.06
				6.49	5000	600	321.7	356.2	321.7	329.0	396.5	1.12	1.71	1.10	0.61	324.52	0.99	1.21	3.88	1.36	1.75	0.79	298.26	1.08
				6.49	5000	750	335.8	366.2	335.8	329.0	396.5	1.16	1.91	1.10	0.61	358.82	0.94	1.21	3.88	1.36	1.75	0.79	306.76	1.09
R7_L5	130x60x15x20x5			6.49	5500	150	186.4	173.7	173.7	290.1	328.0	1.02	0.91	1.10	0.61	169.77	1.02	1.13	4.76	1.51	1.90	0.84	169.77	1.02
				6.49	5500	300	250.5	254.8	250.5	290.1	328.0	1.04	1.29	1.10	0.61	240.17	1.04	1.13	4.76	1.51	1.90	0.84	240.17	1.04
				6.49	5500	450	272.8	288.7	272.8	290.1	328.0	1.07	1.58	1.10	0.61	266.08	1.03	1.13	4.76	1.51	1.90	0.84	255.86	1.07
				6.49	5500	600	287.1	300.4	287.1	290.1	328.0	1.13	1.82	1.10	0.61	302.88	0.95	1.13	4.76	1.51	1.90	0.84	259.61	1.11
				6.49	5500	750	298.5	306.2	298.5	290.1	328.0	1.17	2.03	1.10	0.61	334.90	0.89	1.13	4.76	1.51	1.90	0.84	262.55	1.14
R7_L6	130x60x15x20x5			6.49	6200	150	173.9	165.4	165.4	250.0	258.2	1.03	0.98	1.10	0.61	160.60	1.03	1.03	6.17	1.839	2.00	0.88	160.60	1.03
				6.49	6200	300	221.0	215.0	215.0	250.0	258.2	1.00	1.39	1.10	0.61	214.93	1.00	1.03	6.17	1.839	2.00	0.88	214.93	1.00
				6.49	6200	450	237.6	233.3	233.3	250.0	258.2	1.06	1.70	1.10	0.61	245.19	0.95	1.03	6.17	1.839	2.00	0.88	219.41	1.06
				6.49	6200	600	247.8	240.0	240.0	250.0	258.2	1.09	1.96	1.10	0.61	279.10	0.86	1.03	6.17	1.839	2.00	0.88	219.41	1.09
				6.49	6200	750	254.9	243.7	243.7	250.0	258.2	1.11	2.19	1.10	0.61	308.60	0.79	1.03	6.17	1.839	2.00	0.88	219.41	1.11
R8_L1	120x70x10x15x5			5.06	5500	150	171.7	179.5	171.7	246.2	366.8	1.10	0.97	1.01	0.59	156.60	1.10	1.49	3.67	0.71	1.01	0.59	156.60	1.10
				5.06	5500	300	222.1	275.1	222.1	246.2	366.8	1.05	1.37	1.01	0.59	210.96	1.05	1.49	3.67	0.71	1.01	0.59	210.96	1.05
				5.06	5500	450	245.7	318.3	245.7	246.2	366.8	1.14	1.68	1.01	0.59	242.06	1.02	1.49	3.67	0.71	1.01	0.59	242.06	1.02
				5.06	5500	600	266.1	333.0	266.1	246.2	366.8	1.23	1.94	1.01	0.59	278.95	0.95	1.49	3.67	0.71	1.01	0.59	278.95	0.95
				5.06	5500	750	284.1	340.8	284.1	246.2	366.8	1.32	2.17	1.01	0.59	311.39	0.91	1.49	3.67	0.71	1.01	0.59	311.39	0.91
R8_L2	120x70x10x15x5			5.06	6000	150	162.3	163.8	162.3	222.0	308.3	1.08	1.02	1.01	0.59	149.98	1.08	1.39	4.43	1.037	1.34	0.67	149.98	1.08
				5.06	6000	300	204.1	249.8	204.1	222.0	308.3	1.05	1.45	1.01	0.59	193.51	1.05	1.39	4.43	1.037	1.34	0.67	193.51	1.05
				5.06	6000	450	225.2	273.4	225.2	222.0	308.3	1.16	1.77	1.01	0.59	229.66	0.98	1.39	4.43	1.037	1.34	0.67	217.45	1.04
				5.06	6000	600	242.8	283.6	242.8	222.0	308.3	1.25	2.05	1.01	0.59	264.66	0.92	1.39	4.43	1.037	1.34	0.67	239.06	1.02
				5.06	6000	750	257.4	289.1	257.4	222.0	308.3	1.32	2.29	1.01	0.59	295.44	0.87	1.39	4.43	1.037	1.34	0.67	257.29	1.00
R8_L3	120x70x10x15x5			5.06	6500	150	153.6	159.2	153.6	202.7	262.7	1.07	1.07	1.01	0.59	143.85	1.07	1.30	5.25	1.219	1.52	0.72	143.85	1.07
				5.06	6500	300	188.9	220.1	188.9	202.7	262.7	1.06	1.51	1.01	0.59	179.57	1.05	1.30	5.25	1.219	1.52	0.72	178.68	1.06
				5.06</																				

Table I.3: RLC column (i) geometries, (ii) β_{FT} values, (iii) yield stresses, (iv) buckling load values and ratios, (v) numerical failure loads, (vi) failure load predictions estimates P_{nG} , P_{nFT} and P_{nFT-Fm} , and (vii) numerical-to-predicted failure loads ratios (mm, kN)

Column	Geometry			SFEA					DSM Design													
	$b_w \times b_f \times b_t \times b_s \times t$	β_{FT}	L	f_y	$P_{u,FT}$	$P_{u,Fm}$	P_u	$P_{cr,FT}$	$P_{b,Fm}$	$\frac{P_u}{P_{cr}}$	λ_{FT}	b	a	P_{nFT}	$\frac{P_u}{P_{nFT}}$	R_G	R_{DL}	c	b	a	P_{nFT-Fm}	$\frac{P_u}{P_{nFT-Fm}}$
RLC1_L1	80x55x10x15x4	4.34	4500	150	94.9	94.6	94.6	126.1	182.5	1.06	1.07	0.97	0.58	89.27	1.06	1.45	7.55	0.86	1.12	0.61	89.27	1.06
		4.34	4500	300	116.1	143.0	116.1	126.1	182.5	1.05	1.51	0.97	0.58	111.49	1.04	1.45	7.55	0.86	1.12	0.61	111.36	1.04
		4.34	4500	450	126.4	163.4	126.4	126.1	182.5	1.14	1.85	0.97	0.58	137.37	0.92	1.45	7.55	0.86	1.12	0.61	133.13	0.95
		4.34	4500	600	135.1	168.4	135.1	126.1	182.5	1.22	2.14	0.97	0.58	159.31	0.85	1.45	7.55	0.86	1.12	0.61	151.11	0.89
		4.34	4500	750	142.7	172.1	142.7	126.1	182.5	1.29	2.39	0.97	0.58	178.70	0.80	1.45	7.55	0.86	1.12	0.61	166.72	0.86
RLC1_L2	80x55x10x15x4	4.34	4750	150	91.3	103.1	91.3	118.6	163.8	1.05	1.10	0.97	0.58	86.62	1.05	1.38	8.50	1.06	1.32	0.66	86.62	1.05
		4.34	4750	300	110.0	139.4	110.0	118.6	163.8	1.06	1.56	0.97	0.58	108.23	1.02	1.38	8.50	1.06	1.32	0.66	106.81	1.03
		4.34	4750	450	119.5	146.3	119.5	118.6	163.8	1.15	1.91	0.97	0.58	133.36	0.90	1.38	8.50	1.06	1.32	0.66	122.72	0.97
		4.34	4750	600	127.3	151.4	127.3	118.6	163.8	1.22	2.20	0.97	0.58	154.65	0.82	1.38	8.50	1.06	1.32	0.66	135.42	0.94
		4.34	4750	750	133.8	155.3	133.8	118.6	163.8	1.29	2.46	0.97	0.58	173.48	0.77	1.38	8.50	1.06	1.32	0.66	146.17	0.92
RLC1_L3	80x55x10x15x4	4.34	5000	150	87.9	86.4	86.4	112.0	147.9	1.03	1.13	0.97	0.58	84.09	1.03	1.32	9.50	1.18	1.44	0.70	84.09	1.03
		4.34	5000	300	104.5	126.3	104.5	112.0	147.9	1.06	1.60	0.97	0.58	105.29	0.99	1.32	9.50	1.18	1.44	0.70	102.05	1.02
		4.34	5000	450	113.1	135.9	113.1	112.0	147.9	1.15	1.96	0.97	0.58	129.74	0.87	1.32	9.50	1.18	1.44	0.70	114.32	0.99
		4.34	5000	600	115.3	139.4	115.3	112.0	147.9	1.17	2.27	0.97	0.58	150.45	0.77	1.32	9.50	1.18	1.44	0.70	123.90	0.93
		4.34	5000	750	121.5	141.3	121.5	112.0	147.9	1.24	2.53	0.97	0.58	168.77	0.72	1.32	9.50	1.18	1.44	0.70	131.89	0.92
RLC1_L4	80x55x10x15x4	4.34	5500	150	81.5	88.1	81.5	101.1	122.2	1.03	1.19	0.97	0.58	79.33	1.03	1.21	11.70	1.35	1.61	0.75	79.33	1.03
		4.34	5500	300	95.0	108.1	95.0	101.1	122.2	1.07	1.69	0.97	0.58	100.17	0.95	1.21	11.70	1.35	1.61	0.75	92.85	1.02
		4.34	5500	450	101.8	113.3	101.8	101.1	122.2	1.15	2.07	0.97	0.58	123.43	0.82	1.21	11.70	1.35	1.61	0.75	100.42	1.01
		4.34	5500	600	106.7	116.1	106.7	101.1	122.2	1.20	2.39	0.97	0.58	143.13	0.75	1.21	11.70	1.35	1.61	0.75	106.16	1.01
		4.34	5500	750	110.4	117.3	110.4	101.1	122.2	1.24	2.67	0.97	0.58	160.56	0.69	1.21	11.70	1.35	1.61	0.75	110.84	1.00
RLC1_L5	80x55x10x15x4	4.34	6000	150	75.9	76.8	75.9	92.2	102.7	1.01	1.25	0.97	0.58	74.91	1.01	1.11	14.15	1.55	1.81	0.81	74.91	1.01
		4.34	6000	300	86.7	90.9	86.7	92.2	102.7	1.07	1.77	0.97	0.58	95.81	0.91	1.11	14.15	1.55	1.81	0.81	83.44	1.04
		4.34	6000	450	91.8	96.3	91.8	92.2	102.7	1.13	2.16	0.97	0.58	118.05	0.78	1.11	14.15	1.55	1.81	0.81	86.66	1.06
		4.34	6000	600	95.1	98.1	95.1	92.2	102.7	1.18	2.50	0.97	0.58	136.89	0.69	1.11	14.15	1.55	1.81	0.81	89.02	1.07
		4.34	6000	750	97.2	98.9	97.2	92.2	102.7	1.20	2.79	0.97	0.58	153.56	0.63	1.11	14.15	1.55	1.81	0.81	90.89	1.07
RLC1_L6	80x55x10x15x4	4.34	6500	150	70.8	66.3	66.3	84.8	87.5	0.94	1.30	0.97	0.58	70.75	0.94	1.03	16.81	1.84	2.00	0.88	70.75	0.94
		4.34	6500	300	79.4	79.7	79.4	84.8	87.5	1.07	1.84	0.97	0.58	91.99	0.86	1.03	16.81	1.84	2.00	0.88	74.43	1.07
		4.34	6500	450	82.1	82.7	82.1	84.8	87.5	1.10	2.26	0.97	0.58	113.35	0.72	1.03	16.81	1.84	2.00	0.88	74.43	1.10
		4.34	6500	600	84.8	83.7	83.7	84.8	87.5	1.12	2.61	0.97	0.58	131.45	0.64	1.03	16.81	1.84	2.00	0.88	74.43	1.12
		4.34	6500	750	85.8	84.7	84.7	84.8	87.5	1.14	2.91	0.97	0.58	147.45	0.57	1.03	16.81	1.84	2.00	0.88	74.43	1.14
RLC2_L1	100x60x15x15x4	5.68	4500	150	124.1	129.4	124.1	181.4	264.3	1.09	0.96	1.05	0.60	114.03	1.09	1.46	5.36	0.83	1.17	0.63	114.03	1.09
		5.68	4500	300	161.4	203.6	161.4	181.4	264.3	1.04	1.36	1.05	0.60	154.79	1.04	1.46	5.36	0.83	1.17	0.63	154.79	1.04
		5.68	4500	450	176.0	224.0	176.0	181.4	264.3	1.11	1.67	1.05	0.60	175.96	1.00	1.46	5.36	0.83	1.17	0.63	173.82	1.01
		5.68	4500	600	187.3	236.1	187.3	181.4	264.3	1.18	1.92	1.05	0.60	201.71	0.93	1.46	5.36	0.83	1.17	0.63	195.94	0.96
		5.68	4500	750	197.6	247.4	197.6	181.4	264.3	1.24	2.15	1.05	0.60	224.25	0.88	1.46	5.36	0.83	1.17	0.63	215.02	0.92
RLC2_L2	100x60x15x15x4	5.68	5000	150	115.3	120.8	115.3	157.4	214.2	1.07	1.03	1.05	0.60	107.49	1.07	1.36	6.69	1.10	1.44	0.70	107.49	1.07
		5.68	5000	300	143.4	173.5	143.4	157.4	214.2	1.04	1.46	1.05	0.60	137.54	1.04	1.36	6.69	1.10	1.44	0.70	137.54	1.07
		5.68	5000	450	155.8	191.1	155.8	157.4	214.2	1.13	1.79	1.05	0.60	163.33	0.95	1.36	6.69	1.10	1.44	0.70	152.43	1.02
		5.68	5000	600	165.7	199.6	165.7	157.4	214.2	1.20	2.07	1.05	0.60	187.22	0.89	1.36	6.69	1.10	1.44	0.70	165.16	1.00
		5.68	5000	750	174.2	202.9	174.2	157.4	214.2	1.26	2.31	1.05	0.60	208.14	0.84	1.36	6.69	1.10	1.44	0.70	175.76	0.99
RLC2_L3	100x60x15x15x4	5.68	5500	150	106.8	117.0	106.8	139.4	177.1	1.05	1.10	1.05	0.60	101.43	1.05	1.27	8.29	1.26	1.60	0.75	101.43	1.05
		5.68	5500	300	129.1	152.6	129.1	139.4	177.1	1.06	1.55	1.05	0.60	126.37	1.02	1.27	8.29	1.26	1.60	0.75	124.00	1.04
		5.68	5500	450	139.6	161.2	139.6	139.4	177.1	1.14	1.90	1.05	0.60	153.19	0.91	1.27	8.29	1.26	1.60	0.75	134.53	1.04
		5.68	5500	600	147.8	165.9	147.8	139.4	177.1	1.21	2.20	1.05	0.60	175.60	0.84	1.27	8.29	1.26	1.60	0.75	142.54	1.04
		5.68	5500	750	154.3	168.7	154.3	139.4	177.1	1.26	2.46	1.05	0.60	195.22	0.79	1.27	8.29	1.26	1.60	0.75	149.07	1.04
RLC2_L4	100x60x15x15x4	5.68	6000	150	99.3	103.2	99.3	125.3	148.9	1.04	1.16	1.05	0.60	95.85	1.04	1.19	10.09	1.3				

Column	Geometry			SFEA				DSM Design																
	$b_w \times b_f \times b_l \times b_s \times t$	β_{FT}	L	f_y	$P_{u,FT}$	$P_{u,Fm}$	P_u	$P_{cr,FT}$	$P_{b,Fm}$	$\frac{P_u}{P_{nG}}$	λ_{FT}	b	a	P_{nFT}	$\frac{P_u}{P_{nFT}}$	R_G	R_{DL}	c	b	a	P_{nFT-Fm}	$\frac{P_u}{P_{nFT-Fm}}$		
RLC3_L1	120x70x20x20x5			5.87	5000	150	201.7	193.7	322.8	446.9	1.06	0.89	1.06	0.60	183.20	1.06	1.38	5.53	1.05	1.40	0.69	183.20	1.06	
				5.87	5000	300	276.7	308.0	276.7	322.8	446.9	1.05	1.26	1.06	0.60	263.23	1.05	1.38	5.53	1.05	1.40	0.69	263.23	1.05
				5.87	5000	450	301.7	372.7	301.7	322.8	446.9	1.07	1.54	1.06	0.60	290.21	1.04	1.38	5.53	1.05	1.40	0.69	287.68	1.05
				5.87	5000	600	318.3	406.6	318.3	322.8	446.9	1.12	1.78	1.06	0.60	332.13	0.96	1.38	5.53	1.05	1.40	0.69	313.63	1.02
				5.87	5000	750	332.6	414.8	332.6	322.8	446.9	1.18	1.99	1.06	0.60	368.77	0.90	1.38	5.53	1.05	1.40	0.69	335.36	0.99
RLC3_L2	120x70x20x20x5			5.87	5500	150	190.7	201.5	190.7	282.4	369.7	1.09	0.95	1.06	0.60	174.74	1.09	1.31	6.61	1.20	1.55	0.73	174.74	1.09
				5.87	5500	300	248.2	294.7	248.2	282.4	369.7	1.04	1.34	1.06	0.60	239.48	1.04	1.31	6.61	1.20	1.55	0.73	239.48	1.04
				5.87	5500	450	268.7	320.6	268.7	282.4	369.7	1.08	1.65	1.06	0.60	270.34	0.99	1.31	6.61	1.20	1.55	0.73	258.38	1.04
				5.87	5500	600	283.1	338.4	283.1	282.4	369.7	1.14	1.90	1.06	0.60	309.38	0.92	1.31	6.61	1.20	1.55	0.73	275.68	1.03
				5.87	5500	750	295.6	346.9	295.6	282.4	369.7	1.19	2.12	1.06	0.60	343.51	0.86	1.31	6.61	1.20	1.55	0.73	289.89	1.02
RLC3_L3	120x70x20x20x5			5.87	6000	150	179.5	174.3	174.3	251.3	310.9	1.05	1.01	1.06	0.60	166.75	1.05	1.24	7.89	1.31	1.66	0.76	166.75	1.05
				5.87	6000	300	224.9	240.1	224.9	251.3	310.9	1.03	1.42	1.06	0.60	218.08	1.03	1.24	7.89	1.31	1.66	0.76	218.08	1.03
				5.87	6000	450	242.0	282.4	242.0	251.3	310.9	1.10	1.74	1.06	0.60	254.08	0.95	1.24	7.89	1.31	1.66	0.76	232.10	1.04
				5.87	6000	600	254.4	290.3	254.4	251.3	310.9	1.15	2.01	1.06	0.60	290.78	0.87	1.24	7.89	1.31	1.66	0.76	243.72	1.04
				5.87	6000	750	264.7	294.6	264.7	251.3	310.9	1.20	2.25	1.06	0.60	322.86	0.82	1.24	7.89	1.31	1.66	0.76	253.14	1.05
RLC3_L4	120x70x20x20x5			5.87	6500	150	168.8	175.6	168.8	226.6	265.0	1.06	1.06	1.06	0.60	159.23	1.06	1.17	9.40	1.42	1.78	0.80	159.23	1.06
				5.87	6500	300	205.4	220.8	205.4	226.6	265.0	1.03	1.50	1.06	0.60	198.89	1.03	1.17	9.40	1.42	1.78	0.80	198.88	1.03
				5.87	6500	450	219.9	242.5	219.9	226.6	265.0	1.11	1.84	1.06	0.60	240.54	0.91	1.17	9.40	1.42	1.78	0.80	208.12	1.06
				5.87	6500	600	230.1	247.9	230.1	226.6	265.0	1.16	2.12	1.06	0.60	275.28	0.84	1.17	9.40	1.42	1.78	0.80	214.94	1.07
				5.87	6500	750	238.1	251.2	238.1	226.6	265.0	1.20	2.37	1.06	0.60	305.65	0.78	1.17	9.40	1.42	1.78	0.80	220.38	1.08
RLC3_L5	120x70x20x20x5			5.87	7000	150	158.9	163.1	158.9	206.7	228.6	1.04	1.11	1.06	0.60	152.16	1.04	1.11	11.13	1.57	1.93	0.85	152.16	1.04
				5.87	7000	300	189.0	194.9	189.0	206.7	228.6	1.04	1.57	1.06	0.60	189.40	1.00	1.11	11.13	1.57	1.93	0.85	182.00	1.04
				5.87	7000	450	200.9	212.3	200.9	206.7	228.6	1.11	1.92	1.06	0.60	229.06	0.88	1.11	11.13	1.57	1.93	0.85	184.73	1.09
				5.87	7000	600	209.0	216.3	209.0	206.7	228.6	1.15	2.22	1.06	0.60	262.14	0.80	1.11	11.13	1.57	1.93	0.85	186.69	1.12
				5.87	7000	750	214.8	218.3	214.8	206.7	228.6	1.18	2.48	1.06	0.60	291.06	0.74	1.11	11.13	1.57	1.93	0.85	188.22	1.14
RLC3_L6	120x70x20x20x5			5.87	7500	150	149.8	141.0	141.0	190.2	199.2	0.97	1.16	1.06	0.60	145.51	0.97	1.05	13.01	1.78	2.00	0.88	145.51	0.97
				5.87	7500	300	174.7	171.8	171.8	190.2	199.2	1.03	1.64	1.06	0.60	181.23	0.95	1.05	13.01	1.78	2.00	0.88	166.93	1.03
				5.87	7500	450	184.3	186.3	184.3	190.2	199.2	1.10	2.01	1.06	0.60	219.18	0.84	1.05	13.01	1.78	2.00	0.88	166.93	1.10
				5.87	7500	600	190.3	189.3	189.3	190.2	199.2	1.13	2.32	1.06	0.60	250.84	0.75	1.05	13.01	1.78	2.00	0.88	166.93	1.13
				5.87	7500	750	194.1	219.7	191.7	190.2	199.2	1.15	2.59	1.06	0.60	278.51	0.69	1.05	13.01	1.78	2.00	0.88	166.93	1.15
RLC4_L1	140x70x15x20x5			7.15	3500	150	233.3	232.4	232.4	612.1	897.9	1.06	0.65	1.14	0.62	219.37	1.06	1.47	2.33	0.79	1.21	0.64	219.37	1.06
				7.15	3500	300	417.9	448.7	417.9	612.1	897.9	1.14	0.93	1.14	0.62	366.65	1.14	1.47	2.33	0.79	1.21	0.64	366.65	1.14
				7.15	3500	450	508.9	610.8	508.9	610.8	897.9	1.11	1.13	1.14	0.62	459.61	1.11	1.47	2.33	0.79	1.21	0.64	459.61	1.11
				7.15	3500	600	550.1	703.9	550.1	612.1	897.9	1.07	1.31	1.14	0.62	512.13	1.07	1.47	2.33	0.79	1.21	0.64	512.13	1.07
				7.15	3500	750	573.3	764.3	573.3	612.1	897.9	1.07	1.46	1.14	0.62	534.98	1.07	1.47	2.33	0.79	1.21	0.64	534.98	1.07
RLC4_L2	140x70x15x20x5			7.15	4000	150	229.7	231.3	229.7	495.4	691.6	1.09	0.73	1.14	0.62	210.29	1.09	1.40	3.02	1.02	1.45	0.70	210.29	1.09
				7.15	4000	300	376.0	417.4	376.0	495.4	691.6	1.12	1.03	1.14	0.62	336.92	1.12	1.40	3.02	1.02	1.45	0.70	336.92	1.12
				7.15	4000	450	433.9	511.5	433.9	495.4	691.6	1.07	1.26	1.14	0.62	404.86	1.07	1.40	3.02	1.02	1.45	0.70	404.86	1.07
				7.15	4000	600	461.9	569.5	461.9	495.4	691.6	1.07	1.46	1.14	0.62	432.45	1.07	1.40	3.02	1.02	1.45	0.70	432.45	1.07
				7.15	4000	750	481.5	599.0	481.5	495.4	691.6	1.11	1.63	1.14	0.62	466.41	1.03	1.40	3.02	1.02	1.45	0.70	454.80	1.06
RLC4_L3	140x70x15x20x5			7.15	5000	150	213.0	209.0	209.0	357.1	444.7	1.08	0.86	1.14	0.62	192.97	1.08	1.25	4.62	1.30	1.72	0.78	192.97	1.08
				7.15	5000	300	301.3	334.9	301.3	357.1	444.7	1.06	1.21	1.14	0.62	283.72	1.06	1.25	4.62	1.30	1.72	0.78	283.72	1.06

Column	Geometry			SFEA					DSM Design															
	$b_w \times b_f \times b_l \times b_s \times t$	β_{FT}	L	f_y	$P_{u,FT}$	$P_{u,Fm}$	P_u	$P_{cr,FT}$	$P_{b,Fm}$	$\frac{P_u}{P_{nG}}$	λ_{FT}	b	a	P_{nFT}	$\frac{P_u}{P_{nFT}}$	R_G	R_{DL}	c	b	a	P_{nFT-Fm}	$\frac{P_u}{P_{nFT-Fm}}$		
RLC5_L1	100x70x15x20x5			4.37	6000	150	144.9	170.7	144.9	187.9	272.0	1.05	1.11	0.97	0.58	138.52	1.05	1.45	8.58	0.86	1.12	0.61	138.52	1.05
				4.37	6000	300	174.4	229.1	174.4	187.9	272.0	1.06	1.57	0.97	0.58	173.15	1.01	1.45	8.58	0.86	1.12	0.61	171.91	1.01
				4.37	6000	450	189.5	248.2	189.5	187.9	272.0	1.15	1.93	0.97	0.58	213.27	0.89	1.45	8.58	0.86	1.12	0.61	205.38	0.92
				4.37	6000	600	202.3	252.5	202.3	187.9	272.0	1.23	2.22	0.97	0.58	247.25	0.82	1.45	8.58	0.86	1.12	0.61	233.00	0.87
RLC5_L2	100x70x15x20x5			4.37	6500	150	135.8	151.3	135.8	171.2	231.8	1.03	1.17	0.97	0.58	131.67	1.03	1.35	10.28	1.12	1.38	0.68	131.67	1.03
				4.37	6500	300	160.5	187.4	160.5	171.2	231.8	1.07	1.65	0.97	0.58	165.47	0.97	1.35	10.28	1.12	1.38	0.68	159.26	1.01
				4.37	6500	450	173.6	212.9	173.6	171.2	231.8	1.16	2.02	0.97	0.58	203.80	0.85	1.35	10.28	1.12	1.38	0.68	180.69	0.96
				4.37	6500	600	184.2	219.2	184.2	171.2	231.8	1.23	2.33	0.97	0.58	236.28	0.78	1.35	10.28	1.12	1.38	0.68	197.62	0.93
RLC5_L3	100x70x15x20x5			4.37	7000	150	127.6	140.3	127.6	157.3	199.9	1.02	1.22	0.97	0.58	125.26	1.02	1.27	12.08	1.26	1.52	0.72	125.26	1.02
				4.37	7000	300	148.5	173.0	148.5	157.3	199.9	1.08	1.72	0.97	0.58	158.84	0.93	1.27	12.08	1.26	1.52	0.72	147.39	1.01
				4.37	7000	450	159.6	185.9	159.6	157.3	199.9	1.16	2.11	0.97	0.58	195.64	0.82	1.27	12.08	1.26	1.52	0.72	162.43	0.98
				4.37	7000	600	168.1	190.1	168.1	157.3	199.9	1.22	2.43	0.97	0.58	226.81	0.74	1.27	12.08	1.26	1.52	0.72	174.02	0.97
RLC5_L4	100x70x15x20x5			4.37	7500	150	120.0	132.9	120.0	145.7	174.1	1.01	1.26	0.97	0.58	119.22	1.01	1.20	14.05	1.38	1.64	0.76	119.22	1.01
				4.37	7500	300	137.9	156.9	137.9	145.7	174.1	1.08	1.79	0.97	0.58	153.01	0.90	1.20	14.05	1.38	1.64	0.76	136.19	1.01
				4.37	7500	450	147.0	163.5	147.0	145.7	174.1	1.15	2.19	0.97	0.58	188.46	0.78	1.20	14.05	1.38	1.64	0.76	146.54	1.00
				4.37	7500	600	153.6	165.8	153.6	145.7	174.1	1.20	2.53	0.97	0.58	218.49	0.70	1.20	14.05	1.38	1.64	0.76	154.35	1.00
RLC5_L5	100x70x15x20x5			4.37	8000	150	113.3	108.3	108.3	135.7	153.0	0.95	1.31	0.97	0.58	113.51	0.95	1.13	16.20	1.52	1.78	0.80	113.51	0.95
				4.37	8000	300	128.4	137.8	128.4	135.7	153.0	1.08	1.85	0.97	0.58	147.82	0.87	1.13	16.20	1.52	1.78	0.80	124.77	1.03
				4.37	8000	450	135.7	143.7	135.7	135.7	153.0	1.14	2.27	0.97	0.58	182.07	0.75	1.13	16.20	1.52	1.78	0.80	130.51	1.04
				4.37	8000	750	143.7	148.1	143.7	135.7	153.0	1.21	2.93	0.97	0.58	236.73	0.61	1.13	16.20	1.52	1.78	0.80	134.74	1.04
RLC5_L6	100x70x15x20x5			4.37	8500	150	107.1	105.5	105.5	127.0	135.6	0.98	1.35	0.97	0.58	108.06	0.98	1.07	18.48	1.70	1.96	0.86	108.06	0.98
				4.37	8500	300	119.8	124.4	119.8	127.0	135.6	1.08	1.91	0.97	0.58	143.14	0.84	1.07	18.48	1.70	1.96	0.86	112.52	1.06
				4.37	8500	450	125.4	128.5	125.4	127.0	135.6	1.13	2.34	0.97	0.58	176.30	0.71	1.07	18.48	1.70	1.96	0.86	113.42	1.11
				4.37	8500	600	128.7	130.4	128.7	127.0	135.6	1.16	2.71	0.97	0.58	204.39	0.63	1.07	18.48	1.70	1.96	0.86	114.06	1.13
RLC6_L1	90x50x15x20x3			7.07	3000	150	98.8	94.4	94.4	189.0	281.1	1.05	0.79	1.13	0.62	90.30	1.05	1.49	3.53	0.71	1.13	0.62	90.30	1.05
				7.07	3000	300	151.2	183.1	151.2	189.0	281.1	1.09	1.11	1.13	0.62	139.38	1.09	1.49	3.53	0.71	1.13	0.62	139.38	1.09
				7.07	3000	450	169.7	224.8	169.7	189.0	281.1	1.05	1.36	1.13	0.62	161.36	1.05	1.49	3.53	0.71	1.13	0.62	161.36	1.05
				7.07	3000	600	178.9	242.5	178.9	189.0	281.1	1.08	1.57	1.13	0.62	172.89	1.03	1.49	3.53	0.71	1.13	0.62	172.89	1.03
RLC6_L2	90x50x15x20x3			7.07	3500	150	91.2	97.6	91.2	146.8	207.9	1.09	0.89	1.13	0.62	83.81	1.09	1.42	4.74	0.96	1.39	0.68	83.81	1.09
				7.07	3500	300	125.4	129.5	125.4	146.8	207.9	1.04	1.26	1.13	0.62	120.06	1.04	1.42	4.74	0.96	1.39	0.68	120.06	1.04
				7.07	3500	450	137.1	179.7	137.1	146.8	207.9	1.07	1.55	1.13	0.62	132.24	1.04	1.42	4.74	0.96	1.39	0.68	131.23	1.04
				7.07	3500	600	144.3	187.1	144.3	146.8	207.9	1.12	1.79	1.13	0.62	149.78	0.96	1.42	4.74	0.96	1.39	0.68	143.35	1.01
RLC6_L3	90x50x15x20x3			7.07	4000	150	83.2	91.0	83.2	119.2	159.7	1.07	0.99	1.13	0.62	77.57	1.07	1.34	6.16	1.14	1.57	0.74	77.57	1.07
				7.07	4000	300	106.2	129.0	119.2	159.7	159.7	1.03	1.40	1.13	0.62	102.86	1.03	1.34	6.16	1.14	1.57	0.74	102.86	1.03
				7.07	4000	450	114.8	137.2	114.8	119.2	159.7	1.10	1.72	1.13	0.62	117.50	0.98	1.34	6.16	1.14	1.57	0.74	110.84	1.04
				7.07	4000	600	121.0	148.1	121.0	119.2	159.7	1.16	1.98	1.13	0.62	133.09	0.91	1.34	6.16	1.14	1.57	0.74	117.96	1.03
RLC6_L4	90x50x15x20x3			7.07	4500	150	75.2	74.5	74.5	100.1	126.4	1.04	1.08	1.13	0.62	71.72	1.04	1.26	7.70	1.27	1.69	0.78	71.72	1.04
				7.07	4500	300	91.6	106.7	91.6	100.1	126.4	1.04	1.53	1.13	0.62	89.29	1.03	1.26	7.70	1.27	1.69	0.78	88.33	1.04
				7.07	4500	450	98.6	115.8	98.6	100.1	126.4	1.12	1.87	1.13	0.62	106.43	0.93	1.26	7.70	1.27	1.69	0.78	93.99	1.05
				7.07	4500	600	103.8	118.2	103.8	100.1	126.4	1.18	2.16	1.13	0.62	120.55	0.86	1.26	7.70	1.27	1.69	0.78	98.23	1.06
RLC6_L5	90x50x15x20x3			7.07	5000	150	68.0	71.6	68.0	86.3	102.5	1.03	1.16	1.13	0.62	66.32	1.03	1.19	9.42	1.39	1.81	0.81	66.32	1.03
				7.07	5000	300	80.5	90.7	80.5	86.3	102.5	1.06	1.65	1.13	0.62	82.08	0.98	1.19	9.42	1.39	1.81	0.81	77.03	1.04

Column	Geometry			SFEA				DSM Design														
	$b_w \times b_f \times b_l \times b_s \times t$	β_{FT}	L	f_y	$P_{u,FT}$	$P_{u,Fm}$	P_u	$P_{cr,FT}$	$P_{b,Fm}$	$\frac{P_u}{P_{nG}}$	λ_{FT}	b	a	P_{nFT}	$\frac{P_u}{P_{nFT}}$	R_G	R_{DL}	c	b	a	P_{nFT-Fm}	$\frac{P_u}{P_{nFT-Fm}}$
RLC7_L1	130x70x15x20x5	6.38	4000	150	219.5	214.3	214.3	450.6	673.3	1.06	0.75	1.09	0.61	201.22	1.06	1.49	3.18	0.71	1.09	0.61	201.22	1.06
		6.38	4000	300	351.1	385.7	351.1	450.6	673.3	1.11	1.06	1.09	0.61	317.56	1.11	1.49	3.18	0.71	1.09	0.61	317.56	1.11
		6.38	4000	450	400.1	521.0	400.1	450.6	673.3	1.06	1.30	1.09	0.61	375.87	1.06	1.49	3.18	0.71	1.09	0.61	375.87	1.06
		6.38	4000	600	425.2	523.9	425.2	450.6	673.3	1.08	1.50	1.09	0.61	396.48	1.07	1.49	3.18	0.71	1.09	0.61	396.48	1.07
		6.38	4000	750	444.2	577.1	444.2	450.6	673.3	1.12	1.68	1.09	0.61	438.72	1.01	1.49	3.18	0.71	1.09	0.61	438.72	1.01
RLC7_L2	130x70x15x20x5	6.38	4500	150	212.6	213.8	212.6	378.7	533.4	1.10	0.82	1.09	0.61	192.37	1.10	1.41	3.97	0.98	1.37	0.68	192.37	1.10
		6.38	4500	300	311.7	371.7	311.7	378.7	533.4	1.07	1.16	1.09	0.61	290.23	1.07	1.41	3.97	0.98	1.37	0.68	290.23	1.07
		6.38	4500	450	347.1	436.0	347.1	378.7	533.4	1.06	1.42	1.09	0.61	328.41	1.06	1.41	3.97	0.98	1.37	0.68	328.41	1.06
		6.38	4500	600	367.9	449.6	367.9	378.7	533.4	1.11	1.64	1.09	0.61	360.54	1.02	1.41	3.97	0.98	1.37	0.68	351.74	1.05
		6.38	4500	750	385.5	471.0	385.5	378.7	533.4	1.16	1.83	1.09	0.61	398.95	0.97	1.41	3.97	0.98	1.37	0.68	377.48	1.02
RLC7_L3	130x70x15x20x5	6.38	5000	150	203.1	203.1	203.1	326.8	432.6	1.10	0.88	1.09	0.61	183.95	1.10	1.32	4.87	1.17	1.56	0.73	183.95	1.10
		6.38	5000	300	279.9	329.0	279.9	326.8	432.6	1.05	1.25	1.09	0.61	265.39	1.05	1.32	4.87	1.17	1.56	0.73	265.39	1.05
		6.38	5000	450	306.5	355.9	306.5	326.8	432.6	1.07	1.53	1.09	0.61	291.96	1.05	1.32	4.87	1.17	1.56	0.73	289.29	1.06
		6.38	5000	600	324.9	390.8	324.9	326.8	432.6	1.13	1.77	1.09	0.61	332.66	0.98	1.32	4.87	1.17	1.56	0.73	308.41	1.05
		6.38	5000	750	340.7	394.4	340.7	326.8	432.6	1.19	1.98	1.09	0.61	368.10	0.93	1.32	4.87	1.17	1.56	0.73	324.10	1.05
RLC7_L4	130x70x15x20x5	6.38	5500	150	192.8	171.1	171.1	288.0	357.8	0.97	0.94	1.09	0.61	176.03	0.97	1.24	5.96	1.30	1.68	0.77	176.03	0.97
		6.38	5500	300	252.9	280.2	252.9	288.0	357.8	1.04	1.33	1.09	0.61	243.04	1.04	1.24	5.96	1.30	1.68	0.77	243.04	1.04
		6.38	5500	450	275.0	313.2	275.0	288.0	357.8	1.09	1.63	1.09	0.61	272.48	1.01	1.24	5.96	1.30	1.68	0.77	259.45	1.06
		6.38	5500	600	290.9	320.9	290.9	288.0	357.8	1.15	1.88	1.09	0.61	310.47	0.94	1.24	5.96	1.30	1.68	0.77	271.56	1.07
		6.38	5500	750	304.4	335.9	304.4	288.0	357.8	1.21	2.10	1.09	0.61	343.55	0.89	1.24	5.96	1.30	1.68	0.77	281.33	1.08
RLC7_L5	130x70x15x20x5	6.38	6000	150	182.4	183.4	182.4	258.1	300.8	1.08	0.99	1.09	0.61	168.64	1.08	1.17	7.25	1.43	1.81	0.81	168.64	1.08
		6.38	6000	300	230.7	242.0	230.7	258.1	300.8	1.03	1.41	1.09	0.61	223.04	1.03	1.17	7.25	1.43	1.81	0.81	223.04	1.03
		6.38	6000	450	249.3	269.6	249.3	258.1	300.8	1.10	1.72	1.09	0.61	256.65	0.97	1.17	7.25	1.43	1.81	0.81	232.36	1.07
		6.38	6000	600	262.7	280.7	262.7	258.1	300.8	1.16	1.99	1.09	0.61	292.43	0.90	1.17	7.25	1.43	1.81	0.81	238.67	1.10
		6.38	6000	750	273.3	284.2	273.3	258.1	300.8	1.21	2.22	1.09	0.61	323.58	0.84	1.17	7.25	1.43	1.81	0.81	243.67	1.12
RLC7_L6	130x70x15x20x5	6.38	7000	150	163.7	152.9	152.9	215.3	221.1	0.98	1.09	1.09	0.61	155.33	0.98	1.03	10.23	1.86	2.00	0.88	155.33	0.98
		6.38	7000	300	196.2	190.8	190.8	215.3	221.1	1.01	1.54	1.09	0.61	193.39	0.99	1.03	10.23	1.86	2.00	0.88	188.92	1.01
		6.38	7000	450	208.8	205.0	205.0	215.3	221.1	1.09	1.88	1.09	0.61	232.44	0.88	1.03	10.23	1.86	2.00	0.88	188.92	1.08
		6.38	7000	600	216.6	209.4	209.4	215.3	221.1	1.11	2.18	1.09	0.61	264.85	0.79	1.03	10.23	1.86	2.00	0.88	188.92	1.11
		6.38	7000	750	221.5	210.5	210.5	215.3	221.1	1.11	2.43	1.09	0.61	293.06	0.72	1.03	10.23	1.86	2.00	0.88	188.92	1.11
RLC8_L1	120x60x10x15x4	7.30	3500	150	149.0	152.7	149.0	295.5	428.9	1.10	0.77	1.15	0.62	135.99	1.10	1.45	2.58	0.85	1.28	0.66	135.99	1.10
		7.30	3500	300	234.7	268.3	234.7	295.5	428.9	1.10	1.09	1.15	0.62	212.58	1.10	1.45	2.58	0.85	1.28	0.66	212.58	1.10
		7.30	3500	450	266.0	330.1	266.0	295.5	428.9	1.07	1.33	1.15	0.62	249.22	1.07	1.45	2.58	0.85	1.28	0.66	249.22	1.07
		7.30	3500	600	283.3	368.6	283.3	295.5	428.9	1.09	1.53	1.15	0.62	264.41	1.07	1.45	2.58	0.85	1.28	0.66	263.60	1.07
		7.30	3500	750	297.3	384.2	297.3	295.5	428.9	1.15	1.72	1.15	0.62	290.79	1.02	1.45	2.58	0.85	1.28	0.66	285.53	1.04
RLC8_L2	120x60x10x15x4	7.30	4000	150	142.7	138.1	138.1	242.7	329.2	1.07	0.85	1.15	0.62	128.89	1.07	1.36	3.37	1.11	1.55	0.73	128.89	1.07
		7.30	4000	300	204.2	237.3	204.2	242.7	329.2	1.07	1.20	1.15	0.62	190.94	1.07	1.36	3.37	1.11	1.55	0.73	190.94	1.07
		7.30	4000	450	226.8	275.7	226.8	242.7	329.2	1.07	1.47	1.15	0.62	212.15	1.07	1.36	3.37	1.11	1.55	0.73	212.15	1.07
		7.30	4000	600	241.8	293.2	241.8	242.7	329.2	1.14	1.69	1.15	0.62	236.14	1.02	1.36	3.37	1.11	1.55	0.73	224.95	1.07
		7.30	4000	750	254.9	297.2	254.9	242.7	329.2	1.20	1.89	1.15	0.62	259.69	0.98	1.36	3.37	1.11	1.55	0.73	236.59	1.08
RLC8_L3	120x60x10x15x4	7.30	4500	150	134.5	135.2	134.5	206.2	260.5	1.10	0.92	1.15	0.62	122.22	1.10	1.26	4.37	1.27	1.71	0.78	122.22	1.10
		7.30	4500	300	180.7	194.6	180.7	206.2	260.5	1.05	1.30	1.15	0.62	171.69	1.05	1.26	4.37	1.27	1.71	0.78	171.69	1.05
		7.30	4500	450	198.4	226.6	198.4	206.2	260.5	1.10	1.59	1.15	0.62	190.24	1.04	1.26	4.37	1.27	1.71	0.78	184.06	1.08
		7.30	4500	600	211.6	237.6	211.6	206.2	260.5	1.17	1.84	1.15	0.62	215.04	0.98	1.26	4.37	1.27	1.71	0.78	191.99	1.10
		7.30	4500	750	222.9	235.9	222.9	206.2	260.5	1.23	2.05	1.15	0.62	236.49	0.94	1.26	4.37	1.27	1.71	0.78	198.38	1.12
RLC8_L4	120x60x10x15x4	7.30	5000	150	126.4	126.4	126.4	179.8	211.1	1.09	0.98	1.15	0.62	116.05	1.09	1.17	5.53	1.41	1.85	0.83	116.05	1.09
		7.30																				

Table I.4: WSC column (i) geometries, (ii) β_{FT} values, (iii) yield stresses, (iv) buckling load values and ratios, (v) numerical failure loads, (vi) failure load predictions estimates P_{nG} , P_{nFT} and P_{nFT-Fm} , and (vii) numerical-to-predicted failure loads ratios (mm, kN)

Column	Geometry			SFEA					DSM Design														
	$b_w \times b_f \times b_s \times t$	β_{FT}	L	f_y	$P_{u,FT}$	$P_{u,Fm}$	P_u	$P_{cr,FT}$	$P_{b,Fm}$	$\frac{P_u}{P_{ag}}$	λ_{FT}	b	a	P_{nFT}	$\frac{P_u}{P_{nFT}}$	R_G	R_{DL}	c	b	a	P_{nFT-Fm}	$\frac{P_u}{P_{nFT-Fm}}$	
WSC1_L1	110x60x15x3	7.32	3500	150	100.4	103.5	100.4	180.6	278.9	1.10	0.82	1.15	0.62	91.26	1.10	1.54	1.94	0.71	1.15	0.62	91.26	1.10	
		7.32	3500	300	149.7	179.6	149.7	180.6	278.9	1.09	1.16	1.15	0.62	137.96	1.09	1.54	1.94	0.71	1.15	0.62	137.96	1.09	
		7.32	3500	450	168.5	220.2	168.5	180.6	278.9	1.08	1.42	1.15	0.62	156.43	1.08	1.54	1.94	0.71	1.15	0.62	156.43	1.08	
		7.32	3500	600	180.3	239.1	180.3	180.6	278.9	1.14	1.64	1.15	0.62	170.53	1.06	1.54	1.94	0.71	1.15	0.62	170.53	1.06	
		7.32	3500	750	190.9	248.1	190.9	180.6	278.9	1.21	1.83	1.15	0.62	187.51	1.02	1.54	1.94	0.71	1.15	0.62	187.51	1.02	
WSC1_L2	110x60x15x3	7.32	4000	150	94.0	98.3	94.0	146.0	214.4	1.10	0.91	1.15	0.62	85.42	1.10	1.47	2.50	0.78	1.22	0.64	85.42	1.10	
		7.32	4000	300	128.8	156.5	128.8	146.0	214.4	1.07	1.29	1.15	0.62	120.87	1.07	1.47	2.50	0.78	1.22	0.64	120.87	1.07	
		7.32	4000	450	143.0	180.8	143.0	146.0	214.4	1.12	1.57	1.15	0.62	133.57	1.07	1.47	2.50	0.78	1.22	0.64	133.11	1.07	
		7.32	4000	600	154.3	190.9	154.3	146.0	214.4	1.20	1.82	1.15	0.62	150.95	1.02	1.47	2.50	0.78	1.22	0.64	148.91	1.04	
		7.32	4000	750	164.2	196.2	164.2	146.0	214.4	1.28	2.03	1.15	0.62	165.98	0.99	1.47	2.50	0.78	1.22	0.64	162.45	1.01	
WSC1_L3	110x60x15x3	7.32	5000	150	80.0	83.9	80.0	105.1	137.7	1.07	1.07	1.15	0.62	74.64	1.07	1.31	4.09	1.20	1.64	0.76	74.64	1.07	
		7.32	5000	300	99.9	113.8	99.9	105.1	137.7	1.08	1.52	1.15	0.62	93.04	1.07	1.31	4.09	1.20	1.64	0.76	92.57	1.08	
		7.32	5000	450	111.0	123.4	111.0	105.1	137.7	1.20	1.86	1.15	0.62	110.55	1.00	1.31	4.09	1.20	1.64	0.76	99.66	1.11	
		7.32	5000	600	119.6	127.4	119.6	105.1	137.7	1.30	2.14	1.15	0.62	124.94	0.96	1.31	4.09	1.20	1.64	0.76	105.02	1.14	
		7.32	5000	750	125.7	129.4	125.7	105.1	137.7	1.36	2.40	1.15	0.62	137.38	0.92	1.31	4.09	1.20	1.64	0.76	109.38	1.15	
WSC1_L4	110x60x15x3	7.32	6000	150	68.1	68.7	68.1	82.5	95.7	1.04	1.21	1.15	0.62	65.43	1.04	1.16	6.11	1.44	1.88	0.84	65.43	1.04	
		7.32	6000	300	81.8	83.1	81.8	82.5	95.7	1.13	1.71	1.15	0.62	80.95	1.01	1.16	6.11	1.44	1.88	0.84	73.51	1.11	
		7.32	6000	450	89.7	88.3	88.3	82.5	95.7	1.22	2.10	1.15	0.62	96.18	0.92	1.16	6.11	1.44	1.88	0.84	75.30	1.17	
		7.32	6000	600	94.4	90.2	90.2	82.5	95.7	1.25	2.42	1.15	0.62	108.70	0.83	1.16	6.11	1.44	1.88	0.84	76.59	1.18	
		7.32	6000	750	96.7	91.2	91.2	82.5	95.7	1.26	2.71	1.15	0.62	119.52	0.76	1.16	6.11	1.44	1.88	0.84	77.61	1.18	
WSC1_L5	110x60x15x3	7.32	6500	150	63.3	59.1	59.1	74.7	81.6	0.96	1.27	1.15	0.62	61.40	0.96	1.09	7.27	1.62	2.00	0.88	61.40	0.96	
		7.32	6500	300	74.8	72.5	72.5	74.7	81.6	1.11	1.80	1.15	0.62	76.49	0.95	1.09	7.27	1.62	2.00	0.88	65.58	1.11	
		7.32	6500	450	80.9	76.0	76.0	74.7	81.6	1.16	2.20	1.15	0.62	90.89	0.84	1.09	7.27	1.62	2.00	0.88	65.58	1.16	
		7.32	6500	600	83.9	77.4	77.4	74.7	81.6	1.18	2.54	1.15	0.62	102.71	0.75	1.09	7.27	1.62	2.00	0.88	65.58	1.18	
		7.32	6500	750	84.9	78.1	78.1	74.7	81.6	1.19	2.84	1.15	0.62	112.94	0.69	1.09	7.27	1.62	2.00	0.88	65.58	1.19	
WSC1_L6	110x60x15x3	7.32	7000	150	59.0	53.3	53.3	68.5	70.3	0.92	1.33	1.15	0.62	57.74	0.92	1.03	8.53	1.87	2.00	0.88	57.74	0.92	
		7.32	7000	300	68.7	63.5	63.5	68.5	70.3	1.06	1.88	1.15	0.62	72.75	0.87	1.03	8.53	1.87	2.00	0.88	60.11	1.06	
		7.32	7000	450	73.0	66.0	66.0	68.5	70.3	1.10	2.30	1.15	0.62	86.45	0.76	1.03	8.53	1.87	2.00	0.88	60.11	1.10	
		7.32	7000	600	74.5	67.0	67.0	68.5	70.3	1.12	2.66	1.15	0.62	97.70	0.69	1.03	8.53	1.87	2.00	0.88	60.11	1.12	
		7.32	7000	750	74.8	67.6	67.6	68.5	70.3	1.13	2.97	1.15	0.62	107.42	0.63	1.03	8.53	1.87	2.00	0.88	60.11	1.12	
WSC2_L1	100x50x10x2	9.52	3000	150	55.8	56.9	55.8	96.4	138.4	1.10	0.84	1.28	0.66	50.88	1.10	1.43	1.51	0.90	1.48	0.71	50.88	1.10	
		9.52	3000	300	81.4	94.4	81.4	96.4	138.4	1.08	1.19	1.28	0.66	75.59	1.08	1.43	1.51	0.90	1.48	0.71	75.59	1.08	
		9.52	3000	450	90.9	111.7	90.9	96.4	138.4	1.08	1.46	1.28	0.66	84.23	1.08	1.43	1.51	0.90	1.48	0.71	84.23	1.08	
		9.52	3000	600	97.0	119.2	97.0	96.4	138.4	1.15	1.69	1.28	0.66	92.02	1.05	1.43	1.51	0.90	1.48	0.71	89.96	1.08	
		9.52	3000	750	102.2	122.8	102.2	96.4	138.4	1.21	1.88	1.28	0.66	99.70	1.02	1.43	1.51	0.90	1.48	0.71	95.39	1.07	
WSC2_L2	100x50x10x2	9.52	3500	150	50.6	52.6	50.6	74.4	102.4	1.09	0.96	1.28	0.66	46.58	1.09	1.38	2.02	1.06	1.64	0.76	46.58	1.09	
		9.52	3500	300	67.4	78.5	67.4	74.4	102.4	1.06	1.36	1.28	0.66	63.36	1.06	1.38	2.02	1.06	1.64	0.76	63.36	1.06	
		9.52	3500	450	75.0	88.0	75.0	74.4	102.4	1.15	1.66	1.28	0.66	70.25	1.07	1.38	2.02	1.06	1.64	0.76	67.73	1.11	
		9.52	3500	600	81.0	91.9	81.0	74.4	102.4	1.24	1.92	1.28	0.66	77.90	1.04	1.38	2.02	1.06	1.64	0.76	71.38	1.13	
		9.52	3500	750	85.5	93.8	85.5	74.4	102.4	1.31	2.15	1.28	0.66	84.41	1.01	1.38	2.02	1.06	1.64	0.76	74.34	1.15	
WSC2_L3	100x50x10x2	9.52	4000	150	45.4	47.4	45.4	59.9	78.7	1.07	1.07	1.28	0.66	42.45	1.07	1.31	2.70	1.19	1.76	0.80	42.45	1.07	
		9.52	4000	300	57.4	64.8	57.4	59.9	78.7	1.09	1.51	1.28	0.66	52.89	1.09	1.31	2.70	1.19	1.76	0.80	52.70	1.09	
		9.52	4000	450	64.3	70.1	64.3	59.9	78.7	1.22	1.85	1.28	0.66	61.19	1.05	1.31	2.70	1.19	1.76	0.80	55.29	1.16	
		9.52	4000	600	69.3	72.2	69.3	59.9	78.7	1.32	2.14	1.28	0.66	67.86	1.02	1.31	2.70	1.19	1.76	0.80	57.20	1.21	
		9.52	4000	750	72.6	73.3	72.6	59.9	78.7	1.38	2.39	1.28	0.66	73.52	0.99	1.31	2.70	1.19	1.76	0.80	58.73	1.24	
WSC2_L4	100x50x10x2	9.52	4500	150	40.5	42.0	40.5	50.0	62.3	1.05	1.17	1.28	0.66	38.61	1.05	1.24	3.51	1.30	1.87	0.83	38.61	1.05	
		9.52	4500	300	50.2	53.3	50.2	50.0	62.3	1.14	1.65	1.28	0.										

Column	Geometry			SFEA					DSM Design													
	$b_w \times b_f \times b_s \times t$	β_{FT}	L	f_y	$P_{u,FT}$	$P_{u,Fm}$	P_u	$P_{cr,FT}$	$P_{b,Fm}$	$\frac{P_u}{P_{nG}}$	λ_{FT}	b	a	P_{nFT}	$\frac{P_u}{P_{nFT}}$	R_G	R_{DL}	c	b	a	P_{nFT-Fm}	$\frac{P_u}{P_{nFT-Fm}}$
WSC3_L1	120x70x12x4	6.25	4000	150	146.3	147.4	146.3	253.7	398.4	1.11	0.83	1.09	0.61	131.32	1.11	1.57	2.09	0.71	1.09	0.61	131.32	1.11
		6.25	4000	300	214.3	256.8	214.3	253.7	398.4	1.09	1.18	1.09	0.61	196.66	1.09	1.57	2.09	0.71	1.09	0.61	196.66	1.09
		6.25	4000	450	240.1	315.4	240.1	253.7	398.4	1.09	1.44	1.09	0.61	220.88	1.09	1.57	2.09	0.71	1.09	0.61	220.88	1.09
		6.25	4000	600	259.1	342.8	259.1	253.7	398.4	1.16	1.66	1.09	0.61	244.65	1.06	1.57	2.09	0.71	1.09	0.61	244.65	1.06
		6.25	4000	750	277.1	356.5	277.1	253.7	398.4	1.25	1.86	1.09	0.61	270.94	1.02	1.57	2.09	0.71	1.09	0.61	270.94	1.02
WSC3_L2	120x70x12x4	6.25	4500	150	138.8	141.7	138.8	214.8	315.2	1.11	0.90	1.09	0.61	124.61	1.11	1.47	2.71	0.78	1.16	0.62	124.61	1.11
		6.25	4500	300	189.7	227.1	189.7	214.8	315.2	1.07	1.28	1.09	0.61	177.09	1.07	1.47	2.71	0.78	1.16	0.62	177.09	1.07
		6.25	4500	450	211.2	264.4	211.2	214.8	315.2	1.12	1.56	1.09	0.61	195.96	1.08	1.47	2.71	0.78	1.16	0.62	195.35	1.08
		6.25	4500	600	229.2	280.4	229.2	214.8	315.2	1.22	1.81	1.09	0.61	223.52	1.03	1.47	2.71	0.78	1.16	0.62	220.48	1.04
		6.25	4500	750	245.3	288.5	245.3	214.8	315.2	1.30	2.02	1.09	0.61	247.54	0.99	1.47	2.71	0.78	1.16	0.62	242.19	1.01
WSC3_L3	120x70x12x4	6.25	5000	150	130.7	114.3	114.3	186.7	255.5	0.97	0.97	1.09	0.61	118.36	0.97	1.37	3.39	1.08	1.46	0.70	118.36	0.97
		6.25	5000	300	170.2	198.6	170.2	186.7	255.5	1.07	1.37	1.09	0.61	159.78	1.07	1.37	3.39	1.08	1.46	0.70	159.78	1.07
		6.25	5000	450	189.3	219.7	189.3	186.7	255.5	1.16	1.68	1.09	0.61	181.60	1.04	1.37	3.39	1.08	1.46	0.70	174.11	1.09
		6.25	5000	600	205.4	232.2	205.4	186.7	255.5	1.25	1.94	1.09	0.61	207.14	0.99	1.37	3.39	1.08	1.46	0.70	188.18	1.09
		6.25	5000	750	218.6	237.3	218.6	186.7	255.5	1.33	2.17	1.09	0.61	229.40	0.95	1.37	3.39	1.08	1.46	0.70	199.88	1.09
WSC3_L4	120x70x12x4	6.25	6000	150	115.4	134.0	115.4	149.4	177.6	1.08	1.08	1.09	0.61	107.30	1.08	1.19	5.03	1.39	1.76	0.80	107.30	1.08
		6.25	6000	300	142.0	146.8	142.0	149.4	177.6	1.08	1.53	1.09	0.61	133.68	1.06	1.19	5.03	1.39	1.76	0.80	131.77	1.08
		6.25	6000	450	156.5	160.6	156.5	149.4	177.6	1.19	1.88	1.09	0.61	160.92	0.97	1.19	5.03	1.39	1.76	0.80	138.26	1.13
		6.25	6000	600	167.0	165.4	165.4	149.4	177.6	1.26	2.17	1.09	0.61	183.55	0.90	1.19	5.03	1.39	1.76	0.80	143.05	1.16
		6.25	6000	750	173.6	167.9	167.9	149.4	177.6	1.28	2.42	1.09	0.61	203.28	0.83	1.19	5.03	1.39	1.76	0.80	146.88	1.14
WSC3_L5	120x70x12x4	6.25	6500	150	108.7	98.4	98.4	136.5	151.3	0.96	1.13	1.09	0.61	102.44	0.96	1.11	5.96	1.57	1.94	0.86	102.44	0.96
		6.25	6500	300	131.1	128.4	128.4	136.5	151.3	1.07	1.60	1.09	0.61	127.30	1.01	1.11	5.96	1.57	1.94	0.86	120.27	1.07
		6.25	6500	450	143.0	138.6	138.6	136.5	151.3	1.16	1.96	1.09	0.61	153.24	0.90	1.11	5.96	1.57	1.94	0.86	121.69	1.14
		6.25	6500	600	150.4	141.8	141.8	136.5	151.3	1.18	2.27	1.09	0.61	174.79	0.81	1.11	5.96	1.57	1.94	0.86	122.71	1.16
		6.25	6500	750	154.4	143.9	143.9	136.5	151.3	1.20	2.53	1.09	0.61	193.58	0.74	1.11	5.96	1.57	1.94	0.86	123.50	1.17
WSC3_L6	120x70x12x4	6.25	7200	150	100.4	90.1	90.1	122.4	123.4	0.94	1.20	1.09	0.61	96.29	0.94	1.01	7.32	1.96	2.00	0.88	96.29	0.94
		6.25	7200	300	118.0	108.8	108.8	122.4	123.4	1.01	1.69	1.09	0.61	119.98	0.91	1.01	7.32	1.96	2.00	0.88	107.43	1.01
		6.25	7200	450	126.0	114.4	114.4	122.4	123.4	1.07	2.07	1.09	0.61	144.44	0.79	1.01	7.32	1.96	2.00	0.88	107.43	1.06
		6.25	7200	600	129.8	116.7	116.7	122.4	123.4	1.09	2.39	1.09	0.61	164.75	0.71	1.01	7.32	1.96	2.00	0.88	107.43	1.09
		6.25	7200	750	131.0	118.0	118.0	122.4	123.4	1.10	2.68	1.09	0.61	182.46	0.65	1.01	7.32	1.96	2.00	0.88	107.43	1.10
WSC4_L1	140x70x20x4	7.87	3500	150	177.2	176.4	176.4	440.9	633.8	1.08	0.67	1.18	0.63	163.38	1.08	1.44	1.63	0.89	1.37	0.68	163.38	1.08
		7.87	3500	300	307.3	327.3	307.3	440.9	633.8	1.13	0.95	1.18	0.63	271.03	1.13	1.44	1.63	0.89	1.37	0.68	271.03	1.13
		7.87	3500	450	371.6	434.5	371.6	440.9	633.8	1.10	1.16	1.18	0.63	337.21	1.10	1.44	1.63	0.89	1.37	0.68	337.21	1.10
		7.87	3500	600	400.6	498.6	400.6	440.9	633.8	1.07	1.34	1.18	0.63	372.93	1.07	1.44	1.63	0.89	1.37	0.68	372.93	1.07
		7.87	3500	750	419.1	534.4	419.1	440.9	633.8	1.08	1.49	1.18	0.63	386.66	1.08	1.44	1.63	0.89	1.37	0.68	386.66	1.08
WSC4_L2	140x70x10x4	7.87	4000	150	171.1	170.5	170.5	353.3	489.4	1.09	0.75	1.18	0.63	155.98	1.09	1.39	2.11	1.05	1.52	0.72	155.98	1.09
		7.87	4000	300	274.7	302.0	274.7	353.3	489.4	1.11	1.06	1.18	0.63	247.04	1.11	1.39	2.11	1.05	1.52	0.72	247.04	1.11
		7.87	4000	450	315.6	377.7	315.6	353.3	489.4	1.08	1.29	1.18	0.63	293.44	1.08	1.39	2.11	1.05	1.52	0.72	293.44	1.08
		7.87	4000	600	336.8	413.4	336.8	353.3	489.4	1.09	1.49	1.18	0.63	309.83	1.09	1.39	2.11	1.05	1.52	0.72	309.83	1.09
		7.87	4000	750	352.9	432.2	352.9	353.3	489.4	1.14	1.67	1.18	0.63	338.41	1.04	1.39	2.11	1.05	1.52	0.72	326.45	1.08
WSC4_L3	140x70x10x4	7.87	5000	150	156.0	155.7	155.7	249.6	315.3	1.10	0.89	1.18	0.63	141.56	1.10	1.26	3.25	1.27	1.74	0.79	141.56	1.10
		7.87	5000	300	217.0	239.1	217.0	249.6	315.3	1.07	1.26	1.18	0.63	203.48	1.07	1.26	3.25	1.27	1.74	0.79	203.48	1.07
		7.87	5000	450	239.9	270.9	239.9	249.6	315.3	1.10	1.54	1.18	0.63	223.62	1.07	1.26	3.25	1.27	1.74	0.79	220.46	1.09
		7.87	5000	600	256.4	284.1	256.4	249.6	315.3	1.17	1.78	1.18	0.63	251.53	1.02	1.26	3.25	1.27	1.74	0.79	228.80	1.12
		7.87	5000	750	270.1	290.9	270.1	249.6	315.3	1.23	1.99	1.18	0.63	275.55	0.98	1.26	3.25	1.27	1.74	0.79	235.49	1.15
WSC4_L4	140x70x10x4	7.87	5500	150	147.3	142.1	142.1	217.3	260.9	1.05	0.95	1.18	0.63	134.79	1.05	1.20	4.01	1.37	1.84	0.82	134.79	1.05
		7.87	5500	300	194.9	208.6	194															

Column	Geometry			SFEA					DSM Design															
	$b_w \times b_f \times b_s \times t$	β_{FT}	L	f_y	$P_{u,FT}$	$P_{u,Fm}$	P_u	$P_{cr,FT}$	$P_{b,Fm}$	$\frac{P_u}{P_{nG}}$	λ_{FT}	b	a	P_{nFT}	$\frac{P_u}{P_{nFT}}$	R_G	R_{DL}	c	b	a	P_{nFT-Fm}	$\frac{P_u}{P_{nFT-Fm}}$		
WSC5_L1	140x80x15x4			6.79	6000	150	139.8	151.1	139.8	187.9	274.3	1.08	1.04	1.12	0.61	129.15	1.08	1.46	3.09	0.81	1.22	0.64	129.15	1.08
				6.79	6000	300	177.7	218.4	177.7	187.9	274.3	1.08	1.47	1.12	0.61	164.36	1.08	1.46	3.09	0.81	1.22	0.64	164.36	1.08
				6.79	6000	450	199.7	241.1	199.7	187.9	274.3	1.21	1.80	1.12	0.61	193.69	1.03	1.46	3.09	0.81	1.22	0.64	190.04	1.05
				6.79	6000	600	218.5	250.6	218.5	187.9	274.3	1.33	2.08	1.12	0.61	219.90	0.99	1.46	3.09	0.81	1.22	0.64	212.54	1.03
				6.79	6000	750	232.9	255.7	232.9	187.9	274.3	1.41	2.32	1.12	0.61	242.65	0.96	1.46	3.09	0.81	1.22	0.64	231.82	1.00
WSC5_L2	100x50x10x3			6.79	6500	150	131.3	134.7	131.3	168.6	233.8	1.07	1.10	1.12	0.61	122.64	1.07	1.39	3.67	1.04	1.45	0.70	122.64	1.07
				6.79	6500	300	163.4	192.8	163.4	168.6	233.8	1.11	1.55	1.12	0.61	152.44	1.07	1.39	3.67	1.04	1.45	0.70	150.74	1.08
				6.79	6500	450	183.8	209.2	183.8	168.6	233.8	1.24	1.90	1.12	0.61	182.31	1.01	1.39	3.67	1.04	1.45	0.70	168.54	1.09
				6.79	6500	600	199.9	216.1	199.9	168.6	233.8	1.35	2.19	1.12	0.61	206.98	0.97	1.39	3.67	1.04	1.45	0.70	182.42	1.10
				6.79	6500	750	211.1	219.7	211.1	168.6	233.8	1.43	2.45	1.12	0.61	228.39	0.92	1.39	3.67	1.04	1.45	0.70	193.97	1.09
WSC5_L3	100x50x10x3			6.79	7000	150	123.3	131.6	123.3	153.2	201.7	1.06	1.15	1.12	0.61	116.57	1.06	1.32	4.31	1.19	1.59	0.74	116.57	1.06
				6.79	7000	300	151.5	170.9	151.5	153.2	201.7	1.13	1.63	1.12	0.61	144.48	1.05	1.32	4.31	1.19	1.59	0.74	138.98	1.09
				6.79	7000	450	169.8	182.8	169.8	153.2	201.7	1.26	1.99	1.12	0.61	172.79	0.98	1.32	4.31	1.19	1.59	0.74	150.94	1.13
				6.79	7000	600	183.0	188.0	183.0	153.2	201.7	1.36	2.30	1.12	0.61	196.17	0.93	1.32	4.31	1.19	1.59	0.74	160.05	1.14
				6.79	7000	750	191.1	190.7	190.7	153.2	201.7	1.42	2.57	1.12	0.61	216.47	0.88	1.32	4.31	1.19	1.59	0.74	167.49	1.14
WSC5_L4	100x50x10x3			6.79	7500	150	116.2	121.4	116.2	140.6	175.7	1.05	1.20	1.12	0.61	110.93	1.05	1.25	5.00	1.29	1.70	0.78	110.93	1.05
				6.79	7500	300	141.2	152.0	141.2	140.6	175.7	1.15	1.70	1.12	0.61	137.74	1.03	1.25	5.00	1.29	1.70	0.78	128.14	1.10
				6.79	7500	450	157.2	160.9	157.2	140.6	175.7	1.27	2.08	1.12	0.61	164.72	0.95	1.25	5.00	1.29	1.70	0.78	136.25	1.15
				6.79	7500	600	167.4	164.9	164.9	140.6	175.7	1.34	2.40	1.12	0.61	187.01	0.88	1.25	5.00	1.29	1.70	0.78	142.32	1.16
				6.79	7500	750	173.0	167.0	140.6	175.7	1.35	2.69	1.12	0.61	206.36	0.81	1.25	5.00	1.29	1.70	0.78	147.21	1.13	
WSC5_L5	100x50x10x3			6.79	8500	150	104.1	103.0	103.0	121.5	136.9	1.02	1.29	1.12	0.61	100.87	1.02	1.13	6.52	1.52	1.93	0.85	100.87	1.02
				6.79	8500	300	123.8	121.4	121.4	121.5	136.9	1.14	1.83	1.12	0.61	126.93	0.96	1.13	6.52	1.52	1.93	0.85	108.16	1.12
				6.79	8500	450	134.6	127.2	127.2	121.5	136.9	1.19	2.24	1.12	0.61	151.80	0.84	1.13	6.52	1.52	1.93	0.85	109.78	1.16
				6.79	8500	600	139.7	129.7	129.7	121.5	136.9	1.22	2.59	1.12	0.61	172.34	0.75	1.13	6.52	1.52	1.93	0.85	110.94	1.17
				6.79	8500	750	141.5	131.0	131.0	121.5	136.9	1.23	2.89	1.12	0.61	190.17	0.69	1.13	6.52	1.52	1.93	0.85	111.84	1.17
WSC5_L6	100x50x10x3			6.79	9000	150	99.0	92.2	92.2	114.1	122.1	0.96	1.33	1.12	0.61	96.38	0.96	1.07	7.31	1.69	2.00	0.88	96.38	0.96
				6.79	9000	300	116.2	109.3	109.3	114.1	122.1	1.09	1.89	1.12	0.61	122.53	0.89	1.07	7.31	1.69	2.00	0.88	100.09	1.09
				6.79	9000	450	124.4	114.1	114.1	122.1	114.1	1.14	2.31	1.12	0.61	146.54	0.78	1.07	7.31	1.69	2.00	0.88	100.09	1.14
				6.79	9000	600	127.5	116.1	116.1	122.1	116.1	1.16	2.67	1.12	0.61	166.37	0.70	1.07	7.31	1.69	2.00	0.88	100.09	1.16
				6.79	9000	750	128.2	117.2	117.2	114.1	122.1	1.17	2.98	1.12	0.61	183.58	0.64	1.07	7.31	1.69	2.00	0.88	100.09	1.17
WSC6_L1	130x70x15x3			8.03	5000	150	98.5	107.4	98.5	137.5	209.4	1.08	1.00	1.19	0.63	90.94	1.08	1.52	2.24	0.71	1.19	0.63	90.94	1.08
				8.03	5000	300	127.7	161.3	127.7	137.5	209.4	1.07	1.42	1.19	0.63	119.23	1.07	1.52	2.24	0.71	1.19	0.63	119.23	1.07
				8.03	5000	450	143.1	180.8	143.1	137.5	209.4	1.19	1.74	1.19	0.63	136.01	1.05	1.52	2.24	0.71	1.19	0.63	136.01	1.05
				8.03	5000	600	156.3	188.9	156.3	137.5	209.4	1.30	2.01	1.19	0.63	152.78	1.02	1.52	2.24	0.71	1.19	0.63	152.78	1.02
				8.03	5000	750	166.9	193.0	166.9	137.5	209.4	1.38	2.25	1.19	0.63	167.20	1.00	1.52	2.24	0.71	1.19	0.63	167.20	1.00
WSC6_L2	130x70x15x3			8.03	6000	150	83.7	92.2	83.7	104.2	145.7	1.05	1.15	1.19	0.63	79.47	1.05	1.40	3.37	1.01	1.49	0.71	79.47	1.05
				8.03	6000	300	103.9	122.4	103.9	104.2	145.7	1.14	1.63	1.19	0.63	97.89	1.06	1.40	3.37	1.01	1.49	0.71	95.43	1.09
				8.03	6000	450	117.4	131.3	117.4	104.2	145.7	1.28	2.00	1.19	0.63	115.32	1.02	1.40	3.37	1.01	1.49	0.71	105.73	1.11
				8.03	6000	600	127.2	135.1	127.2	104.2	145.7	1.39	2.31	1.19	0.63	129.53	0.98	1.40	3.37	1.01	1.49	0.71	113.71	1.12
				8.03	6000	750	133.5	137.1	133.5	104.2	145.7	1.46	2.58	1.19	0.63	141.76	0.94	1.40	3.37	1.01	1.49	0.71	120.30	1.11
WSC6_L3	130x70x15x3			8.03	7000	150	72.0	75.0	72.0	84.0	107.2	1.04	1.29	1.19	0.63	69.48	1.04	1.28	4.71	1.25	1.73	0.79	69.48	1.04
				8.03	7000	300	88.0	94.0	88.0	84.0	107.2	1.20	1.82	1.19	0.63	86.07	1.02	1.28	4.71	1.25	1.73	0.79	77.60	1.13
				8.03	7000	450	98.2	98.8	98.2	84.0	107.2	1.33	2.23	1.19										

Column	Geometry			SFEA					DSM Design													
	$b_w \times b_f \times b_s \times t$	β_{FT}	L	f_y	$P_{u,FT}$	$P_{u,Fm}$	P_u	$P_{cr,FT}$	$P_{b,Fm}$	$\frac{P_u}{P_{nG}}$	λ_{FT}	b	a	P_{nFT}	$\frac{P_u}{P_{nFT}}$	R_G	R_{DL}	c	b	a	P_{nFT-Fm}	$\frac{P_u}{P_{nFT+Fm}}$
WSC7_L1	120x60x15x3	8.43	3500	150	106.2	107.4	106.2	203.0	286.4	1.10	0.79	1.22	0.64	96.73	1.10	1.41	1.85	0.98	1.48	0.71	96.73	1.10
		8.43	3500	300	164.0	184.6	164.0	203.0	286.4	1.10	1.11	1.22	0.64	149.45	1.10	1.41	1.85	0.98	1.48	0.71	149.45	1.10
		8.43	3500	450	185.6	225.9	185.6	203.0	286.4	1.07	1.36	1.22	0.64	173.17	1.07	1.41	1.85	0.98	1.48	0.71	173.17	1.07
		8.43	3500	600	198.0	242.4	198.0	203.0	286.4	1.11	1.57	1.22	0.64	184.71	1.07	1.41	1.85	0.98	1.48	0.71	182.45	1.09
		8.43	3500	750	208.1	254.2	208.1	203.0	286.4	1.17	1.76	1.22	0.64	201.61	1.03	1.41	1.85	0.98	1.48	0.71	193.27	1.08
WSC7_L2	120x60x15x3	8.43	4000	150	100.0	100.9	100.0	163.4	220.4	1.10	0.88	1.22	0.64	90.87	1.10	1.35	2.37	1.13	1.63	0.76	90.87	1.10
		8.43	4000	300	141.2	160.9	141.2	163.4	220.4	1.07	1.24	1.22	0.64	131.88	1.07	1.35	2.37	1.13	1.63	0.76	131.88	1.07
		8.43	4000	450	157.0	185.4	157.0	163.4	220.4	1.10	1.52	1.22	0.64	144.63	1.09	1.35	2.37	1.13	1.63	0.76	143.98	1.09
		8.43	4000	600	168.3	195.7	168.3	163.4	220.4	1.17	1.75	1.22	0.64	161.90	1.04	1.35	2.37	1.13	1.63	0.76	151.82	1.11
		8.43	4000	750	177.9	201.1	177.9	163.4	220.4	1.24	1.96	1.22	0.64	176.71	1.01	1.35	2.37	1.13	1.63	0.76	158.19	1.12
WSC7_L3	120x60x15x3	8.43	4500	150	92.9	93.1	92.9	136.2	174.6	1.09	0.96	1.22	0.64	85.22	1.09	1.28	3.04	1.24	1.75	0.79	85.22	1.09
		8.43	4500	300	123.2	137.5	123.2	136.2	174.6	1.06	1.36	1.22	0.64	115.98	1.06	1.28	3.04	1.24	1.75	0.79	115.98	1.06
		8.43	4500	450	136.4	152.0	136.4	136.2	174.6	1.14	1.66	1.22	0.64	129.44	1.05	1.28	3.04	1.24	1.75	0.79	122.63	1.11
		8.43	4500	600	146.7	158.8	146.7	136.2	174.6	1.23	1.92	1.22	0.64	144.90	1.01	1.28	3.04	1.24	1.75	0.79	127.20	1.15
		8.43	4500	750	154.7	162.0	154.7	136.2	174.6	1.30	2.14	1.22	0.64	158.15	0.98	1.28	3.04	1.24	1.75	0.79	130.87	1.18
WSC7_L4	120x60x15x3	8.43	5000	150	86.1	86.5	86.1	116.6	141.7	1.08	1.04	1.22	0.64	79.88	1.08	1.22	3.85	1.34	1.85	0.83	79.88	1.08
		8.43	5000	300	109.1	114.1	109.1	116.6	141.7	1.07	1.47	1.22	0.64	101.90	1.07	1.22	3.85	1.34	1.85	0.83	101.90	1.07
		8.43	5000	450	120.8	126.8	120.8	116.6	141.7	1.18	1.80	1.22	0.64	117.77	1.03	1.22	3.85	1.34	1.85	0.83	105.11	1.15
		8.43	5000	600	129.5	130.8	129.5	116.6	141.7	1.27	2.07	1.22	0.64	131.84	0.98	1.22	3.85	1.34	1.85	0.83	107.43	1.21
		8.43	5000	750	135.3	132.9	132.9	116.6	141.7	1.30	2.32	1.22	0.64	143.90	0.92	1.22	3.85	1.34	1.85	0.83	109.27	1.22
WSC7_L5	120x60x15x3	8.43	6000	150	73.6	65.6	65.6	90.8	98.5	0.93	1.17	1.22	0.64	70.31	0.93	1.08	5.75	1.64	2.00	0.88	70.31	0.93
		8.43	6000	300	89.0	84.4	84.4	90.8	98.5	1.06	1.66	1.22	0.64	86.31	0.98	1.08	5.75	1.64	2.00	0.88	79.68	1.06
		8.43	6000	450	97.2	90.6	90.6	90.8	98.5	1.14	2.03	1.22	0.64	101.18	0.90	1.08	5.75	1.64	2.00	0.88	79.68	1.14
		8.43	6000	600	101.7	92.6	92.6	90.8	98.5	1.16	2.35	1.22	0.64	113.27	0.82	1.08	5.75	1.64	2.00	0.88	79.68	1.16
		8.43	6000	750	103.7	93.5	93.5	90.8	98.5	1.17	2.63	1.22	0.64	123.63	0.76	1.08	5.75	1.64	2.00	0.88	79.68	1.17
WSC7_L6	120x60x15x3	8.43	6500	150	68.4	62.4	62.4	82.0	84.0	0.94	1.24	1.22	0.64	66.10	0.94	1.02	6.84	1.88	2.00	0.88	66.10	0.94
		8.43	6500	300	81.3	74.1	74.1	82.0	84.0	1.03	1.75	1.22	0.64	81.14	0.91	1.02	6.84	1.88	2.00	0.88	71.98	1.03
		8.43	6500	450	87.5	78.1	78.1	82.0	84.0	1.09	2.14	1.22	0.64	95.12	0.82	1.02	6.84	1.88	2.00	0.88	71.98	1.08
		8.43	6500	600	90.2	79.5	79.5	82.0	84.0	1.10	2.47	1.22	0.64	106.49	0.75	1.02	6.84	1.88	2.00	0.88	71.98	1.10
		8.43	6500	750	90.9	80.2	80.2	82.0	84.0	1.12	2.76	1.22	0.64	116.23	0.69	1.02	6.84	1.88	2.00	0.88	71.98	1.11
WSC8_L1	110x50x10x2	11.08	3500	150	62.1	62.7	62.1	109.0	133.5	1.08	0.84	1.37	0.68	57.54	1.08	1.23	2.12	1.33	1.99	0.87	57.54	1.08
		11.08	3500	300	90.6	97.6	90.6	109.0	133.5	1.06	1.19	1.37	0.68	85.45	1.06	1.23	2.12	1.33	1.99	0.87	85.45	1.06
		11.08	3500	450	100.2	109.9	100.2	109.0	133.5	1.05	1.46	1.37	0.68	95.17	1.05	1.23	2.12	1.33	1.99	0.87	95.17	1.05
		11.08	3500	600	105.0	117.7	105.0	109.0	133.5	1.10	1.69	1.37	0.68	102.88	1.02	1.23	2.12	1.33	1.99	0.87	95.70	1.10
		11.08	3500	750	108.2	120.7	108.2	109.0	133.5	1.13	1.89	1.37	0.68	110.31	0.98	1.23	2.12	1.33	1.99	0.87	95.79	1.13
WSC8_L2	110x50x10x2	11.08	4000	150	57.0	57.7	57.0	86.1	103.2	1.07	0.95	1.37	0.68	53.17	1.07	1.20	2.73	1.37	2.00	0.88	53.17	1.07
		11.08	4000	300	76.2	82.3	76.2	86.1	103.2	1.04	1.34	1.37	0.68	72.96	1.04	1.20	2.73	1.37	2.00	0.88	72.96	1.04
		11.08	4000	450	83.1	90.5	83.1	86.1	103.2	1.10	1.64	1.37	0.68	79.99	1.04	1.20	2.73	1.37	2.00	0.88	75.56	1.10
		11.08	4000	600	87.5	93.7	87.5	86.1	103.2	1.16	1.90	1.37	0.68	87.52	1.00	1.20	2.73	1.37	2.00	0.88	75.56	1.16
		11.08	4000	750	90.5	94.2	90.5	86.1	103.2	1.20	2.12	1.37	0.68	93.84	0.96	1.20	2.73	1.37	2.00	0.88	75.56	1.20
WSC8_L3	110x50x10x2	11.08	4500	150	51.6	52.3	51.6	70.4	82.0	1.05	1.05	1.37	0.68	48.88	1.05	1.16	3.41	1.43	2.00	0.88	48.88	1.05
		11.08	4500	300	65.1	68.6	65.1	70.4	82.0	1.06	1.48	1.37	0.68	61.68	1.06	1.16	3.41	1.43	2.00	0.88	61.68	1.06
		11.08	4500	450	70.9	73.2	70.9	70.4	82.0	1.15	1.82	1.37	0.68	69.65	1.02	1.16	3.41	1.43	2.00	0.88	61.78	1.15
		11.08	4500	600	74.7	75.3	74.7	70.4	82.0	1.21	2.10	1.37	0.68	76.20	0.98	1.16	3.41	1.43	2.00	0.88	61.78	1.21
		11.08	4500	750	77.0	76.5	76.5	70.4	82.0	1.24	2.35	1.37	0.68	81.71	0.94	1.16	3.41	1.43	2.00	0.88	61.78	1.24
WSC8_L4	110x50x10x2	11.08	5000	150	46.4	46.5	46.4	59.1	66.6	1.04	1.14	1.37	0.68	44.78	1.04	1.13	4.14	1.52	2.00	0.88	44.78	1.04
		11.08	5000	300	56.7	57.5	56.7	59.1	66.6	1.09	1.62	1.37	0.68	54.43	1.04	1.13	4.14	1.52	2.00	0.88	51.90	

Table I.5: WFSC column (i) geometries, (ii) β_{FT} values, (iii) yield stresses, (iv) buckling load values and ratios, (v) numerical failure loads, (vi) failure load predictions estimates P_{nG} , P_{nFT} and P_{nFT-Fm} , and (vii) numerical-to-predicted failure loads ratios (mm, kN)

Column	Geometry			SFEA					DSM Design													
	$b_w \times b_f \times b_s \times t$	β_{FT}	L	f_y	$P_{u,FT}$	$P_{u,Fm}$	P_u	$P_{cr,FT}$	$P_{b,Fm}$	$\frac{P_u}{P_{cG}}$	λ_{FT}	b	a	P_{nFT}	$\frac{P_u}{P_{nFT}}$	R_G	R_{DL}	c	b	a	P_{nFT-Fm}	$\frac{P_u}{P_{nFT-Fm}}$
WFSC1_L1	110x60x15x3	6.85	4500	150	86.6	95.9	86.6	117.6	172.3	1.07	1.04	1.12	0.61	81.22	1.07	1.47	3.63	0.791	1.20	0.63	81.22	1.07
		6.85	4500	300	109.7	136.6	109.7	117.6	172.3	1.07	1.48	1.12	0.61	102.93	1.07	1.47	3.63	0.791	1.20	0.63	102.93	1.07
		6.85	4500	450	122.6	150.4	122.6	117.6	172.3	1.19	1.81	1.12	0.61	121.61	1.01	1.47	3.63	0.791	1.20	0.63	119.78	1.02
		6.85	4500	600	133.8	156.8	133.8	117.6	172.3	1.30	2.09	1.12	0.61	138.01	0.97	1.47	3.63	0.791	1.20	0.63	134.35	1.00
		6.85	4500	750	142.7	160.5	142.7	117.6	172.3	1.38	2.33	1.12	0.61	152.23	0.94	1.47	3.63	0.791	1.20	0.63	146.85	0.97
WFSC1_L2	110x60x15x3	6.85	5000	150	79.4	77.3	77.3	101.9	139.7	1.02	1.12	1.12	0.61	75.70	1.02	1.37	4.60	1.079	1.49	0.71	75.70	1.02
		6.85	5000	300	98.0	114.6	98.0	101.9	139.7	1.10	1.59	1.12	0.61	93.90	1.04	1.37	4.60	1.079	1.49	0.71	91.98	1.07
		6.85	5000	450	109.8	124.0	109.8	101.9	139.7	1.23	1.94	1.12	0.61	112.22	0.98	1.37	4.60	1.079	1.49	0.71	102.00	1.08
		6.85	5000	600	119.0	128.4	119.0	101.9	139.7	1.33	2.24	1.12	0.61	127.34	0.93	1.37	4.60	1.079	1.49	0.71	109.77	1.08
		6.85	5000	750	125.6	131.3	125.6	101.9	139.7	1.41	2.51	1.12	0.61	140.46	0.89	1.37	4.60	1.079	1.49	0.71	116.21	1.08
WFSC1_L3	110x60x15x3	6.85	5500	150	73.0	72.8	72.8	90.1	115.5	1.03	1.19	1.12	0.61	70.68	1.03	1.28	5.70	1.242	1.65	0.76	70.68	1.03
		6.85	5500	300	88.8	97.0	88.8	90.1	115.5	1.12	1.69	1.12	0.61	87.67	1.01	1.28	5.70	1.242	1.65	0.76	82.37	1.08
		6.85	5500	450	99.0	105.4	99.0	90.1	115.5	1.25	2.07	1.12	0.61	104.77	0.94	1.28	5.70	1.242	1.65	0.76	88.38	1.12
		6.85	5500	600	106.1	108.1	106.1	90.1	115.5	1.34	2.39	1.12	0.61	118.89	0.89	1.28	5.70	1.242	1.65	0.76	92.91	1.14
		6.85	5500	750	110.4	109.5	109.5	90.1	115.5	1.39	2.67	1.12	0.61	131.14	0.84	1.28	5.70	1.242	1.65	0.76	96.59	1.13
WFSC1_L4	110x60x15x3	6.85	6000	150	67.6	70.6	67.6	81.1	97.1	1.02	1.26	1.12	0.61	66.14	1.02	1.20	6.88	1.373	1.78	0.80	66.14	1.02
		6.85	6000	300	81.2	85.5	81.2	81.1	97.1	1.14	1.78	1.12	0.61	82.62	0.98	1.20	6.88	1.373	1.78	0.80	73.81	1.10
		6.85	6000	450	89.4	89.6	89.4	81.1	97.1	1.26	2.18	1.12	0.61	98.74	0.91	1.20	6.88	1.373	1.78	0.80	77.12	1.16
		6.85	6000	600	94.4	90.8	90.8	81.1	97.1	1.28	2.51	1.12	0.61	112.05	0.81	1.20	6.88	1.373	1.78	0.80	79.55	1.14
		6.85	6000	750	97.0	92.6	92.6	81.1	97.1	1.30	2.81	1.12	0.61	123.60	0.75	1.20	6.88	1.373	1.78	0.80	81.50	1.14
WFSC1_L5	110x60x15x3	6.85	6500	150	63.0	61.2	61.2	73.9	82.7	0.99	1.32	1.12	0.61	62.04	0.99	1.12	8.19	1.539	1.95	0.86	62.04	0.99
		6.85	6500	300	74.5	73.0	73.0	73.9	82.7	1.13	1.86	1.12	0.61	78.46	0.93	1.12	8.19	1.539	1.95	0.86	65.58	1.11
		6.85	6500	450	80.9	76.8	76.8	73.9	82.7	1.18	2.28	1.12	0.61	93.77	0.82	1.12	8.19	1.539	1.95	0.86	66.26	1.16
		6.85	6500	600	84.0	78.4	78.4	73.9	82.7	1.21	2.63	1.12	0.61	106.40	0.74	1.12	8.19	1.539	1.95	0.86	66.74	1.18
		6.85	6500	750	85.2	79.2	79.2	73.9	82.7	1.22	2.94	1.12	0.61	117.37	0.67	1.12	8.19	1.539	1.95	0.86	67.11	1.18
WFSC1_L6	110x60x15x3	6.85	7000	150	58.9	53.4	53.4	68.2	71.3	0.92	1.37	1.12	0.61	58.34	0.92	1.05	9.63	1.779	2.00	0.88	58.34	0.92
		6.85	7000	300	68.6	64.6	64.6	68.2	71.3	1.08	1.94	1.12	0.61	74.96	0.86	1.05	9.63	1.779	2.00	0.88	59.81	1.08
		6.85	7000	450	73.0	66.1	66.1	68.2	71.3	1.11	2.38	1.12	0.61	89.59	0.74	1.05	9.63	1.779	2.00	0.88	59.81	1.11
		6.85	7000	600	74.7	67.9	67.9	68.2	71.3	1.14	2.74	1.12	0.61	101.66	0.67	1.05	9.63	1.779	2.00	0.88	59.81	1.14
		6.85	7000	750	75.0	68.4	68.4	68.2	71.3	1.15	3.07	1.12	0.61	112.14	0.61	1.05	9.63	1.779	2.00	0.88	59.81	1.14
WFSC2_L1	100x60x10x3	5.92	4500	150	75.7	86.2	75.7	97.7	148.3	1.06	1.10	1.07	0.60	71.52	1.06	1.52	3.91	0.71	1.07	0.60	71.52	1.06
		5.92	4500	300	94.2	117.5	94.2	97.7	148.3	1.10	1.56	1.07	0.60	89.03	1.06	1.52	3.91	0.71	1.07	0.60	89.03	1.06
		5.92	4500	450	106.6	125.5	106.6	97.7	148.3	1.25	1.91	1.07	0.60	107.60	0.99	1.52	3.91	0.71	1.07	0.60	107.60	0.99
		5.92	4500	600	117.3	134.6	117.3	97.7	148.3	1.37	2.21	1.07	0.60	123.09	0.95	1.52	3.91	0.71	1.07	0.60	123.09	0.95
		5.92	4500	750	125.4	138.6	125.4	97.7	148.3	1.46	2.47	1.07	0.60	136.62	0.92	1.52	3.91	0.71	1.07	0.60	136.62	0.92
WFSC2_L2	100x60x10x3	5.92	5000	150	69.5	77.9	69.5	85.9	120.2	1.04	1.18	1.07	0.60	66.70	1.04	1.40	4.92	1.012	1.37	0.68	66.70	1.04
		5.92	5000	300	85.2	98.6	85.2	85.9	120.2	1.13	1.67	1.07	0.60	83.16	1.02	1.40	4.92	1.012	1.37	0.68	80.58	1.06
		5.92	5000	450	96.1	107.9	96.1	85.9	120.2	1.28	2.04	1.07	0.60	100.51	0.96	1.40	4.92	1.012	1.37	0.68	91.61	1.05
		5.92	5000	600	104.4	111.6	104.4	85.9	120.2	1.39	2.36	1.07	0.60	114.97	0.91	1.40	4.92	1.012	1.37	0.68	100.35	1.04
		5.92	5000	750	109.9	112.4	109.9	85.9	120.2	1.46	2.63	1.07	0.60	127.61	0.86	1.40	4.92	1.012	1.37	0.68	107.69	1.02
WFSC2_L3	100x60x10x3	5.92	5500	150	64.2	63.4	63.4	77.1	99.4	1.02	1.24	1.07	0.60	62.40	1.02	1.29	6.04	1.23	1.59	0.74	62.40	1.02
		5.92	5500	300	77.8	86.1	77.8	99.4	1.15	1.76	1.07	0.60	78.49	0.99	1.29	6.04	1.23	1.59	0.74	72.26	1.08	
		5.92	5500	450	86.8	91.1	86.8	77.1	99.4	1.28	2.15	1.07	0.60	94.86	0.92	1.29	6.04	1.23	1.59	0.74	78.59	1.11
		5.92	5500	600	92.7	93.0	92.7	77.1	99.4	1.37	2.49	1.07	0.60	108.51	0.85	1.29	6.04	1.23	1.59	0.74	83.42	1.11
		5.92	5500	750	96.1	94.3	94.3	77.1	99.4	1.40	2.78	1.07	0.60	120.44	0.78	1.29	6.04	1.23	1.59	0.74	87.36	1.08
WFSC2_L4	100x60x10x3	5.92	6000	150	59.8	61.9	59.8	70.2	83.5	1.02	1.30	1.07	0.60	58.57	1.02	1.19	7.30	1.387	1.74	0.79	58.57	1.02
		5.92	6000	300	71.4	72.2	71.4	70.2	83.5	1.16</												

Column	Geometry			SFEA				DSM Design														
	$b_w \times b_f \times b_s \times t$	β_{FT}	L	f_y	$P_{u,FT}$	$P_{u,Fm}$	P_u	$P_{cr,FT}$	$P_{b,Fm}$	$\frac{P_u}{P_{nG}}$	λ_{FT}	b	a	P_{nFT}	$\frac{P_u}{P_{nFT}}$	R_G	R_{DL}	c	b	a	P_{nFT-Fm}	$\frac{P_u}{P_{nFT-Fm}}$
WFSC3_L1	100x50x10x2	8.66	3500	150	50.1	55.7	50.1	69.1	105.2	1.06	1.03	1.23	0.64	47.06	1.06	1.52	2.52	0.71	1.23	0.64	47.06	1.06
		8.66	3500	300	64.5	80.4	64.5	69.1	105.2	1.07	1.46	1.23	0.64	60.30	1.07	1.52	2.52	0.71	1.23	0.64	60.30	1.07
		8.66	3500	450	72.6	90.9	72.6	69.1	105.2	1.20	1.79	1.23	0.64	69.32	1.05	1.52	2.52	0.71	1.23	0.64	69.32	1.05
		8.66	3500	600	79.7	93.3	79.7	69.1	105.2	1.32	2.06	1.23	0.64	77.45	1.03	1.52	2.52	0.71	1.23	0.64	77.45	1.03
		8.66	3500	750	85.2	96.8	85.2	69.1	105.2	1.41	2.31	1.23	0.64	84.40	1.01	1.52	2.52	0.71	1.23	0.64	84.40	1.01
WFSC3_L2	100x50x10x2	8.66	4500	150	39.5	43.1	39.5	47.3	63.8	1.03	1.25	1.23	0.64	38.36	1.03	1.35	4.30	1.125	1.65	0.76	38.36	1.03
		8.66	4500	300	49.0	50.4	49.0	47.3	63.8	1.18	1.76	1.23	0.64	47.01	1.04	1.35	4.30	1.125	1.65	0.76	43.96	1.11
		8.66	4500	450	55.6	57.8	55.6	47.3	63.8	1.34	2.16	1.23	0.64	54.95	1.01	1.35	4.30	1.125	1.65	0.76	47.24	1.18
		8.66	4500	600	59.8	59.5	59.5	47.3	63.8	1.43	2.49	1.23	0.64	61.39	0.97	1.35	4.30	1.125	1.65	0.76	49.72	1.20
		8.66	4500	750	62.1	60.1	47.3	63.8	1.45	2.79	1.23	0.64	66.90	0.90	1.35	4.30	1.125	1.65	0.76	51.73	1.16	
WFSC3_L3	100x50x10x2	8.66	5000	150	35.6	38.0	35.6	40.9	51.7	1.03	1.34	1.23	0.64	34.66	1.03	1.26	5.45	1.268	1.79	0.81	34.66	1.03
		8.66	5000	300	43.9	44.5	43.9	40.9	51.7	1.22	1.89	1.23	0.64	43.00	1.02	1.26	5.45	1.268	1.79	0.81	37.75	1.16
		8.66	5000	450	49.1	47.7	47.7	40.9	51.7	1.33	2.32	1.23	0.64	50.27	0.95	1.26	5.45	1.268	1.79	0.81	39.40	1.21
		8.66	5000	600	51.8	48.6	48.6	40.9	51.7	1.35	2.68	1.23	0.64	56.16	0.87	1.26	5.45	1.268	1.79	0.81	40.63	1.20
		8.66	5000	750	52.9	49.1	49.1	40.9	51.7	1.37	3.00	1.23	0.64	61.20	0.80	1.26	5.45	1.268	1.79	0.81	41.60	1.18
WFSC3_L4	100x50x10x2	8.66	5500	150	32.5	33.2	32.5	36.2	42.8	1.03	1.42	1.23	0.64	31.40	1.03	1.18	6.71	1.4	1.92	0.85	31.40	1.03
		8.66	5500	300	39.6	37.2	37.2	36.2	42.8	1.17	2.02	1.23	0.64	39.86	0.93	1.18	6.71	1.4	1.92	0.85	32.52	1.14
		8.66	5500	450	43.4	39.8	39.8	36.2	42.8	1.26	2.47	1.23	0.64	46.59	0.85	1.18	6.71	1.4	1.92	0.85	33.05	1.20
		8.66	5500	600	44.8	40.1	40.1	36.2	42.8	1.26	2.85	1.23	0.64	52.05	0.77	1.18	6.71	1.4	1.92	0.85	33.44	1.20
		8.66	5500	750	45.2	40.8	40.8	36.2	42.8	1.28	3.19	1.23	0.64	56.73	0.72	1.18	6.71	1.4	1.92	0.85	33.74	1.21
WFSC3_L5	100x50x10x2	8.66	6000	150	29.9	26.5	26.5	32.5	35.9	0.93	1.50	1.23	0.64	28.59	0.93	1.10	8.11	1.577	2.00	0.88	28.55	0.93
		8.66	6000	300	35.8	32.4	32.4	32.5	35.9	1.13	2.13	1.23	0.64	37.33	0.87	1.10	8.11	1.577	2.00	0.88	28.55	1.13
		8.66	6000	450	38.2	33.7	33.7	32.5	35.9	1.18	2.60	1.23	0.64	43.65	0.77	1.10	8.11	1.577	2.00	0.88	28.55	1.18
		8.66	6000	600	38.8	34.2	34.2	32.5	35.9	1.20	3.01	1.23	0.64	48.76	0.70	1.10	8.11	1.577	2.00	0.88	28.55	1.20
		8.66	6000	750	38.8	34.4	34.4	32.5	35.9	1.20	3.36	1.23	0.64	53.14	0.65	1.10	8.11	1.577	2.00	0.88	28.55	1.20
WFSC3_L6	100x50x10x2	8.66	6500	150	27.7	24.4	24.4	29.7	30.6	0.94	1.57	1.23	0.64	27.01	0.90	1.03	9.66	1.839	2.00	0.88	26.03	0.94
		8.66	6500	300	32.3	28.1	28.1	29.7	30.6	1.08	2.23	1.23	0.64	35.27	0.80	1.03	9.66	1.839	2.00	0.88	26.03	1.08
		8.66	6500	450	33.6	28.7	28.7	29.7	30.6	1.10	2.73	1.23	0.64	41.24	0.70	1.03	9.66	1.839	2.00	0.88	26.03	1.10
		8.66	6500	600	33.8	29.2	29.2	29.7	30.6	1.12	3.15	1.23	0.64	46.07	0.63	1.03	9.66	1.839	2.00	0.88	26.03	1.12
		8.66	6500	750	33.8	29.4	29.4	29.7	30.6	1.13	3.52	1.23	0.64	50.20	0.59	1.03	9.66	1.839	2.00	0.88	26.03	1.13
WFSC4_L1	90x50x10x2	7.20	4500	150	35.8	42.4	35.8	41.8	61.5	1.03	1.30	1.14	0.62	34.79	1.03	1.47	4.57	0.765	1.20	0.63	34.79	1.03
		7.20	4500	300	44.3	52.9	44.3	41.8	61.5	1.21	1.84	1.14	0.62	43.63	1.02	1.47	4.57	0.765	1.20	0.63	43.15	1.03
		7.20	4500	450	50.6	56.1	50.6	41.8	61.5	1.38	2.25	1.14	0.62	51.92	0.98	1.47	4.57	0.765	1.20	0.63	50.78	1.00
		7.20	4500	600	54.9	57.5	54.9	41.8	61.5	1.50	2.60	1.14	0.62	58.74	0.93	1.47	4.57	0.765	1.20	0.63	57.00	0.96
		7.20	4500	750	57.4	58.2	57.4	41.8	61.5	1.57	2.90	1.14	0.62	64.64	0.89	1.47	4.57	0.765	1.20	0.63	62.35	0.92
WFSC4_L2	90x50x10x2	7.20	5000	150	32.3	36.8	32.3	36.4	49.9	1.03	1.39	1.14	0.62	31.35	1.03	1.37	5.78	1.084	1.52	0.72	31.35	1.03
		7.20	5000	300	39.9	43.7	39.9	36.4	49.9	1.25	1.97	1.14	0.62	40.33	0.99	1.37	5.78	1.084	1.52	0.72	36.44	1.09
		7.20	5000	450	44.9	45.9	44.9	36.4	49.9	1.41	2.41	1.14	0.62	47.99	0.94	1.37	5.78	1.084	1.52	0.72	40.20	1.12
		7.20	5000	600	47.7	47.0	47.0	36.4	49.9	1.47	2.78	1.14	0.62	54.29	0.87	1.37	5.78	1.084	1.52	0.72	43.10	1.09
		7.20	5000	750	49.0	47.5	47.5	36.4	49.9	1.49	3.11	1.14	0.62	59.75	0.79	1.37	5.78	1.084	1.52	0.72	45.50	1.04
WFSC4_L3	90x50x10x2	7.20	5500	150	29.5	31.4	29.5	32.4	41.2	1.04	1.47	1.14	0.62	28.35	1.04	1.27	7.12	1.255	1.69	0.77	28.35	1.04
		7.20	5500	300	36.1	36.9	36.1	32.4	41.2	1.27	2.09	1.14	0.62	37.72	0.96	1.27	7.12	1.255	1.69	0.77	31.51	1.14
		7.20	5500	450	39.7	38.2	38.2	32.4	41.2	1.34	2.55	1.14	0.62	44.88	0.85	1.27	7.12	1.255	1.69	0.77	33.57	1.14
		7.20	5500	600	41.3	39.0	39.0	32.4	41.2	1.37	2.95	1.14	0.62	50.78	0.77	1.27	7.12	1.255	1.69	0.77	35.12	1.11
		7.20	5500	750	41.8	39.4	39.4	32.4	41.2	1.39	3.30	1.14	0.62	55.88	0.71	1.27	7.12	1.255	1.69	0.77	36.36	1.08
WFSC4_L4	90x50x10x2	7.20	6000	150	27.3	27.9	27.3	29.3	34.6	1.06	1.55	1.14	0.62	26.45	1.03	1.18	8.61	1.399	1.83	0.82	25.84	1.05
		7.20	6000	300	32.6	31.2	31.2	29.3	34.6	1.21	2.19	1.14	0.62	35.61	0.88	1.18	8.61	1.399	1.83	0.82	27.41	1.14
		7.20	6000	450	35.1	32.4	32.4	29.3	34.6	1.26	2.69	1.14	0.62	42.37	0.76	1.18	8.61	1.399	1.83	0.82	28.37</	

Column	Geometry				SFEA						DSM Design											
	$b_w \times b_f \times b_s \times t$	β_{FT}	L	f_y	$P_{u,FT}$	$P_{u,Fm}$	P_u	$P_{cr,FT}$	$P_{b,Fm}$	$\frac{P_u}{P_{nG}}$	λ_{FT}	b	a	P_{nFT}	$\frac{P_u}{P_{nFT}}$	R_G	R_{DL}	c	b	a	P_{nFT-Fm}	$\frac{P_u}{P_{nFT-Fm}}$
WFSC5_L1	100x60x15x3	5.83	5000	150	72.8	80.1	72.8	91.1	135.1	1.04	1.17	1.06	0.60	70.05	1.04	1.48	4.87	0.715	1.06	0.60	70.05	1.04
		5.83	5000	300	89.2	108.0	89.2	91.1	135.1	1.12	1.65	1.06	0.60	87.30	1.02	1.48	4.87	0.715	1.06	0.60	87.26	1.02
		5.83	5000	450	100.5	120.6	100.5	91.1	135.1	1.26	2.02	1.06	0.60	105.64	0.95	1.48	4.87	0.715	1.06	0.60	105.48	0.95
		5.83	5000	600	109.6	125.1	109.6	91.1	135.1	1.37	2.33	1.06	0.60	120.93	0.91	1.48	4.87	0.715	1.06	0.60	120.67	0.91
		5.83	5000	750	116.3	127.5	116.3	91.1	135.1	1.46	2.61	1.06	0.60	134.30	0.87	1.48	4.87	0.715	1.06	0.60	133.94	0.87
WFSC5_L2	100x60x15x3	5.83	5500	150	66.9	71.3	66.9	80.9	111.7	1.03	1.24	1.06	0.60	65.24	1.03	1.38	6.03	1.059	1.41	0.69	65.24	1.03
		5.83	5500	300	81.9	96.2	81.9	80.9	111.7	1.14	1.75	1.06	0.60	82.02	0.99	1.38	6.03	1.059	1.41	0.69	77.75	1.04
		5.83	5500	450	90.9	102.0	90.9	80.9	111.7	1.28	2.14	1.06	0.60	99.24	0.92	1.38	6.03	1.059	1.41	0.69	87.65	1.04
		5.83	5500	600	97.9	103.2	97.9	80.9	111.7	1.38	2.47	1.06	0.60	113.61	0.86	1.38	6.03	1.059	1.41	0.69	95.43	1.03
		5.83	5500	750	102.5	106.1	102.5	80.9	111.7	1.44	2.76	1.06	0.60	126.17	0.81	1.38	6.03	1.059	1.41	0.69	101.94	1.01
WFSC5_L3	100x60x15x3	5.83	6000	150	62.0	65.7	62.0	73.1	93.9	1.02	1.30	1.06	0.60	60.92	1.02	1.28	7.28	1.238	1.59	0.74	60.92	1.02
		5.83	6000	300	74.3	82.4	74.3	73.1	93.9	1.16	1.84	1.06	0.60	77.71	0.96	1.28	7.28	1.238	1.59	0.74	69.78	1.06
		5.83	6000	450	82.3	85.4	82.3	73.1	93.9	1.28	2.25	1.06	0.60	94.03	0.87	1.28	7.28	1.238	1.59	0.74	75.86	1.08
		5.83	6000	600	87.3	88.7	87.3	73.1	93.9	1.36	2.60	1.06	0.60	107.64	0.81	1.28	7.28	1.238	1.59	0.74	80.50	1.08
		5.83	6000	750	90.2	89.7	89.7	73.1	93.9	1.40	2.91	1.06	0.60	119.55	0.75	1.28	7.28	1.238	1.59	0.74	84.28	1.06
WFSC5_L4	100x60x15x3	5.83	6500	150	57.8	54.3	54.3	66.9	80.0	0.95	1.36	1.06	0.60	57.03	0.95	1.20	8.67	1.375	1.72	0.78	57.03	0.95
		5.83	6500	300	68.3	71.5	68.3	66.9	80.0	1.16	1.92	1.06	0.60	74.13	0.92	1.20	8.67	1.375	1.72	0.78	62.83	1.09
		5.83	6500	450	74.5	74.5	66.9	80.0	1.27	2.36	1.06	0.60	89.69	0.83	1.20	8.67	1.375	1.72	0.78	66.44	1.12	
		5.83	6500	600	77.8	76.0	76.0	66.9	80.0	1.30	2.72	1.06	0.60	102.68	0.74	1.20	8.67	1.375	1.72	0.78	69.13	1.10
		5.83	6500	750	79.4	76.8	76.8	66.9	80.0	1.31	3.04	1.06	0.60	114.03	0.67	1.20	8.67	1.375	1.72	0.78	71.28	1.08
WFSC5_L5	100x60x15x3	5.83	7000	150	54.1	54.0	54.0	61.8	69.0	1.01	1.41	1.06	0.60	53.51	1.01	1.12	10.18	1.546	1.90	0.84	53.51	1.01
		5.83	7000	300	62.9	61.6	61.6	61.8	69.0	1.14	2.00	1.06	0.60	71.09	0.87	1.12	10.18	1.546	1.90	0.84	55.87	1.10
		5.83	7000	450	67.4	64.8	64.8	61.8	69.0	1.20	2.45	1.06	0.60	86.01	0.75	1.12	10.18	1.546	1.90	0.84	57.07	1.14
		5.83	7000	600	69.3	65.7	65.7	61.8	69.0	1.21	2.83	1.06	0.60	98.47	0.67	1.12	10.18	1.546	1.90	0.84	57.93	1.13
		5.83	7000	750	70.0	66.4	66.4	61.8	69.0	1.23	3.16	1.06	0.60	109.35	0.61	1.12	10.18	1.546	1.90	0.84	58.61	1.13
WFSC5_L6	100x60x15x3	5.83	7500	150	50.8	47.6	47.6	57.6	60.1	0.95	1.47	1.06	0.60	50.32	0.95	1.04	11.82	1.791	2.00	0.88	50.32	0.95
		5.83	7500	300	57.9	54.5	54.5	57.6	60.1	1.08	2.07	1.06	0.60	68.47	0.80	1.04	11.82	1.791	2.00	0.88	50.51	1.08
		5.83	7500	450	60.9	56.8	56.8	57.6	60.1	1.13	2.54	1.06	0.60	82.84	0.69	1.04	11.82	1.791	2.00	0.88	50.51	1.12
		5.83	7500	600	61.8	57.3	57.3	57.6	60.1	1.13	2.93	1.06	0.60	94.84	0.60	1.04	11.82	1.791	2.00	0.88	50.51	1.13
		5.83	7500	750	61.9	58.1	58.1	57.6	60.1	1.15	3.28	1.06	0.60	105.32	0.55	1.04	11.82	1.791	2.00	0.88	50.51	1.15
WFSC6_L1	120x60x20x3	7.90	3500	150	114.1	118.9	114.1	213.8	321.2	1.09	0.80	1.18	0.63	104.88	1.09	1.50	2.18	0.71	1.18	0.63	104.88	1.09
		7.90	3500	300	172.6	205.9	172.6	213.8	321.2	1.08	1.13	1.18	0.63	160.37	1.08	1.50	2.18	0.71	1.18	0.63	160.37	1.08
		7.90	3500	450	194.7	230.9	194.7	213.8	321.2	1.06	1.39	1.18	0.63	183.91	1.06	1.50	2.18	0.71	1.18	0.63	183.91	1.06
		7.90	3500	600	207.4	274.1	207.4	213.8	321.2	1.11	1.60	1.18	0.63	197.99	1.05	1.50	2.18	0.71	1.18	0.63	197.99	1.05
		7.90	3500	750	218.0	284.7	218.0	213.8	321.2	1.16	1.79	1.18	0.63	216.87	1.01	1.50	2.18	0.71	1.18	0.63	216.87	1.01
WFSC6_L2	120x60x20x3	7.90	4500	150	98.5	105.2	98.5	143.1	195.8	1.07	0.98	1.18	0.63	91.83	1.07	1.37	3.51	1.085	1.56	0.73	91.83	1.07
		7.90	4500	300	128.8	152.2	128.8	143.1	195.8	1.05	1.38	1.18	0.63	122.94	1.05	1.37	3.51	1.085	1.56	0.73	122.94	1.05
		7.90	4500	450	142.2	168.8	142.2	143.1	195.8	1.13	1.70	1.18	0.63	138.78	1.03	1.37	3.51	1.085	1.56	0.73	132.53	1.07
		7.90	4500	600	153.1	177.9	153.1	143.1	195.8	1.22	1.96	1.18	0.63	156.07	0.98	1.37	3.51	1.085	1.56	0.73	141.23	1.08
		7.90	4500	750	162.0	181.4	162.0	143.1	195.8	1.29	2.19	1.18	0.63	170.95	0.95	1.37	3.51	1.085	1.56	0.73	148.36	1.09
WFSC6_L3	120x60x20x3	7.90	5500	150	83.4	82.5	82.5	106.8	131.4	1.03	1.13	1.18	0.63	80.15	1.03	1.23	5.32	1.32	1.79	0.81	80.15	1.03
		7.90	5500	300	102.1	110.3	102.1	106.8	131.4	1.09	1.60	1.18	0.63	98.95	1.03	1.23	5.32	1.32	1.79	0.81	95.04	1.07
		7.90	5500	450	112.7	118.0	112.7	106.8	131.4	1.20	1.96	1.18	0.63	116.76	0.97	1.23	5.32	1.32	1.79	0.81	99.09	1.14
		7.90	5500	600	120.4	122.6	120.4	106.8	131.4	1.28	2.27	1.18	0.63	131.31	0.92	1.23	5.32	1.32	1.79	0.81	102.07	1.18
		7.90	5500	750	125.3	124.2	124.2	106.8	131.4	1.33	2.53	1.18	0.63	143.83	0.86	1.23	5.32	1.32	1.79	0.81	104.44	1.19
WFSC6_L4	120x60x20x3	7.90	6000	150	77.0	78.4	77.0	95.0	110.4	1.03	1.20	1.18	0.63	74.96	1.03	1.16	6.48	1.438	1.91	0.85	74.96	1.03
		7.90	6000	300	92.6	96.5	92.6	95.0	110.4	1.11	1.70	1.18	0.63	92.31	1.00	1.16	6.48	1.438	1.91	0.85	84.	

Column	Geometry			SFEA						DSM Design												
	$b_w \times b_f \times b_s \times t$	β_{FT}	L	f_y	$P_{u,FT}$	$P_{u,Fm}$	P_u	$P_{cr,FT}$	$P_{b,Fm}$	$\frac{P_u}{P_{nG}}$	λ_{FT}	b	a	P_{nFT}	$\frac{P_u}{P_{nFT}}$	R_G	R_{DL}	c	b	a	P_{nFT-Fm}	$\frac{P_u}{P_{nFT-Fm}}$
WFSC7_L1	110x50x15x2	10.02	3500	150	58.2	60.3	58.2	88.1	123.2	1.07	0.95	1.31	0.66	54.48	1.07	1.40	2.39	1.012	1.61	0.75	54.48	1.07
		10.02	3500	300	78.2	93.4	78.2	88.1	123.2	1.05	1.34	1.31	0.66	74.70	1.05	1.40	2.39	1.012	1.61	0.75	74.70	1.05
		10.02	3500	450	86.7	104.8	86.7	88.1	123.2	1.12	1.64	1.31	0.66	82.39	1.05	1.40	2.39	1.012	1.61	0.75	80.13	1.08
		10.02	3500	600	93.2	110.1	93.2	88.1	123.2	1.21	1.90	1.31	0.66	90.97	1.02	1.40	2.39	1.012	1.61	0.75	84.71	1.10
		10.02	3500	750	98.4	112.4	98.4	88.1	123.2	1.27	2.12	1.31	0.66	98.23	1.00	1.40	2.39	1.012	1.61	0.75	88.44	1.11
WFSC7_L2	110x50x15x2	10.02	4000	150	52.0	56.0	52.0	70.6	94.7	1.05	1.06	1.31	0.66	49.61	1.05	1.34	3.08	1.14	1.74	0.79	49.61	1.05
		10.02	4000	300	66.2	76.7	66.2	70.6	94.7	1.07	1.50	1.31	0.66	61.97	1.07	1.34	3.08	1.14	1.74	0.79	61.97	1.07
		10.02	4000	450	73.9	83.5	73.9	70.6	94.7	1.19	1.84	1.31	0.66	71.25	1.04	1.34	3.08	1.14	1.74	0.79	65.30	1.13
		10.02	4000	600	79.7	86.5	79.7	70.6	94.7	1.29	2.12	1.31	0.66	78.67	1.01	1.34	3.08	1.14	1.74	0.79	67.77	1.18
		10.02	4000	750	83.8	87.8	83.8	70.6	94.7	1.35	2.37	1.31	0.66	84.96	0.99	1.34	3.08	1.14	1.74	0.79	69.75	1.20
WFSC7_L3	110x50x15x2	10.02	4500	150	46.4	50.0	46.4	58.6	75.0	1.03	1.16	1.31	0.66	45.03	1.03	1.28	3.85	1.243	1.84	0.82	45.03	1.03
		10.02	4500	300	57.6	62.6	57.6	58.6	75.0	1.12	1.65	1.31	0.66	54.82	1.05	1.28	3.85	1.243	1.84	0.82	52.15	1.10
		10.02	4500	450	64.4	67.9	64.4	58.6	75.0	1.25	2.02	1.31	0.66	63.03	1.02	1.28	3.85	1.243	1.84	0.82	53.82	1.20
		10.02	4500	600	69.1	69.3	69.1	58.6	75.0	1.34	2.33	1.31	0.66	69.59	0.99	1.28	3.85	1.243	1.84	0.82	55.04	1.26
		10.02	4500	750	71.8	70.0	70.0	58.6	75.0	1.36	2.60	1.31	0.66	75.15	0.93	1.28	3.85	1.243	1.84	0.82	56.01	1.25
WFSC7_L4	110x50x15x2	10.02	5500	150	37.7	38.0	37.7	43.5	50.3	1.02	1.35	1.31	0.66	36.99	1.02	1.16	5.98	1.45	2.00	0.88	36.99	1.02
		10.02	5500	300	45.8	43.0	43.0	43.5	50.3	1.13	1.91	1.31	0.66	45.10	0.95	1.16	5.98	1.45	2.00	0.88	38.17	1.13
		10.02	5500	450	50.3	46.7	46.7	43.5	50.3	1.23	2.34	1.31	0.66	51.86	0.90	1.16	5.98	1.45	2.00	0.88	38.17	1.22
		10.02	5500	600	52.3	47.5	47.5	43.5	50.3	1.24	2.70	1.31	0.66	57.26	0.83	1.16	5.98	1.45	2.00	0.88	38.17	1.24
		10.02	5500	750	52.9	47.8	47.8	43.5	50.3	1.25	3.02	1.31	0.66	61.83	0.77	1.16	5.98	1.45	2.00	0.88	38.17	1.25
WFSC7_L5	110x50x15x2	10.02	6000	150	34.5	33.5	33.5	38.6	42.3	1.00	1.44	1.31	0.66	33.56	1.00	1.10	7.28	1.603	2.00	0.88	33.56	1.00
		10.02	6000	300	41.4	37.9	37.9	38.6	42.3	1.12	2.03	1.31	0.66	41.69	0.91	1.10	7.28	1.603	2.00	0.88	33.86	1.12
		10.02	6000	450	44.5	39.6	39.6	38.6	42.3	1.17	2.49	1.31	0.66	47.94	0.83	1.10	7.28	1.603	2.00	0.88	33.86	1.17
		10.02	6000	600	45.5	40.1	40.1	38.6	42.3	1.19	2.87	1.31	0.66	52.93	0.76	1.10	7.28	1.603	2.00	0.88	33.86	1.19
		10.02	6000	750	45.7	40.3	40.3	38.6	42.3	1.19	3.21	1.31	0.66	57.16	0.71	1.10	7.28	1.603	2.00	0.88	33.86	1.19
WFSC7_L6	110x50x15x2	10.02	6500	150	31.7	29.0	29.0	34.7	36.0	0.95	1.51	1.31	0.66	30.66	0.95	1.04	8.68	1.818	2.00	0.88	30.49	0.95
		10.02	6500	300	37.4	33.0	33.0	34.7	36.0	1.08	2.14	1.31	0.66	38.92	0.85	1.04	8.68	1.818	2.00	0.88	30.49	1.08
		10.02	6500	450	39.4	33.6	33.6	34.7	36.0	1.10	2.62	1.31	0.66	44.76	0.75	1.04	8.68	1.818	2.00	0.88	30.49	1.10
		10.02	6500	600	39.7	34.3	34.3	34.7	36.0	1.12	3.02	1.31	0.66	49.42	0.69	1.04	8.68	1.818	2.00	0.88	30.49	1.12
		10.02	6500	750	39.8	34.5	34.5	34.7	36.0	1.13	3.38	1.31	0.66	53.36	0.65	1.04	8.68	1.818	2.00	0.88	30.49	1.13
WFSC8_L1	120x50x15x2	11.62	3000	150	67.5	69.3	67.5	128.8	170.3	1.07	0.80	1.41	0.69	63.07	1.07	1.32	1.67	1.175	1.87	0.83	63.07	1.07
		11.62	3000	300	102.7	114.8	102.7	128.8	170.3	1.06	1.13	1.41	0.69	96.48	1.06	1.32	1.67	1.175	1.87	0.83	96.48	1.06
		11.62	3000	450	115.9	135.7	115.9	128.8	170.3	1.05	1.39	1.41	0.69	110.69	1.05	1.32	1.67	1.175	1.87	0.83	110.69	1.05
		11.62	3000	600	122.7	145.0	122.7	128.8	170.3	1.09	1.60	1.41	0.69	117.41	1.05	1.32	1.67	1.175	1.87	0.83	113.92	1.08
		11.62	3000	750	127.5	149.6	127.5	128.8	170.3	1.13	1.79	1.41	0.69	125.44	1.02	1.32	1.67	1.175	1.87	0.83	115.56	1.10
WFSC8_L2	120x50x15x2	11.62	3500	150	62.0	63.1	62.0	98.3	126.6	1.07	0.92	1.41	0.69	58.04	1.07	1.29	2.23	1.231	1.93	0.85	58.04	1.07
		11.62	3500	300	85.4	96.1	85.4	98.3	126.6	1.05	1.30	1.41	0.69	81.71	1.05	1.29	2.23	1.231	1.93	0.85	81.71	1.05
		11.62	3500	450	94.7	107.9	94.7	98.3	126.6	1.10	1.59	1.41	0.69	89.16	1.06	1.29	2.23	1.231	1.93	0.85	86.59	1.09
		11.62	3500	600	101.0	112.6	101.0	98.3	126.6	1.17	1.83	1.41	0.69	97.09	1.04	1.29	2.23	1.231	1.93	0.85	87.49	1.15
		11.62	3500	750	105.7	105.7	98.3	126.6	1.23	2.05	1.41	0.69	103.73	1.02	1.29	2.23	1.231	1.93	0.85	88.20	1.20	
WFSC8_L3	120x50x15x2	11.62	4000	150	55.8	56.8	55.8	78.4	97.5	1.05	1.03	1.41	0.69	53.09	1.05	1.24	2.88	1.299	2.00	0.88	53.09	1.05
		11.62	4000	300	72.3	78.8	72.3	78.4	97.5	1.06	1.45	1.41	0.69	68.37	1.06	1.24	2.88	1.299	2.00	0.88	68.37	1.06
		11.62	4000	450	80.3	86.1	80.3	78.4	97.5	1.17	1.78	1.41	0.69	76.04	1.06	1.24	2.88	1.299	2.00	0.88	68.83	1.17
		11.62	4000	600	86.1	88.5	86.1	78.4	97.5	1.25	2.05	1.41	0.69	82.81	1.04	1.24	2.88	1.299	2.00	0.88	68.87	1.25
		11.62	4000	750	89.7	89.9	89.7	78.4	97.5	1.31	2.29	1.41	0.69	88.47	1.01	1.24	2.88	1.299	2.00	0.88	68.90	1.30
WFSC8_L4	120x50x15x2	11.62	4500	150	50.1	51.2	50.1	64.7	77.2	1.04	1.13	1.41	0.69	48.37	1.04	1.19	3.59	1.38	2.00	0.88	48.37	1.04
		11.62	4500	300	62.7	63.1	62.7	64.7	77.2	1.10	1.60	1.41	0.69	58.92	1.06	1.19	3.59	1.38	2.00	0.88	56.78	1.10
		11.62	4500	450																		